METRO-HAUL

METRO High bandwidth, 5G Application-aware optical network, with edge storage, compute and low latency

Grant No. 761727

Deliverable D3.2

First validation of the METRO-HAUL node architecture and optical solutions

Editor:	Eduardo Magalhães, TU/e
Deliverable nature:	Report (R)
Dissemination level: (Confidentiality)	Public (PU)
Contractual delivery date:	May 2019
Actual delivery date:	4 July 2019
Suggested readers:	Optical Networks Researchers and Engineers; Product Managers; Architects and Technology specialists.
Version:	1.0
Total number of pages:	95
Keywords:	

Abstract

D3.2 reports the first validation of the METRO-HAUL node architecture and the interconnection, transmission and switching optical solutions developed in T3.1-T3.3 in different disaggregated scenarios. The deliverable also includes an early description of the METRO-HAUL node control and management environment and the developed software for controlling all the OIE developed in T3.4.

[End of abstract]

Disclaimer

The research leading to these results has received funding from the European Union Horizon 2020 Programme under grant agreement number METRO-HAUL 761727

Impressum

[Full project title] METRO High bandwidth, 5G Application-aware optical network, with edge storage, compute and low latency

[Short project title] METRO-HAUL

[Number and title of work-package] WP3 - Metro Node and Optical Transmission Solutions

[Number and title of task] T3.1, T3.2, T3.3, T3.4

[Document title] First validation of the METRO-HAUL node architecture and optical solutions

[Editor: Name, company] Eduardo Magalhães, TU/e

[Work-package leader: Name, company] Emilio Riccardi, TIM

[Estimation of PM spent on the Deliverable]

Executive Summary

The METRO-HAUL project was created to provide a bold vision, framework and enabling components for future metro transport networks, technologically capable of supporting advanced 5G use cases and services. These new metro networks would need to handle far higher traffic volumes, and support a diverse set of applications and services, without requiring a vast expansion of fiber infrastructure. This 5G-capable metro transport network would also need to support a holistic multi-layer, and multi-domain provisioning approach, capable of operating both optical transport infrastructure, and IT resources such as compute, function and storage capabilities.

The METRO-HAUL project initially defined a set of 5G service use cases, which led to the development of a framework and deployment architectures, thus leading to a functional definition of the METRO-HAUL node requirements, for both the Access Metro Edge Nodes (AMENs), and the Metro Core Edge Nodes (MCENs). This document represents the activity of METRO-HAUL Work Package 3 (WP3). The WP3 team investigates and designs of new, efficient and flexible data plane architectures for Metro Access, Metro Core Nodes and optical metro-wide networks, supporting both filtered and (semi-)filterless optical solutions and fully exploiting the Elastic Optical Network paradigm. The proposed WP3 solutions are designed to be controllable and monitored by a common SDN and NFV framework, developed in collaboration with the METRO-HAUL control plane work of Work Package 4 (WP4).

The WP3 investigation work has led to the definition of physical metro node architecture and subsequent requirements for supporting flexible 5G access requirements, datacom-telecom convergence and disaggregation of network functionalities, all underpinned by a commoditised flexible optical layer. This new 5G metro optical infrastructure must also meet the need to support low cost optical and energy efficient optical switching elements, capable of high capacity and flexible transmission technologies, supporting both filtered and semi-filterless optical networks.

During the first half of the project, three classes of metro optical WDM transport systems were identified and used within the METRO-HAUL project. These were derived based on the use cases and application requirements and evaluated to be the most suitable solutions for the evolution of metro networks. The three classes differ in terms of switching and transmission technologies, overall guaranteeing cost-effectiveness and high-performance despite of the specific metro application scenario which could vary quite significantly according to the considered optical reach (from few tens of km up to 150-200km), fiber availability and topology (ring, mesh, horseshoe), geographic/demographic conditions (e.g., rural to densely populated areas).

This document, D3.2 “First validation of the METRO-HAUL node architecture and optical solutions”, reports the current results of the second year of activities in WP3 of the METRO-HAUL project. It demonstrates how the METRO-HAUL reference framework, together with a selection and preliminary implementation of candidate metro optical node and transceiver solutions, may be deployed and operated using a common open API. Furthermore, we also highlighted how the METRO-HAUL Monitoring and Data Analytics (MDA) system, which provides node and service telemetry data, is used for real-time operation and optimization of optical infrastructure.

The combined solution of flexible optical technology capable of varying deployment scenarios operated via a common open API and with embedded MDA capabilities, represents a significant step towards practical METRO-HAUL infrastructure for next generation 5G services.

List of Authors

	Name	Partner
	Anna Chiadò Piat, Alessandro Percelsi, Morro Roberto, Emilio Riccardi	TIM
	Laia Nadal, Michela Svaluto Moreolo, Josep Mª Fàbrega	CTTC
	Teresa Yu Bi, Arash Beldachi	UNIBRIS
	Luis Velasco, Marc Ruiz, Jaume Comellas, Gabriel Junyent	UPC
	Filippo Cugini, Francesco Fresi, Alessio Giorgetti, Andrea Sgambelluri	CNIT
	Jorge E. López de Vergara, Guillermo Julián-Moreno, Tobías Alonso, José F. Zazo, Sergio López-Buedo, Gustavo Sutter	Naudit HPCN
	Evangelos Kosmatos, Chris Matrakidis, Alexandros Stavdas	OLC
	Michael Parker	LEX
	Robert Emmerich, Johannes Fischer, Pablo Wilke Berenguer	Fraunhofer
	Eduardo Magalhães, Nicola Calabretta	TU/e
	João Pedro, Antonio Eira, Nelson Costa, Paulo Gomes	CORIANT PT
	Antonio D'Errico	TEI
	Annika Dochhan	ADVA DE
	Boitier Fabien, Layec Patricia, Almonacil Sylvain	NBLF
Checked by:	Emilio Riccardi	TIM
	Daniel King	ODC

Revision History

Revision	Date	Responsible	Comment
0.0	01/04/2019	Editor	Initial version
1.0	04/07/2019		Checked version

Table of contents

List of Figures

List of Tables

1 Introduction

This document D3.2 “First validation of the METRO-HAUL node architecture and optical solutions” describes the most relevant results of the second year’s activity within Work Package 3, “Metro Node and Optical Transmission Solutions” in the METRO-HAUL project. This effort is underpinned by several WP3 tasks, including:

- **Task 3.1** – An architecture definition of METRO-HAUL nodes considering datacom-telecom convergence and the exploration and classification of advanced multi-technology multi-vendor or disaggregated modular Optical Infrastructure Elements, “whiteboxes” ecosystems.
- **Task 3.2** – This task is split into two sub-tasks:
  - **Task 3.2.1** explores and develops optical switching solutions for innovative programmable “optical whitebox” with integrated control and monitoring
  - **Task 3.2.2** develops hitless function and transport protocol programmable access core interface solutions to face 5G access requirements.
- **Task 3.3** – Identifies the with interoperability issues and optimal transmission solutions for both filtered (T3.3.1) and (semi-)filterless (T3.3.2) optical network paradigms and compares and identifies in terms of complexity, flexibility and cost which specific transmission technique is better suited for
- **Task 3.4** – This task is split into two sub-tasks:
  - **Task 3.4.1** aims to demonstrate a cost-effective integrated performance monitoring system architecture ranging from optical to packet and service monitoring with local analytics evaluation
  - **Task 3.4.2** aims to design and implement a Common Optical Node Control software for generic optical whiteboxes, facing control and management plan in a unified way. A selected subset of the key data plane solutions in term of nodes OEI and control and monitoring subsystems

This document also leverages on Deliverable D3.1 “Selection of metro node architectures and optical technology options” related to the first year’s WP3 activity. In particular, D3.1 identified the framework for the design and planning of optical WDM metro networks suitable for supporting 5G access networking and its expected requirements. It introduced the concept of “disaggregation”, originally began in the world of “Hyperscale Operators”, which is applied in METRO-HAUL at the optical level.

Disaggregation is a general approach to reduce CapEx and OpEx by sourcing HW directly and in sizeable volumes from the original design manufacturers (ODM), and then selectively exploiting and adopting free and open source software. To be successfully exploited, it requires several factors, including (i) the presence in the market of general-purpose equipment at relatively low cost and with high performance, (ii) the separation of the operating system software from the HW (i.e. the Software Defined Networking – SDN - approach), and (iii) the presence of Open Programming Interfaces (OpenAPI) that abstract the complexity of the underlying hardware.

This document reports the remarkable METRO-HAUL contributions into the disaggregation of optical metro networks. In particular, D3.2 highlights the cost-effective, high-performance optical systems, subsystems and technologies under development within the project, optimized for the various metro network systems and segments, and provided with properly defined common API and unified, innovative programmable capabilities.

This D3.2 document is structured as follows:

Section 2 reports on the reference scenario. First, it summarizes the driving concept of disaggregation and its specific flavours considered by METRO-HAUL when applied to optical metro networks. Then, it reports on the metro network scenarios of interest for the Operators involved in the Project (i.e., TIM, BT and Telefónica). The scenarios are described accounting for specific geographical and architectural requirements, including topologies, distances, traffic needs, number of nodes, geographic/demographic setting of the nodes/network (e.g., rural/urban), and considering the amount and type of traffic to be transported. This section is strictly dependent on Work Package 2 results and in particular on Deliverable 2.3 “Network Architecture Definition, Design Methods and Performance Evaluation”.

Section 3 summarizes the general METRO-HAUL infrastructural framework, and in particular the three classes of Optical WDM Transport Systems identified within METRO-HAUL: (i) WDM-Sys1: Flexible, high capacity WDM transport System based on MD-ROADMs; (ii) WDM-Sys2: Low cost, simple topology WDM transport System based on degree-2 ROADMs; and (iii)WDM-Sys3: Low cost, simple topology WDM transport System based on Filterless OADMs. These three classes of systems exploit the innovative METRO-HAUL components detailed in Section 5.

Section 4 outlines the criteria used to define the methodology and the Key Performance Indicators (KPIs) for the evaluation of the different devices and sub-systems that compose the METRO-HAUL infrastructure.

Section 5 details the innovative METRO-HAUL solutions for devices and subsystems. First, it reports on the considered optical switching technologies, including low-cost MD-ROADM, semi-filterless and filterless solutions, and innovative filtered photonic integrated solution. Then, it details transceivers solutions together with their transmission performance: (i) a programmable sliceable transceiver based on multicarrier modulation (MCM); (ii) a transceiver solution for dispersion-tolerant direct detection; (iii) an elastic transponder with low resolution DAC and ADCs for metro networks; and (iv) a digital sliceable bandwidth variable transponder for filterless networks. Furthermore, the section reports on the PON termination to metro nodes together with the related abstraction and validation methodology and on the programmable packet switching solution for interconnection at the edge. Finally, this section describes the proposed probe-based monitoring solution at the data-link layer.

Section 6 reports on the design, implementation and preliminary validation of the software components serving as agents of the data plane devices and subsystems. As reported in D3.1, METRO-HAUL has adopted the OpenROADM model for the optical network equipment (O-NE) performing optical switching (e.g., WSS-based ROADM, photonic integrated switching matrices) and the OpenConfig YANG model for O-NE of type transponder. In this deliverable, the implementation of the software agents for either type of O-NE is reported.

Section 7 details the innovative METRO-HAUL node control and management environment to support active and passive monitoring, telemetry, and data analytics through a centrally-managed multi-node agent.

Section 8 concludes the document.

2 Application reference context

2.1 Disaggregation scenarios

The concepts of disaggregation and whitebox were introduced by the IT community, where the hardware and switches were decoupled from the operating system that was installed on it. This enabled different vendors to offer either the software or the hardware, leading to larger competition and avoiding vendor lock-in scenarios. The Open Compute Project (OCP) started in 2011 to create open hardware specifications for servers, and later in 2013, they evolved this concept to the switches area.

In the early days of the telecommunications, the TELCOs used to do all the procedures to offer the phone service to the customer. These tasks started with the hardware definition, prototyping, manufacturing, testing, integrating as well as all the operational aspects including installation, commissioning, and maintenance. Little by little, different tasks were outsourced to companies specialized to carry out such functions. Nowadays, the vast majority of TELCOs purchase their network elements to system integrators that define the hardware solution (switch, router, or transponder), purchase the components from third parties and carry out the integration of the devices as well as the software development to carry out the network element functions. Regarding the operational aspects, there are two flavors. There are vendors that perform the installation, commissioning, and maintenance, while there are others that rely on partners to do such activities. If we consider the elements that compose a network element, we can identify the following roles and activities [1][2]:

- Bare-metal. Hardware system formed with different components (chipset, memory, pluggables, etc.).
- Network Operating System (NOS). Software installed in the bare-metal to support the networking functionalities (L2, L3, etc.).
- Box System. This is a selection of a NOS and a Bare-metal.
- System integration. This is the process of testing and validating that the box system is performing as described in the specs.
- System maintenance. This is the process of installing, testing, repairing and decommissioning the box systems in the field.

If we consider that a network element is decoupled in hardware and software, then different roles appear in relation with the network operator. The two first roles are the bare-metal provider, which supply their hardware, and the NOS provider, which offers the operating system installable in the hardware. A mandatory requirement for those providers is that each component may be deployed into a decoupled fashion with its counterpart. If either the hardware or the NOS vendors limit the interoperability, the disaggregation of the solution does not offer any advantage. The TELCO requires a box system to perform the network function.

Consequently, there must be a whitebox solution that combines hardware and software. The whitebox provider role is a supplier who currently commercializes a box system as an integrated product. If the NOS and the bare metal are open components that allow operating with third-party components, then the solution is an open whitebox or, simply, whitebox.

On the other hand, if there are proprietary elements, this solution is known as a branded whitebox or “Brite-box” (a branded whitebox switch). If we explore the idea of a whitebox in a production environment, it is required to have a whitebox integrator that deals with system integration. The

system integrator works for the correct software and hardware integration, to be in charge of the L2/L3 support and maintenance services, and to participate in the certification activities, the integration with OSS/BSS, the training of operational teams, etc.

Optical Transport DWDM networks for TELCOs are deployed on a metro/regional basis. The motivation for this approach is a combination of factors: legacy deployments, technology redundancy, different optical performance requirements (metro vs. long-haul), lack of interoperability, and simply commercial reasons. These deployments include all system elements, the transponders that generate the optical signals, the line system in charge of amplification and lambda switching and also the Network Management System (NMS). The NMS is operated manually and, sometimes, is integrated with other systems (e.g., OSS) through Application Programmable Interfaces (APIs). When considering how disaggregation is applied to optical networking, three alternatives appear: aggregated (Figure 1a), partially disaggregated (Figure 1b) and fully disaggregated (Figure 1c).

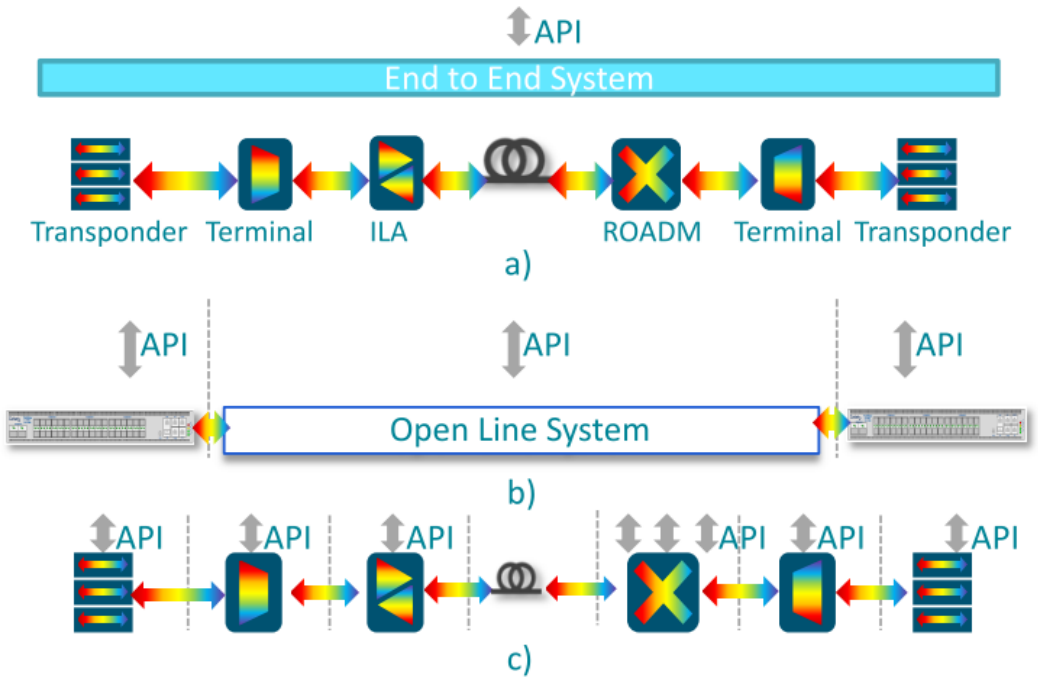

Figure 1: Optical network architecture alternatives: a) Aggregated, b) Partial disaggregation between transponder and line systems, and c) disaggregation among all optical infrastructural elements

A *partially disaggregated* scenario is composed of two main elements the Open Terminals (OT) and the Open Line System (OLS). The OTs are the transponders/muxponders, while the OLS consists of the ®OADMs,, wavelength multiplexors, optical amplifiers, etc. In this approach, optical transponders are disaggregated from the mono-vendor transport infrastructure (i.e., Analog WDM layer – A-WDM), which supports optical channels from external transponders as third parties client signals. The rationale behind this approach is that the operational life of the A-WDM layer is much longer than that of transponders, whose lifetime is governed by the continuous increase in capacity needed, requiring a very strong pace of innovation and therefore a shortened replacement cycle.

Furthermore, placing the analogue domain under the responsibility of a single vendor means leaving the development, testing and management of complex control, equalization loops and analogue heuristics solely to the responsibility of the vendor. Also, horizontal interoperability issues among

analogue O-NEs, again implying analogue optical design (including linear and non-linear transmission impairment control), are left to the system vendor responsibility. Partial disaggregation has also been addressed by the OpenConfig Initiative, which defined YANG models that have been considered by METRO-HAUL for the TP modelling.

A *full disaggregated* scenario opens to the direct control to all elements of a line system (e.g., ROADMs) which operate as stand-alone entities. In this approach, the involvement of the TELCO in the WDM-Sys lifecycle is strong, certainly not limited to vertical integration of control and management SW. O-NEs from both the A-WDM and digital layers are potentially purchased from different vendors, leaving interworking at the control and data plane to the system integrator. Therefore, most of the control intelligence is moved to the WDM controller (necessarily vendor agnostic) which becomes the most critical element of the whole chain, having to face also all the analogue transmission issues (equalization, transient suppression, etc.). Furthermore, the detailed specification for both Single-Wavelength-Interfaces (SWI) and Multi-Wavelength Interface (MWI) is needed to support horizontal integration; likewise, a standardization of the SBI is paramount. Planning and design of such a multi-vendor network require specialized technical skills that often only vendors have. Alternatively, vendor automatic agnostic planning and design tools could be employed if they were available to the market, and sufficiently comprehensive to be used by a skilled user and not necessarily an optical design expert. A TELCO could profitably utilise them to automatically provide the bill of material, equipment configuration and interconnection schemes for a multi-vendor disaggregated environment. Full disaggregation has also been addressed by the OpenROADM initiative which defines a Multi-Source Agreement (MSA) including multiwave interface between the ROADMs and a single wave interface from the transponders. In METRO-HAUL, the OpenROADM YANG model has been considered for ROADM modelling.

A further level of full disaggregation decomposes the optical infrastructure elements into their most relevant building blocks. For example, a ROADM is decomposed into optical amplifiers, WSS and monitors. This level of disaggregation targets the way a white box is built by assembling the internal components. Thus, it may be suitable for system integrators and not for TELCOs, which require the presence of a system integrator. This level of disaggregation has been considered and carefully investigated during the first year of the METRO-HAUL project (see D3.1 [3] and demo in [4]). During the second year, the focus has been devoted to those above partial and first full disaggregated scenarios without further considering the full disaggregation option applied to subcomponents (since not considered a relevant priority for system integrators which already rely on specifically designed interfaces for subcomponent integration).

2.2 Metro areas (from WP2)

METRO-HAUL is aiming to exploit the flexibility and cost-advantages of the disaggregation and white box technologies being developed in the WP3 of the project, by deploying these general-purpose equipment innovations into the metro network, where there are a variety of technical architectures available according to the topologies, distances, traffic needs and number of nodes describing the interface between the 5G fixed & wireless access and the photonic core network. The specific network requirements and definitions of these metro architectures are being developed in the WP2. Figure 2 below indicates the high-level schematic architecture showing how the metro transport network is located between the 5G access and photonic core networks. In particular the two key nodes: Access Metro Edge Node (AMEN) and Metro Core Edge Node (MCEN) are indicated, where much of the disaggregation and white box equipment will be deployed to take advantage of the

different and flexible metro architecture options, e.g. ring and horseshoe topologies, as described in the deliverable D2.3 [5]. In addition, as also outlined in the D2.3, the forecast traffic growth, currently (and projected into the future for the next decade) of a compound annual growth rate (CAGR) of 25% also needs to be taken into account when considering the white box and disaggregation functionalities of the nodal equipment and their upgradeable future-proofing.

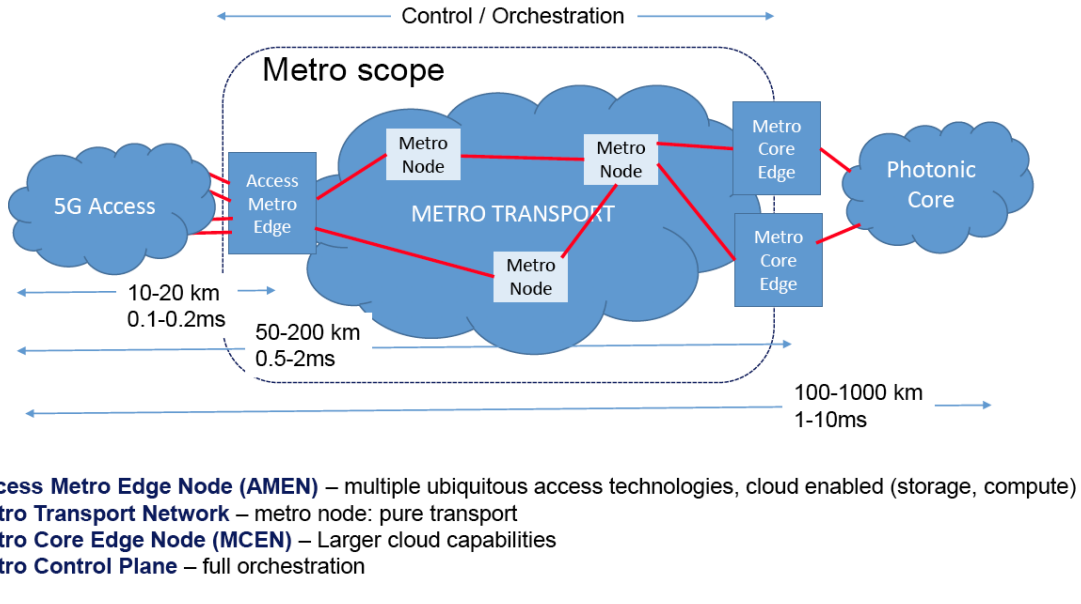

Figure 2: METRO-HAUL Network Scope and Reference Architecture.

Thus the rationale of METRO-HAUL is that it does not propose a one-size-fits-all architecture, but rather a technology toolbox that can be used selectively for different application scenarios. In the scope of METRO-HAUL, these scenarios relate mostly to the geographic/demographic setting of the nodes/network (e.g., rural/urban), which influences the traffic volume/pattern, and also, in the specific case of the optical transport network, the distances to be covered by optical interfaces.

The first version of topologies and network scenarios provided by operators was reported in D3.1 [3]; they reflect the actual deployed operator networks or networks planned to be deployed in the short term. These operator topologies and network scenarios have been used to derive the unified METRO-HAUL reference topology presented in this subsection (again from D2.3).

METRO-HAUL assumes that the range of distances of the metro network segment is between 50 and 100 km, which fall within the typical transmission distances within a mix of urban and dense urban areas. Certain suburban or rural areas may require fibre distances longer than 100 km and up to 200 km.

In addition, two main types of “node functionality” (often referred to as “nodes” themselves), are defined in METRO-HAUL: the AMEN, which gathers traffic from access networks and hosts a limited set of network services; and the MCEN, which assures metro domain internetworking, provides an extended set of centralised services and allows the interconnection with the backbone. Topologies are strictly connected to such functionalities, because each topological node can host one of the two, or both, such functionalities. This general and high-level framework on how access, aggregation and core functionalities can be put together to build an AMEN or an MCEN are described in Section 3.2 “Guidelines for METRO-HAUL Central Office Design and Assembly” of D3.1 [3].

The reference network topology structure is therefore depicted in Figure 3. The network is organized into two tiers: an aggregation tier composed of horseshoe (or ring) subnetworks made of aggregation nodes and two core nodes (the last ones constitute the end-tail nodes of the horseshoe), and a core tier made of core nodes interconnected by a mesh of links.

According to the geotypes specified in D2.3, the fiber length of a horseshoe depends on the specific geotype. Hereafter, *L* is the symbol used to identify the total horseshoe fiber length, i.e. the total length of the chain of AMEN nodes in km. Dense urban environments should have a total fiber length shorter than 20 km for the majority part of their aggregation networks, while the nimority will have lengths between 20 and 50 km. Urban areas should be characterized by the majority of horseshoe lengths being less than 50 km, with most of the remaining part consisting of lengths of up to 100 km. Horseshoes in Sub-urban areas should be a balanced mix of cases with lengths less than 50 km, and lengths between 50 and 100 km, with some few exceptions where the length is equal to or greater than 100 km. Finally, rural districts are expected to show longer horseshoes, but with a minority of them still less than 100 km, the majority being with lengths ranging from 100 to 200 km and, another minority set that is greater than or equal to 200 km.

This model and the associated ranges of distances reproduce, with some adaptations, the real network scenarios proposed by operators, and can also be applied to other geographical and operator specific contexts.

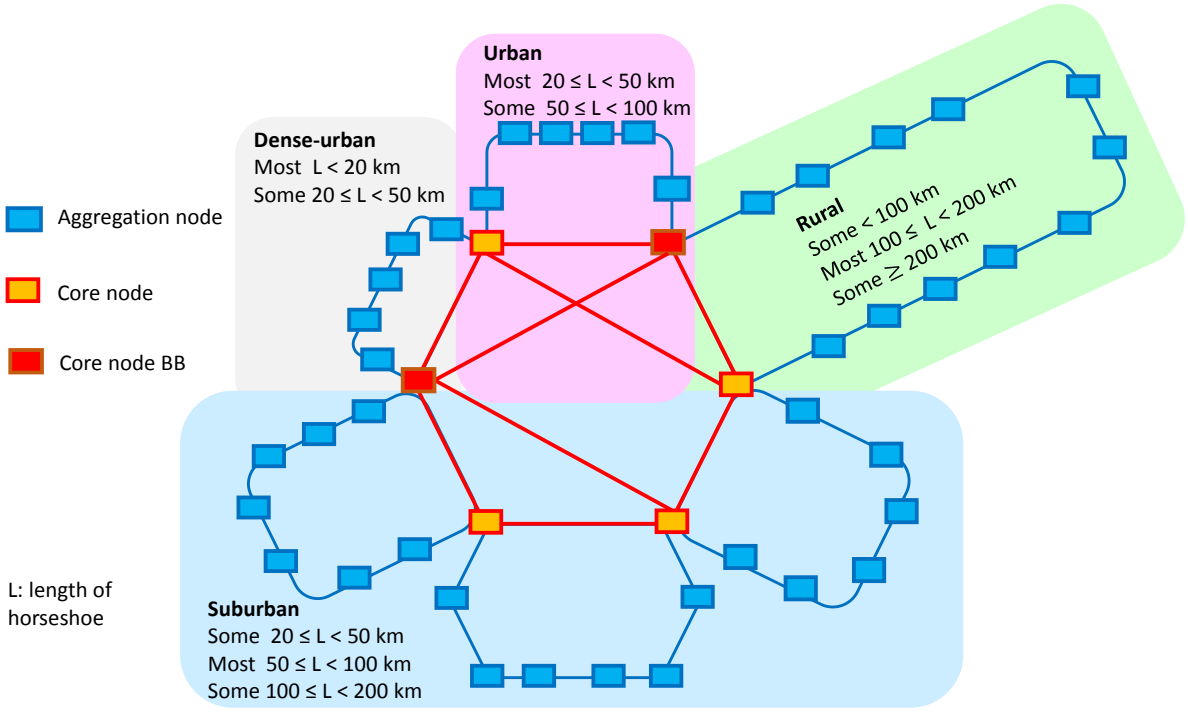

Figure 3: Reference METRO-HAUL horseshoe topology D2.3 [5]

Table 1 reports the ranges of distances for the aggregation networks with the horseshoe topology, and assuming that each horseshoe covers a homogeneous set of AMEN nodes. The exact share of each distance range per geotype context, as well as the percentage of horseshoes belonging to each geotype context about all of the horseshoes in the network, are very dependent on the specific geographic and demographic characteristics of each country and operator. Hence, the values in Table 1 should be taken as indicative, comprising averaged educated guesses from the available operator data.

Table 1: Horseshoe length ranges for homogeneous geo-types areas (D2.3 [5])

Geotype context (homogeneous)	Total distances range for horseshoe topology				
	L <20 km	20 ≤ L < 50 km	50 ≤ L < 100 km	100 ≤ L < 200 km	L ≥ 200 km
Dense urban	YES (majority)	YES (minority)	NO	NO	NO
Urban	NO	YES (majority)	YES (minority)	NO	NO
Suburban	NO	YES (minority)	YES (majority)	YES (rare)	NO
Rural	NO	NO	YES (minority)	YES (majority)	YES (rare)

Concerning the meshed network interconnecting the core nodes, the degree of mesh will depend on the specific implementation, but in general, one can expect a slightly meshed network with node degree values between 3 and 6, depending of course on the number of core nodes belonging to the metro core network. Regarding the role of core nodes within the METRO-HAUL framework, they can exploit in general both AMEN and MCEN functions (and so they can be labelled as MCEN nodes) with only a subset of them that could be connected with the long-distance backbone. In Figure 3, the MCEN nodes interconnected with the backbone are the two red ones, while the remaining four orange ones form the central metro core mesh. Regarding the number of nodes in the metro core meshed network, it can range from a few nodes (4) to tens of nodes (40), depending on both the area covered and the traffic collected from the aggregation subnetworks.

Typical link distances and network diameter of the metro core mesh depend on the geographical context covered by the network. *Table* 2 shows typical node number, nodal degree, link lengths and network diameters of metro networks covering the two contexts of a city (the city area and its close surroundings only) and a wide metro-regional area.

Table 2: Length ranges in a Slightly Meshed Network for homogeneous geo-types areas (D2.3 [5])

Feature	Metropolitan Core			Regional Core		
	Minimum	Average	Maximum	Minimum	Average	Maximum
Node number	4	12	20	8	20	40
Node degree	2	3	5	2	4	6
Link distance	1 km	5 km	20 km	1 km	70 km	120 km
Net. diameter	10 km	20 km	50 km	100 km	200 km	400 km

How the traffic subtypes generate flows in the metro network and towards the backbone is depicted in D2.3 [5]. The network is schematically represented with three domains: Metro aggregation, Metro Core, and Backbone. Topologies are not relevant and can be horseshoes or rings in the aggregation and a mesh in the Core.

3 METRO-HAUL Infrastructure solutions

The macroscopic METRO-HAUL infrastructure, spanning a regional or metropolitan network is reported in Figure 4. The infrastructure is composed of a set of heterogeneous resources, mainly:

- An optical metro network (in yellow), that provides high bandwidth, low latency connections between metro locations.
- Packet switched networks (in blue), providing connectivity to customers, NVFI servers and related endpoints.
- Passive Optical Networks (PON), interfacing the access network
- ETSI NFVI Points of Presence (NFVI PoP) encompassing multiple compute nodes in which virtualized network functions can be executed. It is assumed that such compute nodes (i.e., virtualization servers) are attached to the packet switched networks, e.g. using Ethernet interfaces.

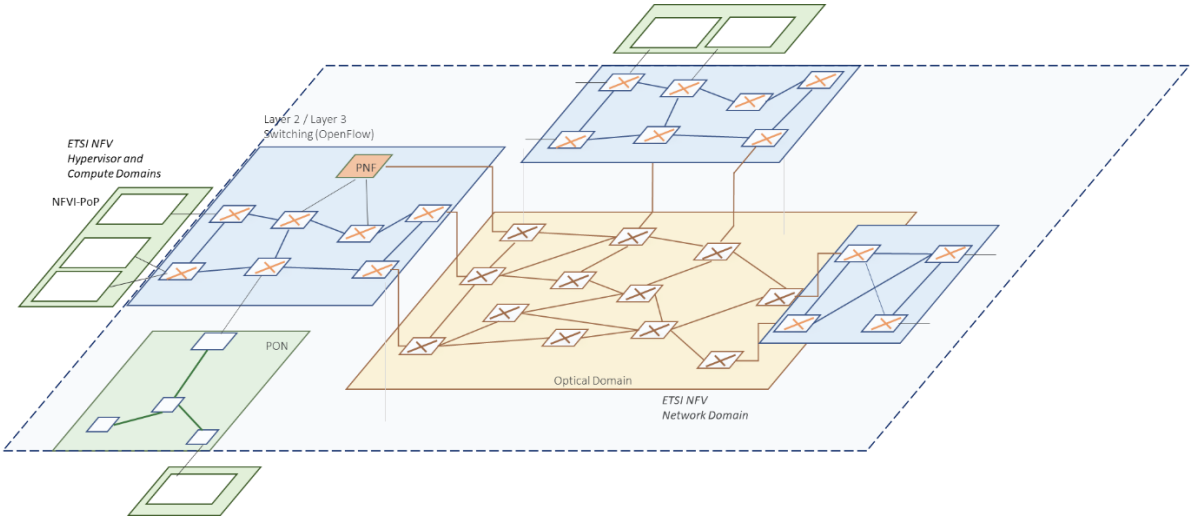

Figure 4: Macroscopic METRO-HAUL infrastructure

Work Package 3 focuses on the optical metro network, providing innovative solutions to architect and design cost-effective, energy-efficient, agile and programmable metro WDM networks that are scalable for 5G access and future requirements. The goal is to effectively interfacing both 5G access and multi-Tbit/s elastic core networks.

In deliverable D3.1 [3], the most relevant options for WDM transport systems were presented and discussed in the context of short/long term applicability and partial/full disaggregation.

According to the physical infrastructures of the Metro-Regional networks owned by the three Operators involved in the project (TIM, BT and Telefonica), three classes of Optical WDM Transport Systems have been identified by METRO-HAUL.

1) WDM-Sys1: Flexible, high capacity WDM transport System based on MD-ROADMs

This first class of systems is characterized by fully flexible optical switching solutions (e.g. MD-ROADM) and highly efficient flexible coherent transceivers optimized for metro/regional reach (less, or approximately up to 200-450 km). This class is designed for high traffic node interconnections, including meshed topologies, implemented through modular chasses with “Data center” form factor or standard “ETSI” telecom form factor, targeting either partial or full disaggregation.

2) WDM-Sys2: Low cost, simple topology WDM transport System based on degree-2 ROADMs

This second class of systems is characterized by low-cost degree 2 Add&Drop system with limited functionalities and lower flexibility and scalability, together with low-cost Coherent or Direct Detection Transceivers optimized for short reach (less, or approximately up to 80-120 km). This class is designed for peripheral nodes interconnection with linear or ring topologies, having to handle relatively few optical connections with limited requirements on reconfiguration. The final implementation will have to be compliant with modular chasses with "Data center" form factor, for either partial or full disaggregation.

3) WDM-Sys3: Low cost, simple topology WDM transport System based on Filterless OADMs

This third class of systems is characterized by a pure filterless architectures with low-cost Coherent or Burst mode interfaces (like in PONs) optimized for even shorter metro distances. This class is designed for peripheral areas using linear topologies and relatively few optical connections with limited requirements on reconfiguration. Implementation with "data center" form factor, for partial or fully disaggregation (possibly reusing existing access technologies (PON) for CO's interconnection)

Table 3 reports the complete list of METRO-HAUL components specified during the first year of the project, together with their possible applicability in each of the classes above of systems.

Table 3: Metro Haul Hardware Components

Metro Haul Hardware Components					
	Components	**Lead Partner**	**Sys1**	**Sys2**	**Sys3**
D1	Low cost MD-ROADM	TIM	X	X	
D2	two-degree ROADM prototype for design and investigation of fully disaggregated solution	CNIT	X		
D3	ROADM O-NE based on splitter and wavelength blocker architecture for semi-filterless solutions	ADVA		X	
D4	Innovative photonic integrated optical switching solution for add/drop module of ROADM	TEI/CNIT	X	X	
D5	A multi-purpose loss-less photonic integrated wavelength selective switch (2 to N degrees)	TU/E	X	X	
D6	Filterless OADM	HHI			X
D7	Programmable sliceable transceiver based on multicarrier modulation (MCM)	CTTC	X	X	X
D8	Transceiver solutions for dispersion-tolerant direct detection	CNIT		X	X
D9	Spectral-efficiency tunable transceiver with probabilistic-shaping	Bristol	X		
D10	Elastic transponders with low resolution DAC and ADCs for metro networks	NOKIA	X	X	X
D11	digital sliceable bandwidth variable transponder for filterless networks	HHI		X	X
D12	Programmable packet switching solution for interconnection of access and core segments	Bristol	X	X	X
D13	PON termination to metro node and its abstraction	OLC			X
D14	100 Gbit/s passive probe	NAUDIT			
D15	100 Gbit/s Active Probe	NAUDIT			
D16	Ericsson SPO1400 ROADM	TEI	X	X	X
D17	Coriant Groove G30 muxponders	TIM/Coriant	X	X	X

D18	ADVA's coherent transponders	ADVA	X	X	X
D19	Voyager Muxponder	BT/ Bristol	X	X	
D20	Lumentum Transport ROADM white-box	TIM/CNIT	X		
D21	Bristol ROADM	Bristol	X		

4 Objectives, methodologies, and performance indicators for METRO-HAUL infrastructure

This section describes the criteria used to define the methodology and the Key Performance Indicators (KPIs) for the evaluation of the different devices and sub-systems that compose the METRO-HAUL infrastructure. Those criteria take into account the general goals of METRO-HAUL project, which are to provide high capacity and cost-efficient optical transport infrastructure, able to cope with high traffic volumes, and to integrate it with application-aware edge computing nodes, to facilitate service deployment and optimize transport bandwidth requirements.

Using these goals, WP2 has defined nine project-wide macro KPIs, that are described in details in Section 2 of Deliverable D.2.3 [5], and are reported here, for completeness, in Table 4, also showing their mapping to the 5G-PPP KPIs listed in Table 5.

Table 4: METRO-HAUL general KPIs and mapping to 5G-PPP performance KPIs D2.3 [5]

METRO-HAUL KPIs	5G PPP Performance KPIs					
	P1	**P2**	**P3**	**P4**	**P5**	**P6**
MH1. Optical PtP connection set-up time			X	X	X	
MH2. METRO-HAUL E2E PtP connection set-up time			X	X	X	
MH3. Set-up time of network service slice across METRO-HAUL	X		X		X	
MH4. Capacity of METRO-HAUL controller	X				X	
MH5. Fault/degradation detection time				X		
MH6. Capacity of METRO-HAUL infrastructure	X			X	X	
MH7. New optical components/systems	X	X	X			
MH8. CapEx reduction	X				X	
MH9. Energy consumption		X				

Table 5: 5G-PPP Performance KPIs D2.3 [5]

	Performance KPIs
P1	Providing 1000 times higher wireless area capacity and more varied service capabilities compared to 2010.
P2	Saving up to 90% of energy per service provided.
P3	Reducing the average service creation time cycle from 90 hours to 90 minutes.
P4	Creating a secure, reliable and dependable Internet with a “zero perceived” downtime for services provision.
P5	Facilitating very dense deployments of wireless communication links to connect over 7 trillion wireless devices serving over 7 billion people.
P6	Enabling advanced user-controlled privacy.

METRO-HAUL KPIs can be classified into three subsets.

The first subset is composed of KPIs that can be measured in an experimental environment, like one of the project’s demonstrators. They are in particular MH1, that is defined as the time needed to activate from the SDN controller an optical point-to-point connection through the optical layer, MH2, that is the time needed to activate from the SDN controller an end-to-end point-to-point connection involving both the packet layer and the optical layer, MH3, defined as the time needed to set-up a service slice across METRO-HAUL network through the orchestrator Open Source MANO, and MH5,

defined as the time from when a fault or degradation actually happens until it is detected by an agent node, or the network controller through a monitoring point.

The second subset regards KPIs that can be assessed through measurement or emulation activities performed on single components instead of an end-to-end system demonstrator; they are in particular MH4 and MH7. MH4 regards the SDN controller capacity, and is defined as the number of optical devices that can be controlled at a time, so it is related to the number of NETCONF sessions that can be managed by an instance of the controller; its measurement can be carried on in a lab environment, where controlled devices are emulated in virtual containers. MH7 is related to single physical devices or sub-systems, and evaluates their degree of innovation concerning their commercial state-of-the-art counterparts to meet some of the specific needs of a 5G enabled Metro network, considering one or more of the following parameters:

- Transmission capacity of an optical interface [Gb/s].
- The transparent reach of an optical interface [km].
- Cost of an optical component/system [cost units].
- Power consumption of an optical component/system [W].
- The footprint of an optical component/system [RU].

Depending on the specific characteristic, this KPI can be measured experimentally in a dedicated testbed, or evaluated based on modelling data.

Finally, the third subset encompasses the KPIs related to techno-economic evaluations of the overall METRO-HAUL solution. In particular MH6 is the capacity of METRO-HAUL infrastructure, defined as the aggregate amount (measured in Tb/s) of service instances that can be supported by a METRO-HAUL domain, MH8 is the Capex reduction, defined as the relative investment cost for deploying a joint IT/optical infrastructure across a METRO-HAUL domain compared to a reference baseline architecture and MH9 is the Energy consumption, defined as the relative power consumption of deploying a joint IT/optical infrastructure across a METRO-HAUL domain, compared to a reference baseline architecture.

Section 5 reports the description of all the physical devices and sub-systems that have been developed in METRO-HAUL, those devices find a place in different network segments, performing different functionalities, and each of them is characterised by very peculiar elements of innovation. For this reason, different KPIs have been defined specifically for each component. Never the less, all possible relationships between the METRO-HAUL macro KPIs defined in D2.3 [5], and the KPIs defined for each specific device in Section 5 have been identified and highlighted. In particular, almost all the devices have at list one KPI that corresponds to one of the parameters listed in the definition of MH7. Moreover, some of the KPIs of specific components can concur to a better performance of one of the other D2.3 macro KPIs.

5 METRO-HAUL Devices and sub-systems evaluation

This section details the first validation of METRO-HAUL technologies and solutions for next-generation metro optical nodes and interfaces. More specifically, the METRO-HAUL optical node prototypes include:

1) Multi-degree ROADM targeting the OpenROADM MSA YANG Device model validation and enhancement;
2) ROADM solution based on splitter and wavelength blocker architecture for semi-filterless solutions;
3) Innovative photonic integrated optical switching solution for add/drop module of (disaggregated) ROADM;
4) Multi-purpose modular and loss-less photonic integrated wavelength selective switches for WDM cross-connect switch (N degree) and add/drop node (2 degree).

On the other hand, at the interface/transmission levels, the following METRO-HAUL prototypes were developed and validated:

1) Programmable sliceable transceiver based on multicarrier modulation (MCM);
2) Transceiver solutions for dispersion-tolerant direct detection;
3) Spectral-efficiency tunable transmitter with probabilistic-shaping;
4) Elastic transponders with low-resolution DAC and ADCs for metro networks;
5) Commercial transponder enhanced with specifically designed NETCONF/YANG modules;
6) Digital sliceable bandwidth variable transponder for filterless networks;
7) Coherent transponders to be used in the filterless architectures.

Additionally, the integration to core and access is specifically addressed by focusing on:

1) Programmable packet switching solution for interconnection of access and core segments;
2) PON termination to the metro node and its abstraction;

Finally, monitoring systems have been developed through the METRO-HAUL project, ranging from the optical layer to the data-link layer. More specifically, in this deliverable, a passive monitor probe at the data-link layer is described.

5.1 Optical switching technologies

5.1.1 Low-cost MD-ROADM

A multi-degree ROADM prototype based on a commercial component (Lumentum TrueFlex® Twin High Port Count WSS,) has been developed within METRO-HAUL project. The most relevant features of this device are the reduced number of WSSs per degree, which makes it significantly low cost, and the programmability using a NETCONF agent and of an OpenROADM compliant YANG model, which should facilitate its possible future interoperability with other vendors devices in a fully disaggregated environment.

The device can be configured as a three or two degrees ROADM, with one or two add-drop modules respectively. Taking into account METRO-HAUL reference topologies defined in deliverable D2.3 [5], it could then be useful both in the horseshoe topology aggregation areas of metro networks, and in small metropolitan core areas (10-20km of network diameter, considering Table 5 of D2.3 [5]).

A description of the device architecture, already presented in the document describing the METRO-HAUL internal Milestone M3.4, is here reported for completeness.

Lumentum TrueFlex® Twin High Port Count WSS is provided on an evaluation board and is configurable through an RS-232 interface; it contains two identical independent modules, both with 21 mono-directional optical ports. Each of the two modules can be programmed to create one or more spectral windows (i.e. media channels) within the C-band, between the so-called *common* port (*c*) and each of the other 20 (*p1-p20*) ports (Figure 5).

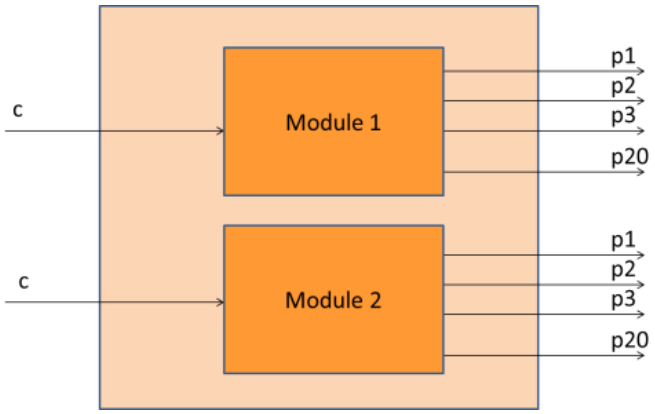

Figure 5: Twin 1 x20 WSS functional scheme

Several media channels, not necessarily contiguous, can be configured at the same time, each characterized by a central frequency, a spectral width and an attenuation (in the range from 0 to 25 dB), with the constraint that, for each module, spectral windows cannot overlap. Therefore, the common port cannot be connected with more than one port using the same spectrum portion. The component supports both fixed and flexible grid modes of operation.

Due to a peculiar "directivity" behaviour (reported in the device documentation and experimentally verified), when a media channel is configured between the common port and an add-drop port, the same spectral window is also created between several other pairs of ports. In particular (referring to the ports numbering shown in Fig. 1), when a media channel is configured between port ***c*** and a given port ***px***, an identical media channel is automatically arranged between the pairs of ports ***py*** and ***pz***, where *x*, *y* and *z* follow this basic rule:

$$y + z = x \qquad (1)$$

Leveraging this "directivity" behaviour, the component was suitably wired and configured to use it as a complete bidirectional non-blocking ROADM, with native colourless and directionless capabilities. In particular, connecting the device ports as shown in Figure 6, and adding one

mux/demux module (a commercial 40 channels 100GHz fixed grid), a 3-degrees directionless and colored ROADM with an internal switch-and-select architecture is achieved.

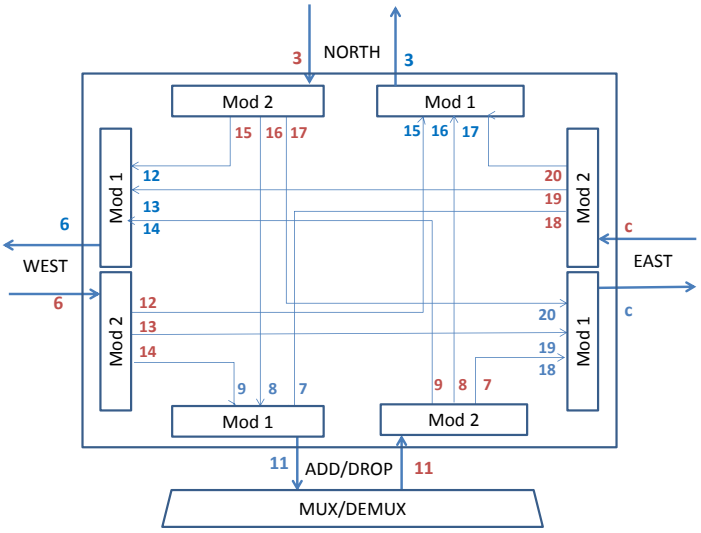

Figure 6: ROADM with switch-and-select architecture

This solution allows to use disjointed spectrum portions in the transit directions between different line interfaces; moreover, the same portion of the spectrum in transit between a pair of line interfaces can be used to carry traffic from the third line interface to the local ADD-DROP port, thus obtaining a non-blocking architecture.

As an example, referring to Figure 6, if x=18, two identical media channels could be created between ADD-DROP (y=11, z=7) and EAST degree and between NORTH (y=3, z=15) and WEST (y=6, z=12) degrees. This behavior, coded in Eq. (1), must be carefully addressed at network control level in a meshed topology to avoid unwanted detrimental optical loops.

In addition to the components shown in Figure 6, optical amplifiers (booster and/or preamplifiers) could be needed, to recover both the attenuation of fiber links in the network and the insertion loss of WSS modules. However, it should be noted that for this prototype, the measured insertion loss between ROADM lines is around 10 dB, which is pretty in-line with the figures of a traditional switch-and-select ROADM built with interconnected discrete WSS modules (typically eight WSS modules for a 3-degrees ROADM with directionless and coloured add-drop). So, even if the number of required optical amplifiers may be the same, this implementation drastically reduces the required number of WSS modules (by a factor of four concerning the traditional layout of 3-degrees ROADM node), saving CapEx.

This solution could be easily modified to exploit other suitable applications in metro/access areas. For example, replacing the mux/demux with a simple coupler/splitter (for instance, 1:8) would add the colorless feature to this ROADM (using coherent interfaces). Another interesting application for the metro area is the 2-degrees ROADM installed in ring topologies, to collect traffic from several sites to a hub node (e.g. in backhauling applications). Converting one of the three line side (e.g. the NORTH one) to a second add/drop connected to another mux/demux, the “directivity” behavior would allow to create the same media channel simultaneously between, for example, one mux/demux and the WEST line and between the other mux/demux and the EAST line, to support dual-homing optical protection scheme, as shown in Figure 7.

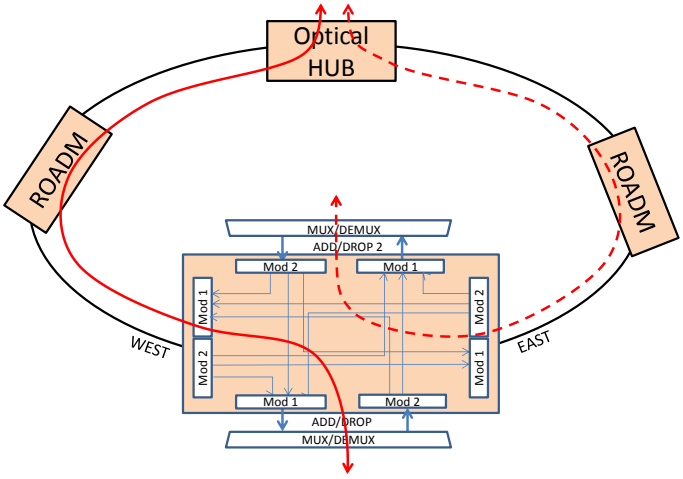

Figure 7: 2-degrees ROADM in a ring topology with dual-homing protection

Some specific KPIs have been defined for this device, and are reported in the following tables.

KPI	**Connection setup time**
Context/ Description	This KPI regards the measurement of the time needed to set up an express link (bidirectional connection between two line ports of the ROADM), or an Add-Drop link (bidirectional connection between a line port and an add-drop port of the ROADM).
Target	The target expected value is in the range of seconds
Assessment	The KPI is evaluated measuring the time between the connection request sent by the SDN controller and the acknowledgement of connection successfully set up received by the same controller. It is part of the general effort made in METRO-HAUL to automate and speed up network services configuration.
Relationship to project KPIs	This KPI concurs to the performance of METRO-HAUL general KPIs MH1 (optical PtP connection set-up time), MH2 (METRO-HAUL E2E PtP connection set-up time), and MH3 (Set-up time of a network service slice across METRO-HAUL)

KPI	**Insertion loss**
Context/ Description	This KPI regards the measurement of the insertion loss across a connection between two line ports or a line and an add-drop port of the ROADM. The KPI aims to verify that, despite the low cost of the component, the performance is in line with what would be expected by a commercial ROADM
Target	The target expected value is around 10 dB
Assessment	The KPI can be measured by setting up a connection between two ports, connecting the input port at one side of the connection to a CW laser source, send a signal with a known input power at different wavelengths within the C band and measure the received power at the output port on the other side of the connection with an Optical Spectrum Analyser.
Relationship to project KPIs	

KPI	**Number of WSS per single Degree or Add-Drop module**
Context/ Description	This KPI is defined as the number of WSS inside the ROADM divided by the number of Degrees and Add-Drop modules. It is related to the general effort made in METRO-HAUL to reduce the cost of hardware in the network.

Target	The target expected value is less then what would be expected by a commercial ROADM (thus less than two WSS per single Degree or Add-Drop module)
Assessment	The KPI can be measured by analyzing the ROADM architecture: 2 WSSs are used in a three Degrees and one Add-Drop module configuration, or in a two Degrees and two Add-Drop modules configuration, so the number of WSS per Degree or Add-Drop module is 0.5.
Relationship to project KPIs	This KPI corresponds to METRO-HAUL general KPI MH7 (new optical components/systems), considering, in particular, the cost and the footprint of an optical component/system; it also concurs to the performance of KPI MH8 (CapEx reduction)

KPI	**Programmability**
Context/ Description	This KPI is related to the availability of a YANG model compliant to OpenROADM v2.2 Device Model, and a NETCONF agent integrated into ONOS SDN controller for the control and management of the ROADM. It is part of the general effort made in METRO-HAUL to implement an open and SDN controllable network.
Target	The target expected result is to be able to set up and tear down bidirectional connections between two line ports or one line port and one add-drop port of the ROADM and to be able to retrieve information from the device about inventory data and the operational state of the ports
Assessment	The KPI can be measured by actually perform some of the above operations from ONOS controller
Relationship to project KPIs	

5.1.2 Semi-filterless solutions

One flavor of semi-filterless solutions in optical networks with coherent transmission would be to add wavelength blockers (WB) in the add-drop nodes instead of using fully functional WSS [6]. Another flavor would be to partially filter the dropped channels [7]. Both approaches target different issues in the network: In a pure drop and waste architecture, wavelengths are lost after they have been dropped by splitters since the signal which is already dropped continues in the network. If this wavelength can be blocked, this will enable its re-use. If for example, a horseshoe architecture is considered, where two terminals (MCENs) are connected with 5 nodes in between. At each node, 8 channels should be dropped, and 8 additional channels should be added. In the case of pure filterless architecture, 88 channels are needed for this operation, while in the case of wavelength blockers in each node, 48 channels are sufficient. The additional filters in the drop paths address the limited output power that falls onto a single receiver if a high order splitter is used – since all channels reach the receiver photo diodes, the total power has to stay below the maximum allowed input power, although the neighboring channels might be considered as "noise".

Based on the architecture above, a certain amount of power is needed for the useful signal to be detected. As an example, commercial receivers might specify an input power between 0 and -17 dBm for a given OSNR. In that case, at maximum a 1:50 splitter can be used without additional losses in the drop path, to ensure a maximum input of 0 dBm will keeping the power for one channel at -17 dBm. Additional filters would reduce the unwanted power, even group filters for only part of the spectrum will introduce some relief on these constraints.

ADVA focusses on the design of systems with coherent transmission and wavelength blockers in the nodes, and at this point does not consider any filters in the drop path. Some theoretical considerations on the system performance have been performed and supported by joint measurements together with Fraunhofer HHI [8]. The results are presented in the following.

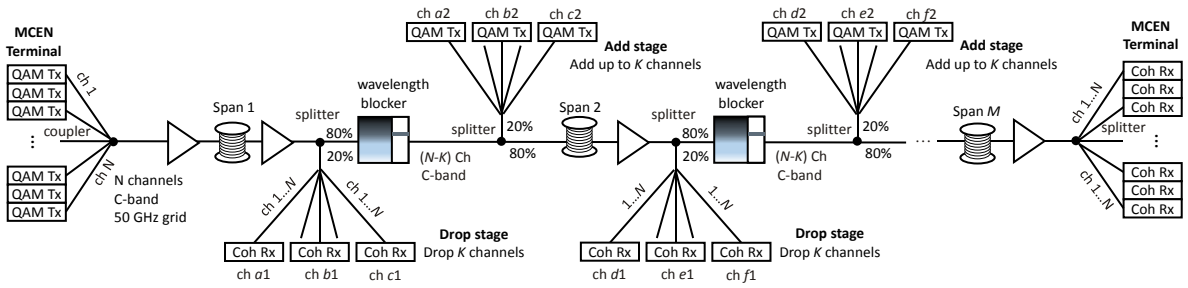

Figure 8: Structure of the semi-filterless network concept with wavelength blockers. Up to N channels can be transmitted, at each Add/Drop stage K channels are dropped and added (QAM Tx: quadrature amplitude modulation transmitter, Coh Rx: coherent receiver)

The structure of the considered network is shown in Figure 8. At the MCEN terminal node, *N* channels (e.g. 96 50-GHz spaced channels in the C-band) are coupled together with couplers, showing ~ 20 dB loss. The coupler is followed by an Erbium doped fiber amplifier (EDFA) as a booster and the first fiber span. After the span, an additional EDFA is used as a pre-amplifier for the dropped channels and as a booster for the continuing channels. A further EDFA could be added for very long spans but is not necessary for most urban metro distances. A fraction R_{drop} = 20% of the signal power is coupled out at the drop stage, while 80 % continues to the WB. This is the splitting ratio for the devices used in the experiments and should be optimized according to the requirements of the considered network. The 20 % output is followed by a 1x*K* splitter, to drop *K* channels, which are detected by *K* coherent receivers. These channels are blocked in the express path by the WB. In addition to the blocking

functionality, the power of each remaining channel is measured and equalized. This enables the use of cheaper EDFAs without flattening filters. The *K* free wavelength slots can be filled with new channels, which are combined by a *K*x1 coupler and inserted into the spectrum by another 20/80 coupler. The resulting signal is transmitted over the next span. At the end of the horseshoe, i. e. at the second MCEN node, the remaining channels are split and fed to coherent receivers.

As already stated, the limitations in the drop path are determined by the dynamic range of the coherent receivers, i.e. the range from a minimum power $P_{min,Rx}$ per channel (at low OSNR) that is required to detect an error-free signal to a maximum power $P_{max,Rx}$ accepted by a receiver (Rx), which results from the total power of all channels. Since the output power P_{amp} of cost-effective conventional EDFAs is limited (typically to ~ 20 dBm), the drop ratio has to be $R_{drop} < (P_{max,Rx} \cdot K)/(P_{amp})$ and $R_{drop} > (P_{min,Rx} \cdot K \cdot N)/P_{amp}$ in an *N* channel system. This assumes that for each *K* a dedicated 1x*K* splitter is used, and no additional attenuation is present. Assuming P_{amp}= 20 dBm, a 96-channel system, where 8 channels should be dropped, and a dynamic range between $P_{Rx,max}$ = +3 dBm and $P_{Rx,min}$ = -23 dBm for the Rx, the ratio should be 3.8 %<R_{drop}<16 %. For the add ratio, R_{add}, holds that the input power of each added channel needs to be equal to the channels passing through the wavelength blocker, i.e.

$$\frac{P_{Tx}}{K} \cdot R_{add} = \frac{P_{amp}(1-R_{drop})}{a_{WB} \cdot N}(1 - R_{add}), \text{ and therefore}$$

$$R_{add} = \frac{P_{amp}(1-R_{drop})}{\frac{P_{Tx}}{k} a_{WB} N + P_{amp}(1-R_{drop})}. \qquad (1)$$

Here, P_{Tx} is the output power of the transmitter (Tx), which can be in the ideal case be adjusted in a range of some dB and a_{WB} is the insertion loss of the WB. For the example above, and P_{Tx} = 3 dBm, a_{WB} =12 (8 dB raw loss of WB +4 dB for compensation of +-2 dB of channel power variations), the minimum drop ratio leads to an add ratio of R_{add} = 20 % and the maximum drop ratio leads to an add ratio of 17.9 %. In this case the loss of the node with minimum add ratio would be either 13.2 dB (R_{drop} = 3.8 %) or 13.7 dB (R_{drop}=16 %). A higher add ratio would increase the loss. For a fiber loss of 0.25 dB/km and a variable gain of the EDFA of up to 30 dB, the maximum span length would be 65.2 km (R_{drop}=16 %), which lies well in the span range of a metro network.

Another important parameter in the system is the OSNR. In some state-of-the-art coherent transponders, additional optical amplifiers are integrated at the Tx. Besides increasing $P_{Tx,max}$, they also add broadband noise to the signal if they do not use a tuneable amplified spontaneous emission (ASE) filter after the amplifier. If, e.g. the OSNR of the Tx is 40 dB, after coupling 96 channels with the same Tx, the OSNR is then reduced to 20.2 dB. The OSNR reduction along the transmission line can be calculated from the power levels and the noise figure of the EDFAs (see, e.g. [9], chapter 4.2.3), i.e. the OSNR after the *M*th span would be

$$OSNR_{M,EDFA} = \frac{OSNR_{TX,N} P_{in,EDFA}}{P_{in,EDFA} + Mhf_c B_{ref} F_N OSNR_{TX,N}}. \qquad (2)$$

Here, $OSNR_{Tx,N}$ is the OSNR per channel after coupling together *N* channels, $P_{in,EDFA}$ the input power to the EDFA after the span, *h* Planck's constant, f_C the frequency of the signal carrier and B_{ref}, the reference bandwidth in Hz for measuring the OSNR, per definition 0.1 nm in wavelength, which corresponds to ~ 12.5 GHz. F_n is the noise figure of the EDFA. If in each node unfiltered channels are added, additional noise overlaps the noise from the transmission. If *K* channels are added, the $OSNR_{add,K}$ for each channel would be the OSNR of the transmitter itself divided by the numbers of

added channels. E.g. if the OSNR of the Tx is 40 dB, after coupling together 8 channels, this would be reduced to 31 dB. The OSNR after adding channels can be calculated by

$$OSNR_{Add} = \frac{OSNR_{through} OSNR_{add,K}}{OSNR_{through} + OSNR_{add,K}}, \quad (3)$$

Where $OSNR_{through}$ are the channels which are passing through the node. Now, combining this, the OSNR after the Mth node with K channels added in each node would be

$$OSNR_{M,E+A} = \frac{P_{in,EDFA}}{Mhf_c B_{ref} F_N + P_{in,EDFA}\left(\frac{M}{OSNR_{add,K}} + \frac{1}{OSNR_{TX,N}}\right)}. \quad (4)$$

Since the strongest OSNR degradation occurs at the MCEN, one might think of using a multiplexer filter there and only have a filterless coupling in the AMENs. All the calculations and assumptions here were made for fixed power and gain values with variations. In further investigations, gain ripples and power variations of up to 3 dB should be taken into account.

The experimental setup corresponded to the structure shown in Figure 8. Two commercially available coherent transponders (see D18 in other Deliverables/Milestones, e.g. MS3.4), capable of terminating 200 Gbit/s DP-16QAM or 100 Gbit/s DP-QPSK signals were used as channels under test (CUTs). Forward error correction was included, leading to a symbol rate of ~ 34 GBaud. The pre-FEC BER was calculated from the corrected errors. Although the FEC for the transponders here was higher than 2e-2, we considered 2e-2 as an FEC limit, since this commonly used for soft-decision FEC. The 88 interferer channels (loaders) were shaped out of an ASE noise source, using two EDFAs and a subsequent Finisar waveshaper as in [10]. The spectrum ranged from 191.55 THz to 196 THz, and the CUTs are put at the 5th and the 85th channel slot (191.75 THz and 195.8 THz respectively) to determine differences due to EDFA noise tilt. All transmit channels were added at the MCEN terminal node on the left. Between the spans, couplers and WBs with R_{drop} = 20 % and R_{add} = 20 %, as shown in Figure 8, were inserted. The WBs had a loss of 12 dB. According to Eq. (1), in this setup, R_{add}=20 % would be optimum if 9 channels are added and $P_{TX,max}$= 3 dBm. The investigated topology consisted of 4×40 km standard single-mode fiber spans (SSMF). The 40-km spans had a loss of 10 dB each. Although the power of the channels can be equalized by the WB ROADMs, the noise of the EDFAs shows a small tilt, leading to a tilted OSNR as well. Longer wavelengths (and thus smaller frequencies, e.g. channel 5) have a higher OSNR than shorter wavelengths (e.g. channel 85).

Since in this setup R_{add} and R_{drop} are fixed, the experiment focused on the influence of transmit OSNR. The OSNR $OSNR_{TX,N}$ after combining all channels was varied. If a pure filterless coupling is used, the OSNR of one channel would be 19.5 dB higher than this value (90 channels ~ 19.5 dB). The OSNR and the bit error ratio (BER) for each CUT were determined at each drop stage and after the last EDFA. The loss from the drop coupler to the Rx was 13 dB, which is equivalent to dropping up to 20 channels. The total input power to the Rx was 2.5 dBm, i.e., 17 dBm per channel. Figure 9 shows the evolution of the OSNR over the 4 spans. The 40-km spans degrade the OSNR significantly only if the Tx OSNR is high – for values less than 20 dB the decrease is quite slow. The values for $OSNR_{TX,N}$ = 30 dB at channel 5 and $OSNR_{TX,N}$ = 27.1dB at channel 85 were measured simultaneously as were the values for 22.4 dB and 19.6 dB, and 20.3 dB and 17.7 dB, respectively. The BER values corresponding to the OSNRs shown in Figure 9 are plotted in Figure 10 for DP-QPSK and DP-16QAM. It can be seen that the Tx OSNR is a critical parameter, and 22 dB Tx OSNR would be needed to bridge all spans with full capacity, if the BER should stay below 2e-2. Considering a 90 channel terminal in which each transmitter adds broadband noise, this requires an OSNR of at least 42 to 45 dB at the transmitter, if a noise tilt of 3 dB is present. However, referring to (4), also the noise from added channels needs to be taken into account, which was not done during the experiment.

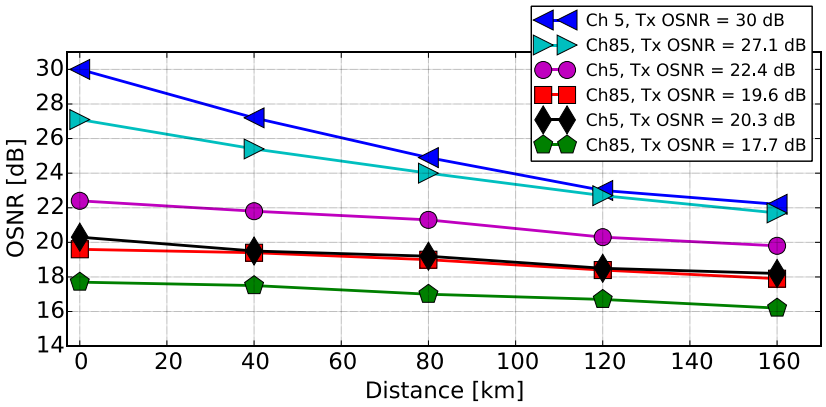

Figure 9: OSNR vs. distance for different Tx OSNR

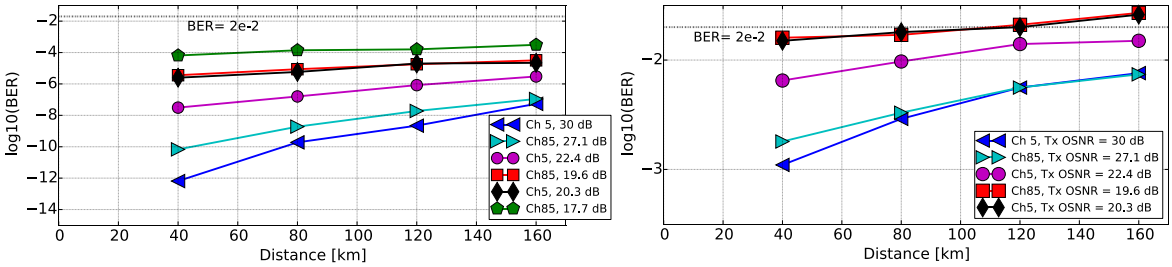

Figure 10: Left: BER vs. distance for DP-QPSK and OSNR of Figure 9. Right: BER vs. distance for DP-16QAM and OSNR measured in Figure 9. 30/27.1 dB and 22.4/19.6 dB are measured simultaneously, for 20.3 dB only channel 5 could be detected

The study together of ADVA and Fraunhofer HHI shows that the add and drop ratios for the splitters have to be chosen carefully, dependent on system parameters. The transmitter OSNR is a critical parameter if no ASE filters are used in the add paths.

KPI	**Connection setup time**
Context/ Description	This KPI regards the measurement of the time needed to set up an express link (bidirectional connection between two line ports of the ROADM), or an Add-Drop link (bidirectional connection between a line port and a client port of the ROADM). It is part of the general effort made in METRO-HAUL to automate and speed up network services configuration.
Target	The target expected value is in the range of seconds.
Assessment	The KPI is evaluated measuring the time between the connection request sent by the SDN controller and the acknowledgement of connection successfully set up received by the same controller .
Relationship to project KPIs	This KPI concurs to the evaluation of project KPI MH1: Optical PtP connection setup time.

KPI	**Capacity of network compared to filterless architecture**
Context/ Description	This KPI compares the total possible capacity of the network which can be achieved by using wavelength blockers instead of pure splitter based architectures.
Target	The target is to enable the use and re-use of all 96 wavelengths that are available in the C-band with 50-GHz channel grid.
Assessment	Simple calculation

Relationship to project KPIs	This KPI concurs to KPI MH6: Capacity of METRO-HAUL infrastructure

KPI	**Capex reduction compared fully functional WSS**
Context/ Description	This KPI compares the actual capital expenditure if a wavelength blocker ROADM solution in a ring or horseshoe topology is used instead of a fully functional WSS.
Target	The target is to at least reduce the capex by half.
Assessment	
Relationship to project KPIs	This KPI concurs to project KPI MH8: CapEx reduction.

5.1.3 Innovative filtered photonic integrated solution

5.1.3.1 An innovative photonic integrated optical switching solution for add/drop module of ROADM

In WDM optical transport networks all-optical nodes are currently available and are based on multi-directional-switching ROADM's (Reconfigurable Add and Drop Multiplexers) capable of rerouting traffic on every single wavelength directly in the optical domain [11][12].

Concerning ROADM nodes, operators are expecting an increasing level of flexibility to allow adding or dropping of any set of wavelengths from any link direction to any add/drop access port [13].

The dynamic colourless, directionless and contentionless add/drop access give the operator the possibility to optimise the resources utilisation, eliminate manual intervention, support re-routing functions in case of faults in a cost-effective way.

Wavelength switching can be done directly in the optical domain, reducing the number of optoelectrical conversions in the network and aggregating or disaggregating traffic carried on multiple wavelengths. Optical switching can be obtained by using optical fibre switches and Wavelength Selective Switches (WSS) [14].

Leveraging on Silicon Photonics integration, it is possible to design a simple ROADM architecture, based on a scalable matrix of optical switching elements, allowing for lower power consumption, lower footprint, lower cost and higher capacity concerning state of the art [15].

The envisaged ROADM should be all optical and designed to efficiently reconfigure the optical path of each WDM channel coming from any direction towards any direction add and drop channels from and to any direction. In integrated and scalable switching matrix architectures it is desirable, to reduce cost, footprint and power consumption, to perform bidirectional switching for dropping and adding of channels at the same wavelength by the same switching element.

Furthermore, the photonic integrated switch allows for transparent interconnection of different equipment vendors transceivers and transponders with tunable wavelength and baud rate. The solution is based on silicon photonics and realised within EU-FP7 IRIS project activities, enhanced in METRO-HAUL by TEI and CNIT with control functions in the framework of the network disaggregation scenario, i.e. the White box concept.

The solution aims to be significant progress beyond state of the art for next-generation cost-effective, energy-efficient, programmable and elastic optical metro networks, with its ambition described across three primary dimensions.

- A novel architecture for interfacing between 5G backhaul and the multi-Tbit/s core;
- New optical metro-network technologies;
- Flexible control, management & orchestration plane.

Figure 11 reports a possible network architecture to be realized in the project, where a white box based on a silicon photonics chip properly drives and routes wavelength channels from and to different network directions, transceivers and transponders. The innovative photonic integrated optical switching solution is modelled according to the Open ROADM YANG model.

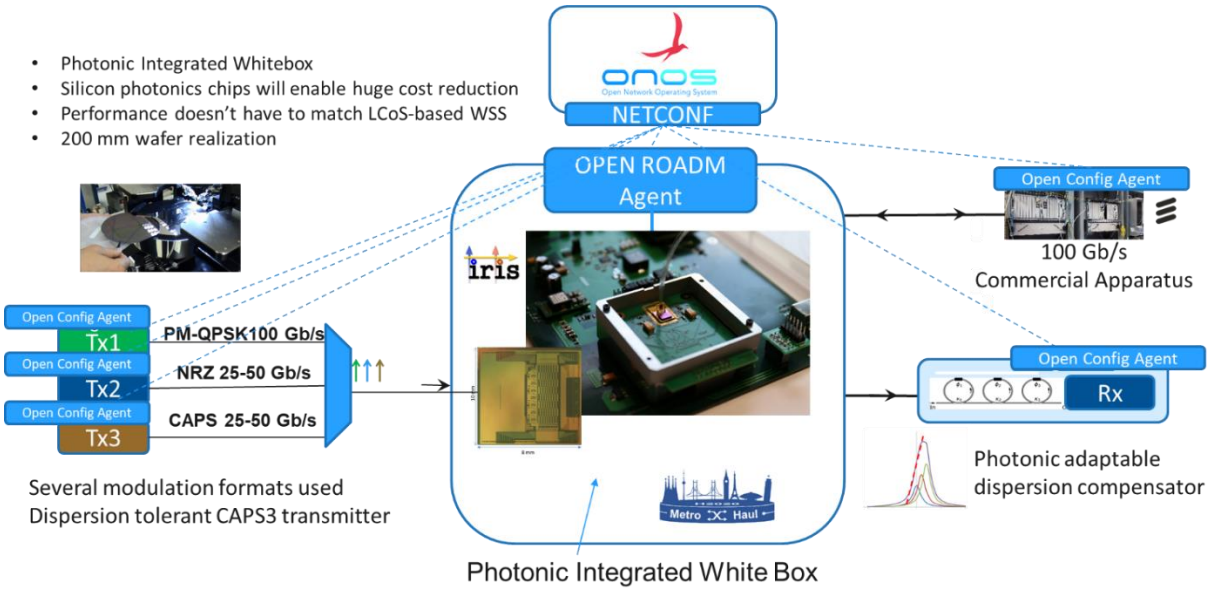

Figure 11: An innovative photonic integrated optical switching solution for add/drop module of Open ROADM. A silicon photonics switch to routes traffic transparently in the optical domain and operates as a white box in a disaggregated network

The switch matrix used as a whitebox

IRIS White box consists of 2 boards where the 2 packaged optical wavelength switch modules have been installed on their electronic board developed by Ericsson (see Figure 12). Each packaged module can be interfaced through an electronic board and optical input/output frontend with a dedicated fan in/out.

Thanks to these electronic and optical ports it is possible to connect several transmission lines for wavelength routing and accordingly to measure different system parameters: optical power, number of routed channels, board temperature, insertion losses and others. Most of the monitoring is performed through photodiodes distributed on the White box board sequentially polled in such a way that optimization of the entire switch performance can be first evaluated and then executed by adequately tuning the board temperature, the microring resonances, and other parameters. Each heater is identified by a number "#" which can be set automatically through an agent. A lookup table here reported permits to check the value assigned to a specific heater allowing the agent to perform any optimization action in the white box. For the map of the lookup table, please refer to Figure 12. Concerning the signal pass-band, the requirement was based on the support of both intensity modulation-direct detection transmission at 10 and 25 Gb/s and coherent QPSK transmission at 100 Gb/s.

The optimization action can be automatized to perform research on the values that optimize the setting of the chip.

The photonic integrated optical switch is controlled as a white box ROADM element through custom-built software agents based on NETCONF/YANG. A NETCONF server implementing OpenROADM YANG models has been defined as the northbound interface.

Within METRO-HAUL a specific driver has been developed in python to communicate with the NETCONF agent and to control the underlying hardware, leveraging on USB communication and custom syntax. In particular, the python driver allows both the setup and the monitoring of a cross-connection with the granularity of all the involved subcomponents (i.e., ingress, middle and egress

points). Figure 12 (a) summarizes the key parameters to perform such actions. The table presents in red the tuple (id, value) of the heaters to be configured for setting up a cross connection. While, labelled in blue, photo-detector (with related id) to check power level are included.

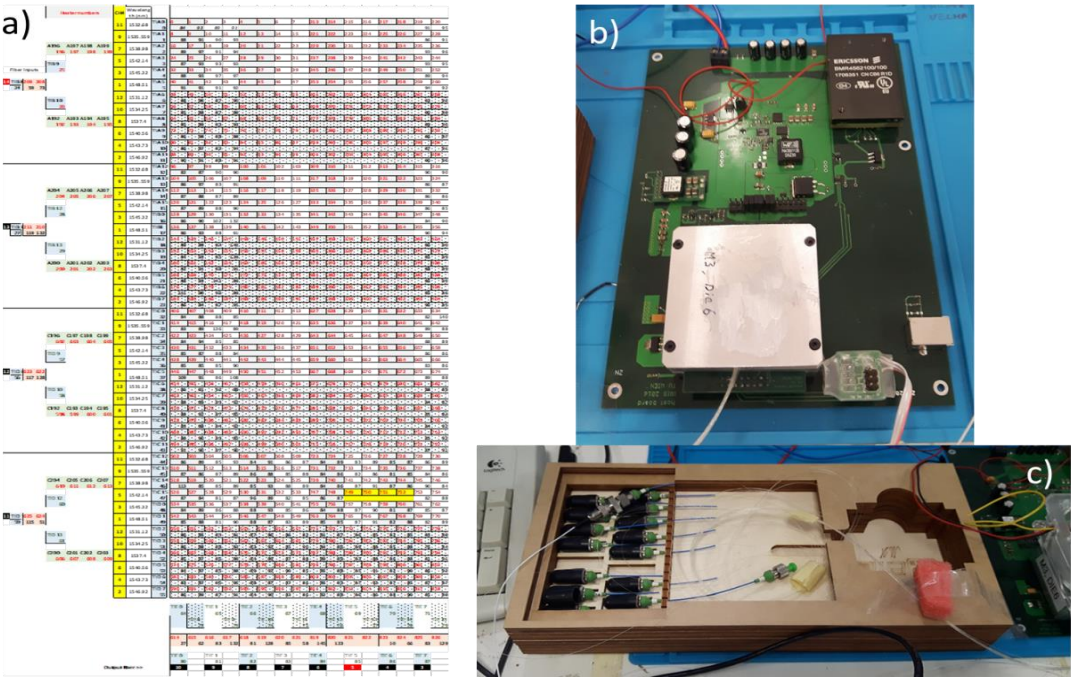

Figure 12: a) The lookup table of reference to be used by the OpenROADM agent to drive the White box; b) one single IRIS board mounted on Ericsson Electronic Board; c) the relevant fanout of the optical switch module

5.1.3.2 A multi-purpose loss-less photonic integrated wavelength selective switch (2 to N degrees)

The TUe based metro access node, and overall metro network operation are shown in the middle part of Figure 13. We implemented two variants of metro access nodes: 1) connected both with antennas and edge computing nodes named as “Edge Node”, and 2) which is only connected with antenna access named as a “Normal Node”. Each node consists of low-cost optical gates based FOADM and an optical-electrical interface.

The metro network operates in a time-slotted way and under the control of an out-of-band supervisory channel (red line in the schematic below), which fast controls the nodes by carrying the destination information of the data channels in each time slot.

The control module of the nodes reads the destination information and controls the fast reconfigurable add-drop multiplexer to decide which WDM channels should be dropped and thus to which wavelengths the access data traffic will be added. The metro access network is connected with the metro core network by a gateway node.

The gateway node works as an edge node in the metro access network, and it also works as an interface between metro access and metro core. It is capable of aggregation and forwards the traffics that need to be sent to the centralized datacenter (DC), and distribution of traffic between metro access nodes.

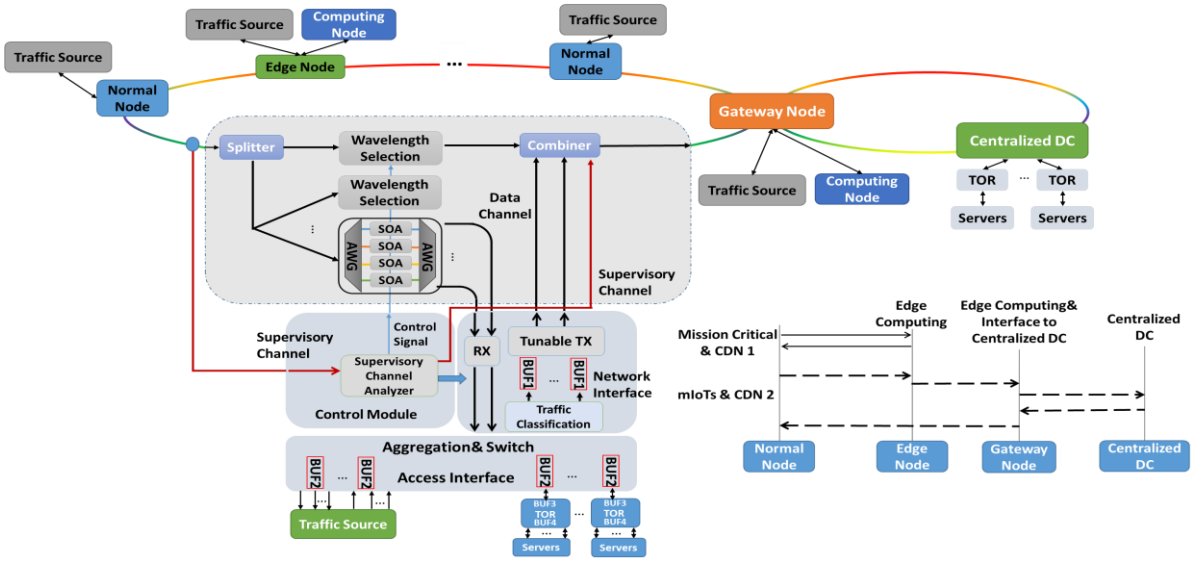

Figure 13: Schematic of Tue node-based metro access node as well as an illustration of the metro network operation

The fast reconfigurable add-drop multiplexer module consists of a semiconductor optical amplifier (SOA) gates-based wavelength selectors to achieve drop and continue of any wavelength channel. Also, the SOA gates in the wavelength selector modules allow fast (nanoseconds) switching of optical traffic and per channel power equalization. The schematic of the TUe node supporting fast waveband switching is shown in Figure 13. To speed-up the switching time and the power equalization operation, the node is equipped with a fast in-band optical label processing for each channel. The optical label provides information on the node destination; therefore, no specific wavelength has to be assigned to individual add/drop port. This results in better utilization of the wavelength resources, which can be flexibly employed for increasing the network dynamicity and capacity. Each optical channel contains one/multiple wavelengths which can be tailored according to the desired channel capacity.

At each node, WDM channels are first demultiplexed and then divided by a 1x2 coupler into a drop arm and continue arm. In the continue arm, the traffic is fed into the SOA based optical gate controlled by the FPGA based controller. The SOA technology guarantees nanosecond switching and adjustable optical gain for power equalization operation. In the drop arm, a Label Extractor (LE) separates the in-band label from the payload by using a narrow-band fiber brag grating (FBG). The power is split into two parts, the first one is used for real-time monitoring to facilitate rapid channel equalization and the other is processed on-the-fly and in asynchronous fashion by the Label Processor (LP) to recover the label information. According to this, the FPGA determines if the packet has to be dropped/forwarded or dropped and forwarded (for multicasting) by controlling the SOAs in both arms. Note that all labels are processed in parallel, which allows the controller to have the full vision of available slots and reconfigure the node in nanoseconds scale.

The optical-electrical interface consists of an access interface, network interface, and control module. The access interface aggregates and switches the incoming 5G data traffic. The 5G data traffic is first analyzed by the destination analyzer and classified based on the same destination and application (forming multiple slicing) and aggregated in buffer cells in the network interface, ready to be transmitted as soon as a time slot in one of the wavelength channels is available. Tunable transmitters inside the network interface are employed to transmit at any available wavelengths to fully utilize the wavelength resource in a statistical multiplexing fashion and solve network

contention. For each time slot, if N wavelength channels are available for adding traffic, then the free channels will be allocated to the slices by the proportion of their required bandwidth. Note that the bandwidth resource allocation of slices is also related to their requirements on reliability.

The control module of the node is responsible for enabling SOA gates of the wavelength blockers and the tunable filters based on the processed information carried by the supervisory channel. Moreover, it also monitors the free wavelengths and sets the wavelength of the fast tunable transmitters to add traffic into the network without collision. If there is no free wavelength, the packet remains stored in the electronic buffer. Finally, the control module modifies the supervisory channel according to the data channel dropped and added before sending it out to the next node.

5.1.4 Filterless solutions

The last and simplest class of optical switching technologies, filterless metro optical networks (FMN), have the following properties in common:

1. O-NEs in the WDM Analogue transport layer (A-WDM) that implements a pure filterless architecture together with simple line terminals (degree 1 O-NEs)
2. O-NEs in the Digital to WDM adaption layer (DtoWDM) with low-cost coherent solutions optimized for short reach, e.g., less than 200 km
3. a design optimized for peripheral nodes interconnection to a central MCEN node with straight-line or horseshoe topologies (see Figure 14), which handle few optical connections with limited requirements on reconfiguration
4. use of small form factor transceivers
5. possibility for the low-cost and seamless upgrade of existing C-band networks, including the L-band.

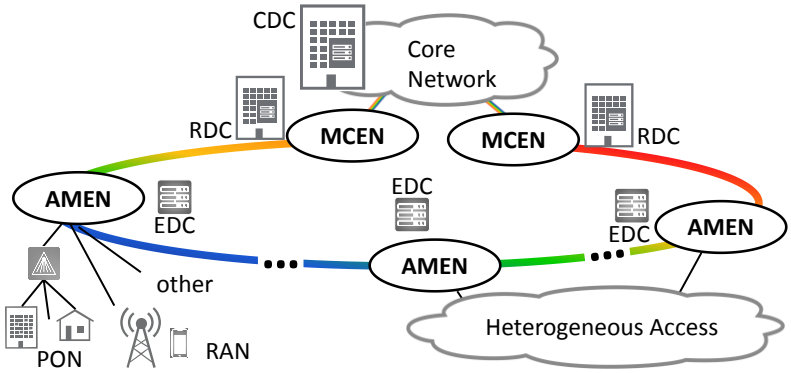

Figure 14: Metro horseshoe topology. (CDC: central data centre, RDC: regional data centre, EDC: edge data centre, MCEN: metro core edge node, AMEN: access metro edge node) [8]

For experimental validation of filterless concepts, an open filterless testbed infrastructure was setup at HHI, providing various concepts such as the drop path of the Drop & Waste network topology including different modulation formats and channel spacing's in the C+L-band. Figure 15 shows an exemplary structure of the network as a build for experimental validation in the laboratory. At the MCEN terminal node (Tx stage), *N* channels are coupled together with passive optical couplers (coupling of, e.g. *N* = 188 channels in the C- and L-band shows approximately 23 dB loss). The coupler is followed by an Erbium doped fibre amplifier (EDFA) as a booster and the first fibre span with variable lengths of 20 km, 40 km, 60 km and up to 80 km. After each span, an additional EDFA is used as a pre-amplifier for the dropped channels. This pattern is repeated for subsequent drop stages and fibre spans.

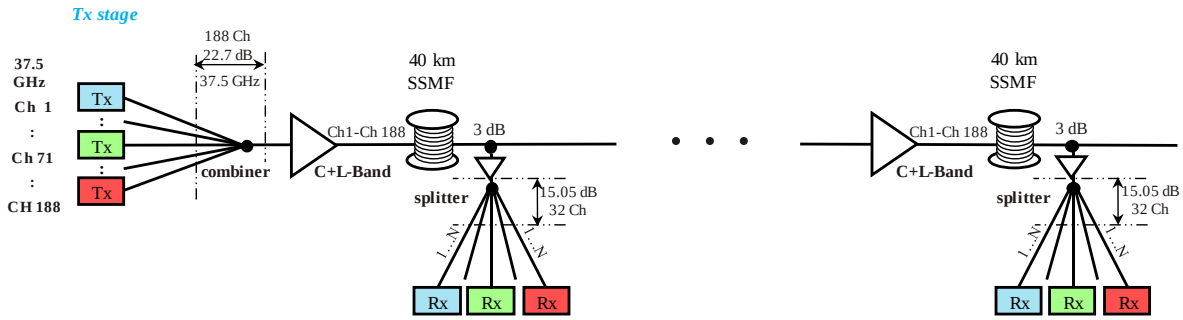

Figure 15: Concept for a testbed for the downstream of a dual fibre network and drop path of a drop-and-waste network

First evaluations using such an FMN testbed were presented in deliverable D3.1 and [16]. There, upgrade scenarios from a C-band only operation to a C- and L-band operation focused on the use of L-band transmission for the short reach links (few hops) in the FMN. C-band channels facing lower fibre loss and transceiver equipment with higher sensitivity were suggested to be used for long reach links (multiple hops).

To further decrease the cost of L-band upgrades, the possibility of EDFA-free transmission in the L-band was investigated in [17]. The network architecture considered in [17] is outlined in Figure 14. We assume a chain/horseshoe topology where a set of tributary nodes communicate directly with a hub node through the C-band. In legacy MANs, such connectivity is typically hardwired, with the C-band express architecture comprising a fixed optical add/drop multiplexer (FOADM) structure, with dedicated frequencies assigned for add/drop channels at each node. New latency-sensitive services, such the ones demonstrated within METRO-HAUL, impose that data processing must be pushed towards the edge. While ideally, each tributary node (central office) could provide co-localized data-center (DC) capabilities, constraints on the available footprint at each site may preclude this. In this case, the traffic requirements for low-latency services evolve towards more direct connectivity between legacy tributary nodes (i.e., to the nearest DC, not necessarily at the hub).

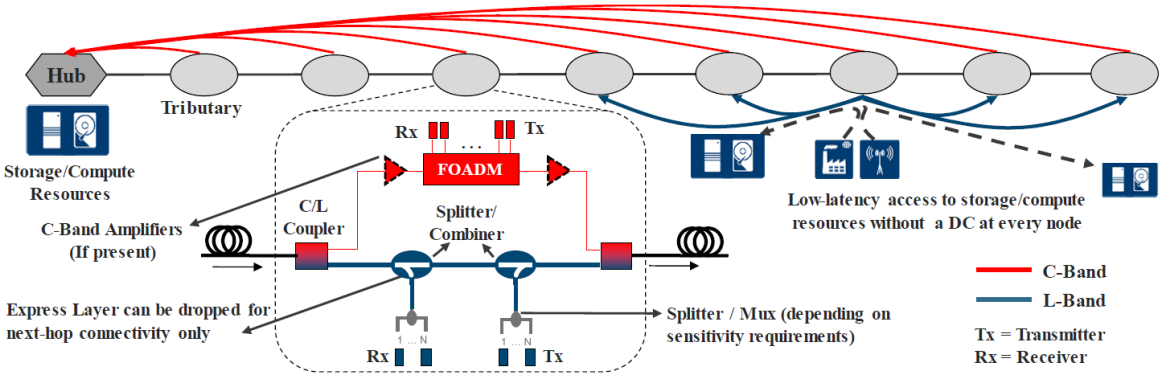

Figure 16: Dual-band MAN with filtered C-band and filterless unamplified L-band

Supporting these requirements may be achieved by upgrading all tributary nodes to reconfigurable OADMs (ROADMs), adding flexibility at the expense of a costlier infrastructure, and subtracting capacity from the available C-band towards the core.

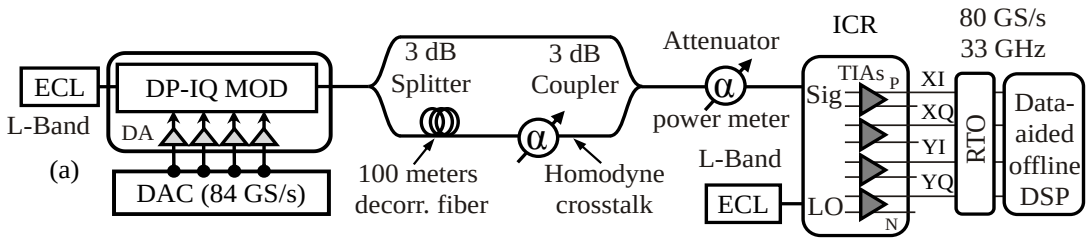

Figure 17: Experimental setup for the estimation of the sensitivity and cross-talk tolerance of the Rx

Alternatively, extra capacity and connectivity may be unlocked by resorting to transmission in the L-band, with minimum disruption to current network operation, by introducing C/L couplers (splitters) after (before) C-band amplifiers. Given this functional split enabling both bands to operate independently, there is also an opportunity to use a differentiated L-band express architecture to target services with low latency edge computing requirements. As Figure 16 illustrates, we evaluate a very low-cost L-band system without amplification and employing a filterless express architecture,

targeted at short transparent connections between tributary nodes. The absence of amplification in the L-band reduces the reach of deployable lightpaths, but also partially offsets the frequency reuse limitations of a traditional filterless network, since interfering signals in the same frequency are naturally attenuated upstream. Depending on the performance limits of such a system, it is possible to consolidate the number of nodes requiring DC resources, while still providing low-latency access to nearby compute resources for every node and without compromising the achievable capacity in the C-band. In [17], we evaluated the design trade-offs and expectable capacity of the L-band system, based on experimental evaluations and add/drop architecture options. The experimental setup is shown in Figure 17.

Figure 18 shows the measured sensitivity for the Rx under evaluation when transmitting QPSK and 16-QAM signals. As expected, QPSK shows much better sensitivity than 16-QAM. As an example, in Figure 18 a), a received power of about -33 dBm is sufficient to correctly detect a QPSK signal if soft-decision (SD, threshold BER = 2e-2) forward error correction (FEC) is employed whereas almost 7 dB of additional optical power is required to correctly detect a 16-QAM signal in the same conditions, as shown in Figure 18 b). Moreover, if hard-decision (HD, threshold BER = 3.8e-3) FEC is employed instead, a penalty of about 2 and 3 dB is obtained for QPSK and 16-QAM, respectively. Homodyne crosstalk, which determines the frequency reuse in adjacent nodes, is also much more critical when the 16-QAM transmission is employed. If a 16-QAM signal is transmitted at the crosstalk level leading to 1 dB of Rx penalty, as shown in Figure 18 c), a crosstalk tolerance reduction exceeding 5 dB for SD-FEC is observed concerning QPSK. Additionally, interfering channels power must be about 20 dB below signal power for the negligible impact of crosstalk when transmitting 16-QAM. Unamplified and filterless transmission in the L-band has been proposed as a low-cost solution for a simple upgrade of legacy MANs, providing additional capacity in short reach links, low latency connections. Based on experimental results characterizing receiver sensitivity and the impact of homodyne crosstalk, the detailed discussion in [17] shows that the suggested system upgrade supports QPSK transmission on L-band with frequency reuse across metro-sized single spans, and over two hops totalling roughly 35 km of fibre. For 16-QAM, the reach is limited to single-hop connections at about 40 km, and frequencies are only reusable after the next express node.

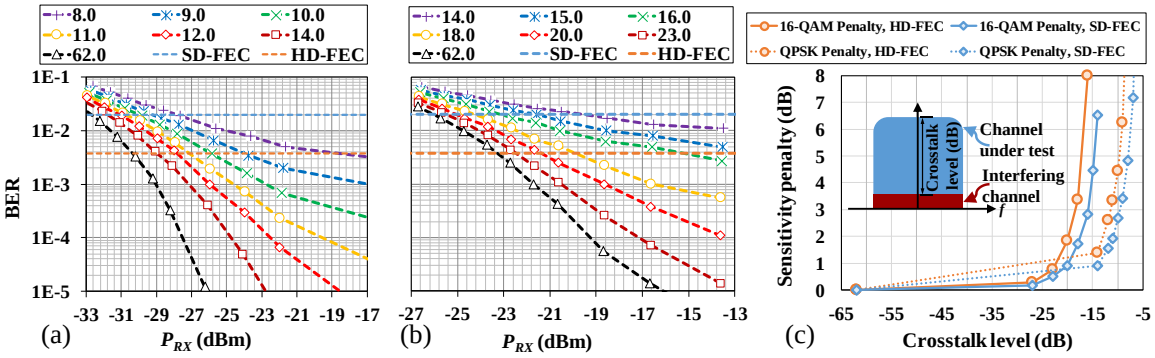

Figure 18: Sensitivity of Rx for 32 GBd a) QPSK and b) 16-QAM signals with attenuation variation (in dB) of the interfering channel given in the legends and c) sensitivity penalty at HD- and SD-FEC thresholds with a depiction of the crosstalk level as insert

While filterless metro networks have been shown to be attractive for straight-line/horseshoe topologies, it is an unsuitable solution for meshed networks, such as envisioned for the real-time low-latency object tracking demonstration in Berlin. Therefore, the semi-filterless topology discussed in 5.1.2 will be used in the Berlin demonstrator.

5.2 Transceivers and transmission performances

5.2.1 A programmable sliceable transceiver based on multicarrier modulation (MCM)

A programmable sliceable transceiver based on multicarrier modulation (MCM) is proposed within METRO-HAUL (MH) project as a suitable solution for transmission in metro optical networks adopting direct detection (DD) reception. In particular, the proposed transceiver is tailored for the metro aggregation segment defined as a part of the MH reference network in deliverable D2.3. The aggregation network is assumed to have a horseshoe topology, where each horseshoe covers a set of AMEN nodes. Thus, a simple and low-cost infrastructure is envisioned to cover distances from 50km to 100km (corresponding to the distances of urban and dense urban areas). Accordingly, a sliceable bandwidth/bitrate variable transceiver (S-BVT) based on cost-effective optoelectronic subsystems and simplified digital signal processing (DSP) solutions are adopted to address the stringent cost target of metro aggregation network infrastructure (see Figure 19). The transceiver architecture description is detailed/reported in D3.1, and it is briefly summarized hereafter to also include recent advances/improvements. Offline DSP, including (de)mapping, (I)FFT, CP and TS, addition/removal and RF upconversion/downconversion, is considered. A simple front-end with Mach-Zehnder modulators (MZMs) driven by tuneable laser sources (TLS) are included at the sliceable bandwidth/bitrate variable transmitter (S-BVTx). At the receiver side, simple photo-detectors (PINs) with transimpedance amplifiers (TIAs) are used to perform DD. The proposed S-BVT is composed of two bandwidth/bit rate variable transceiver modules (BVTs) that can create/receive two different slices at different data rates. Additional modules can be included in the S-BVT architecture to further increase the system capacity in a grow-as-needed approach. The multiple slices are aggregated into a high-capacity flow using a wavelength selective switch (WSS), which also serves as an optical filter. Specifically, single side band (SSB) modulation is implemented to enhance system resilience against chromatic dispersion. An additional WSS is included at the receiver to distribute the received slices.

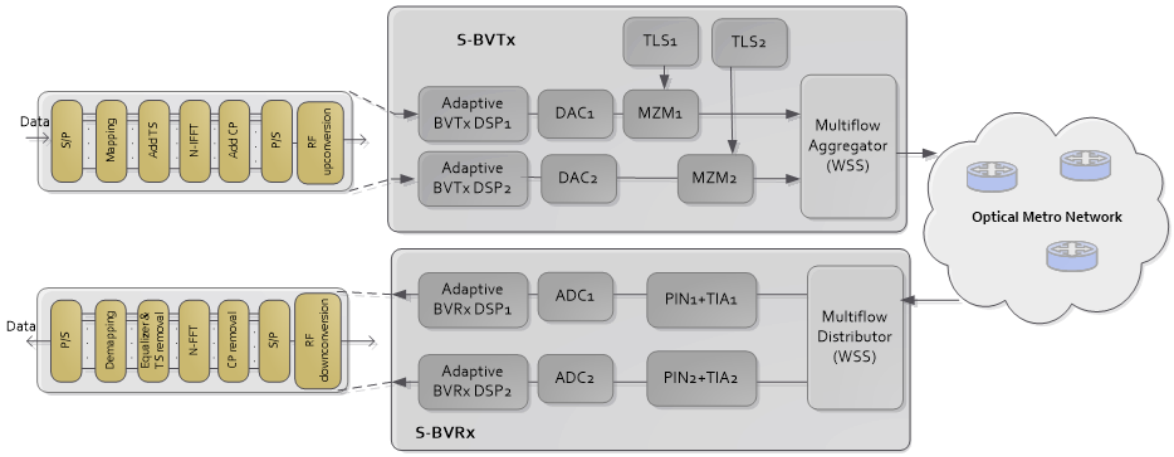

Figure 19. Programmable S-BVT architecture composed of two BVT modules based on MCM and DD

The proposed programmable S-BVT includes advanced functionalities including slice-ability, reach/rate adaptability and reconfigurability. MCM allows the implementation of bit and power loading (BL/PL) algorithms, such as the Levin Campello, where the number of bits and power values per subcarrier can be modified according to the channel profile. By the adoption of the SDN paradigm, the transceiver can be suitably configured/programmed to adapt to the dynamic variation of network capacity, transmission reach and path conditions. Specifically, different system parameters such as the bandwidth occupancy, FEC, loading algorithm selection, MZM bias and equalization type can be reconfigured to fully exploit the system flexibility. SDN agents based on the

OpenConfig model are being developed, enabling the control of different programmable elements such as TLSes, WSSes, optical amplifiers (OAs) and DSP. In particular, the OpenConfig model aims to achieve disaggregated network interoperability and multi-vendor optical devices/elements configuration [18]. Hence, the same agent can control all the building blocks of a single S-BVT, independently from the provider.

Different specific key performance indicators (KPIs) of the S-BVT have been identified, as detailed in Table 6. In particular, this includes: (i) Slice-ability, which is measured by enabling two slices of the S-BVT. The two slices can be aggregated at the transmitter side and distributed, at an intermediate network node, towards different destinations. (ii) Bit error rate (BER), which can be measured by counting the number of errors at the receiver side. Different target BER can be fixed according to the specified forward error correction (FEC). (iii) Capacity: 50 Gb/s target capacity is assumed to evaluate the performance of the S-BVT. (iv) Bit rate variability: thanks to the subcarrier granularity, enabled by the implementation of MCM, fine bit rate variability (of the order of tens of MHz, depending on the number of subcarriers and the slice bandwidth occupation, e.g. 20GHz/256) can be achieved. Hence, the system capacity can be adapted to the traffic demand and network condition by varying the modulation format per subcarrier according to the implemented BL/PL algorithm. (v) Transceiver programmability, which is achieved by the implementation of SDN agents based on the OpenConfig model. Following this data model, a particular client is assigned to an optical channel. Specifically, the central frequency, output power and operational mode of the optical channel can be configured. The operational mode field is vendor-specific and provides different channel mode/configuration to be selected, such as modulation, symbol rate and FEC. FEC mode can be interesting in the case of adopting programmable S-BVTs based on MCM to set the target performance as an input of a loading algorithm, which can be applied, as advanced functionality, to maximize the system capacity. According to the identified programmable transmission parameters, the DSP, TLSes, WSSes and OAs of the S-BVT are reconfigured, promoting efficient use of the metro network resources.

Table 6: Specific KPIs for the programmable S-BVT

KPI	Target SPECS	Means of verification
Slice-ability	2 slices	Number of slices
BER	HD-FEC (4.62e-3) SD-FEC (2e-3)	Error counting
Capacity	50 Gb/s per slice	(BW*bps) Bandwidth occupancy per bit per symbol
Bit rate variability	10 Gb/s-50 Gb/s per slice	Subcarrier granularity (slice BW/subcarrier number)
Programmability (OpenConfig model)	Laser central wavelength (TLS) Laser output power Operational mode	SDN agents controlling DSP, TLS, WSS and OA

On the other hand, general KPIs defined within the MH project and detailed in section 4, and deliverable D2.3 have also been measured/evaluated for the programmable S-BVT. This includes MH1 (Optical PtP connection set-up time), MH6 (Capacity of METRO-HAUL infrastructure), MH8 CapEx reduction and MH9 (Energy consumption) KPIs. Regarding MH1 KPI, the two slices of the S-BVT are configured in about 80 s. This takes into account the control messages to set-up a channel (9

ms) and the configuration of the related hardware (80s). The two lasers, optical amplifiers and WSS filters take 40 s to be configured, while the digital-to-analog converter (DAC)/analog-to-digital converter (ADC) stage takes at least 40 s. It is worth notice that the DSP related to the DAC/ADC configuration is performed off-line and it is the most time-consuming part, as takes at minimum 40 s to load data in the DACs and acquire the received signals at the scope (ADC). To perform accurate BER measurements, this time can increase to 3 minutes. To measure MH6 KPI, the S-BVT performance in terms of capacity has been assessed. Firstly in B2B and then after 35 km and 50 km paths of the ADRENALINE network, ensuring a target data rate of 50 Gb/s per slice. The modular S-BVT architecture provides variable capacity, scalable with the number of enabled slices. By adopting cost-effective optoelectronic subsystems (DD is considered) and simplified DSP solutions, at the S-BVT, a CapEx reduction is achieved, dealing with MH8 KPI.

Moreover, about MH8 and MH9 KPIs, the cost, power consumption and footprint of the S-BVT can be further reduced thanks to the photonic integration of key parts. A way to measure the cost and power consumption of the S-BVT is to consider equivalent form factors [19]. In particular, the proposed 100G S-BVT (50G X 2) can evolve towards 800G S-BVT (200G X 4). Hence, CFP2 form factor transceiver is a suitable option for the envisioned programmable S-BVT. Specifically, 800G transceiver is close to CFP2-class power consumption, which is about 12 W. Near the 79% of this power consumption is due to DSP. The relative cost of the 800G DMT transceiver, concerning the 100G transceiver, is 2.2 [19]. As an evolutionary path, smaller form factors such as QSFP28 can be considered further reducing the cost and power consumption of the proposed solution [20].

Finally, the performance of the programmable S-BVT is evaluated considering as a use case the aggregation segment of the MH reference network. The transmission performance in terms of distances, total nodes traversed, and data rate is experimentally assessed.

Table 7. Transmission performance

Scenario	Node technology	# of nodes	Filter BW (GHz)	Data rate (Gb/s)
B2B	WSS	7	50	60
B2B	WSS	7	25	39
35 km ADRENALINE	WSS	8	50	50
35 km ADRENALINE	WSS	8	25	31

The ADRENALINE network, which is a fixed/flexi-grid dense wavelength division multiplexing (DWDM) network with white box reconfigurable optical add-drop multiplexer (ROADM)/ optical cross-connect (OXC) nodes has been considered for the experiments [21]. However, as the ADRENALINE testbed presents a mesh topology, a single hop-path of the network plus a module emulating cascading filters, as in [22], are taken into account to address the horseshoe topology of the metro aggregation segment. A node architecture based on WSS filters of 25 GHz and 50 GHz is considered. A target BER of 4.62e-3 corresponding to a hard-decision FEC (HD-FEC) is fixed. According to Table 7, 50 Gb/s target capacity is achieved after traversing up to 8 nodes with 50 GHz filters and the 35 km ADRENALINE path.

Conversely, the data rate is reduced of about 20 Gb/s with 25 GHz cascading filters due to the filter narrowing effect, even in B2B configuration.

Additionally, the 50 km ADRENALINE path has also been assessed to evaluate the maximum distance that can support the proposed transceiver at the target capacity without introducing any dispersion compensator. In this case, 50 Gb/s per slice is also maintained with HD-FEC. Longer distances can be covered at the expenses of reducing the data rate or increasing the number of S-BVT building blocks to guarantee a target capacity. In particular, 40 Gb/s per slice is achieved, at 4.62e-3 BER, after 100 km of standard single mode fiber (SSMF), with an optical amplifier every 50 km. The data rate is reduced to 30 Gb/s per slice after 200 km. Additionally, SD-FEC can also be considered to relax BER requirements enabling higher data rate/reach.

5.2.2 Transceiver solutions for dispersion-tolerant direct detection

Within METRO-HAUL project, a DD Transceiver offering high dispersion tolerance at high bit-rate has been developed by exploiting a combination of alternative modulation formats together with Silicon photonics integrated modules. The main target is to increase both the bit rate and the optical reach concerning conventional OOK or PAM modulation formats while maintaining cost and power consumption as low as possible. The transceiver is suitable for capacity and distances envisaged in METRO-HAUL for metropolitan optical networks and can fit both the case of filtered and quasi-filterless networks (where channel filtering is embedded at the receiver to ensure compliance with direct detection). The adopted modulation formats offer enhanced tolerance to chromatic dispersion through a proper combination of coding and pulse shaping, the "combined amplitude and phase shift" (CAPS) codes [23]: while the receiver maintains the same hard threshold symbol-by-symbol detection used for OOK, the generation of CAPS codes requires an encoder with 2^n states (being n the CAPS order) and the use of a 2-channels DAC (in-phase and quadrature components) for proper shaping of the complex signaling pulse (Figure 20(left)). A simplified implementation scheme [24] provides an approximation of the CAPS signals with much simpler analog electronics and is depicted in Figure 20 (right): the modulated signal is obtained by associating a quadrature component to a duobinary coded signal, using an IQ-MZM. Such a component is simply given by two attenuated replicas of the duobinary signal itself, respectively anticipated and delayed by a symbol time. Hence, the scheme, named IQ-duobinary (IQduo), only requires a digital differential precoder and analog electronic blocks (sum, symbol-time delays, analog filters) instead of the CAPS encoder and the DAC. CAPS parameters α and β, as well as the gains g1 and g2 for IQduo, need to be chosen by design for maximizing dispersion tolerance and can be finely tuned to optimize performance according to the desired reach.

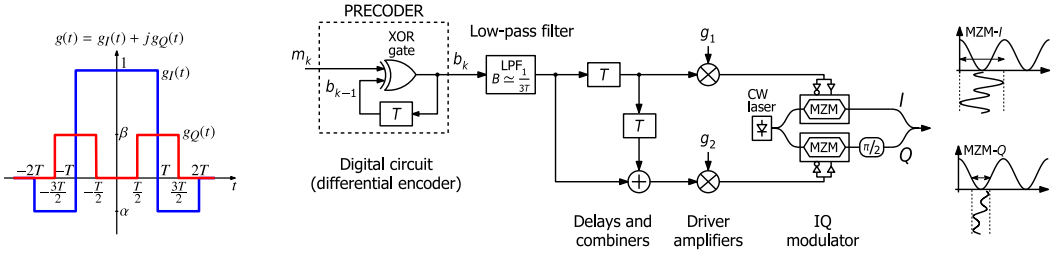

CAPS signaling pulse (complex)

IQ-duobinary transmitter

Figure 20: CAPS signalling pulse (left) and IQDuobinary transmitter scheme (right)

The tolerance to chromatic dispersion concerning simple OOK or PAM4 is strongly increased while maintaining the same receiver used for OOK, at the expense of a marginally higher cost of the transmitter. At a bit-rate of 50Gb/s, CAPS and IQduo provide dispersion tolerance up to 20km and 15km of uncompensated G.652 SMF, respectively. Figure 21 shows how 50Gb/s CAPS and IQduo formats outperform conventional OOK and PAM4 signalling schemes in terms of the maximum reach and required optical power at the receiver [25],[26]. Reference pre-FEC BER = 10^{-3} is considered, assuming implementation of a standard HD-FEC with 7% overhead.

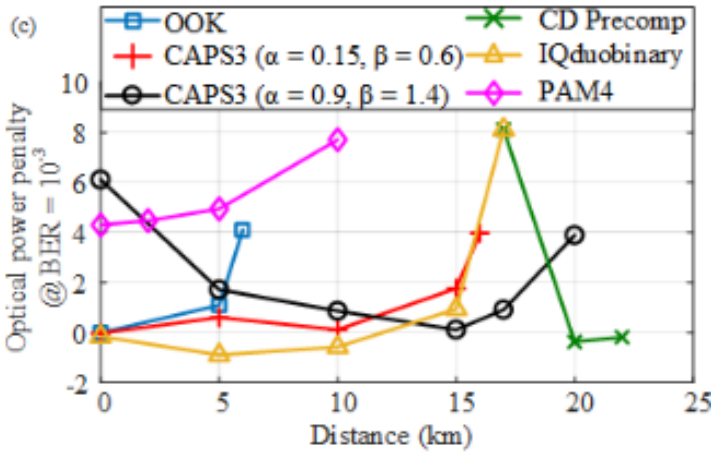

Figure 21: Optical power penalty at BER = 10^{-3} for CAPS and IQduobinary modulation schemes delivering a bit rate of 50 Gb/s. The optical power penalty is calculated relative to a reference required received optical power of OOK in back-to-back to achieve BER of 10^{-3}

To enable further reach extension for C-band high bit-rate transmission without requiring complex DSP, dispersion compensating devices based on integrated photonics are embedded in the optical transceiver. This optical dispersion compensator (ODC) is based on all-pass microring resonators [27] and has been designed and implemented in sub-blocks. Each sub-block can compensate the chromatic dispersion of a 10 km G.652 SMF, at a wavelength of 1550 nm, and is implemented as a cascade of three all-pass microring resonators opportunely designed. By combining ODC and optical switches (e.g. Mach-Zehnder switches), the transponder can be configured for operation on a wide range of fiber lengths (Figure 22) [28]. Table 8 summarizes main Transceiver features and specifications, while Table 9 provides details on the achievable optical reach at 25 Gb/s and 50 Gb/s with different ODC configuration.

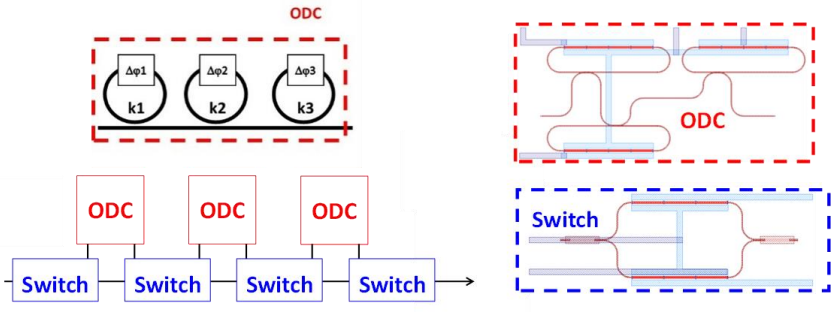

Figure 22. Schematic of the three microrings ODC and the reconfigurable ODC module (left); mask layout of the ODC and the optical switch (right)

The transceiver is fully programmable and is configured through a NETCONF agent based on the OpenConfig model, developed within METRO-HAUL. The transceiver encompasses several components that are configured depending on the connection to be established as well as the link condition, e.g. line rate, laser wavelength, number of active ODC modules. All parameters are internally configured via specific software modules (drivers) and proprietary APIs controlling the underlying hardware. A NE handler implemented in Python maintains the current view of the transceiver and incorporates the different drivers for the communication with the sub-blocks device through the APIs of the different components. The NE handler interfaces with a NETCONF/OpenConfig agent module to enable transceiver configuration in agreement with the

YANG models of the device. The NETCONF server is implemented using ConfD framework and acts as the northbound interface of the agent for the communication with the SDN controller and/or an OAM (Operation, Administration and Maintenance) handler.

Table 8. Transceiver specifications

Tx feature	Tx SPECS
Max capacity per lambda	50 Gb/s up to 50 km
Optical reach (G.652 SMF)	50 Gb/s: 50 km 25 Gb/s:100 km 12.5 Gb/s: >200 km
Transmitter Bandwidth (-3 dB)	18 GHz (50Gb/s) 9 GHz (25Gb/s)
Line Rate	26.75 – 53.5 Gb/s
Programmable elements	Central wavelength Laser output power Line rate N° of active ODC modules
Output power range	0 – 10 dBm
Tunability range	1528 nm – 1568 nm 191.300 THz – 196.300 THz
Reference FEC (Target BER)	7% HD-FEC (3.8e-3)
Reconfigurable parameters within OpenConfig model	Laser central wavelength Laser output power N° of active ODC modules
Monitoring parameters	Pre-FEC BER
Potential capabilities	Programmability, Reconfigurability, Low cost
Specific sub-KPIs	Optical reach, bit rate, low cost, reconfigurability, power consumption compliant to QSFP form factor.
Rx feature	**Rx SPECS**
Photoreceiver type	PIN / TIA
Input power range	-10 / +5 dBm
Receiver bandwidth	40 GHz
Minimum required OSNR in BtB	19 dB at 50Gb/s, 7% HD-FEC (BER=3.8x10^{-3})

Table 9. Optical reach for different modulation formats at 25 Gb/s and 50 Gb/s with and without ODCs. Longer reaches can be enabled by different ODC configurations

Speed	Modulation Format	w/o ODC	1 ODC	2 ODC	3 ODC
25 Gb/s	CAPS	80 km	90 km	100 km	110 km
	IQduo	70 km	80 km	90 km	100 km
50 Gb/s	CAPS	20 km	30 km	40 km	50 km
	IQduo	17 km	27 km	37 km	47 km

Table 10 shows a lookup table reporting transmitter configuration for different targeted reach, referred to the structure depicted in Figure 22: depending on the required reach, switches and ODC modules are activated to guarantee correct operation. Through APIs, a multichannel DC voltage/current source is programmed to provide the correct control signals to the optical switches and micro-ring resonators.

Table 10. Transmitter configuration for different target reach at 50Gb/s operation

Reach [km]	SW #1	SW #2	SW #3	SW #4	Active ODCs	CAPS settings
0-15	BAR	BAR	BAR	BAR	-	Normal operation
15-25	CROSS	CROSS	BAR	BAR	[#1]	Normal operation
25-35	CROSS	BAR	CROSS	BAR	[#1,#2]	Normal operation
35-45	CROSS	BAR	BAR	CROSS	[#1,#2,#3]	Normal operation
45-50	CROSS	BAR	BAR	CROSS	[#1,#2,#3]	Extended reach

Specific KPIs have been identified such as optical reach (up to 200km at a reduced bit rate of 12.5Gb/s), bit rate (up to 50Gb/s), cost-effectiveness (simple architecture exploiting photonic integrated devices), reconfigurability compliant to NETCONF/OpenConfig, affordable power consumption (compliant to QSFP form factor). Nevertheless, the proposed transceiver addresses general KPIs defined within the MH project and specifically MH6 “Capacity of METRO-HAUL infrastructure”, MH8 “CapEx reduction” and MH9 “Energy consumption”: a transmission capacity up to 50Gb/s per lambda is achieved with optical reach suitable for the metro segment while keeping low cost and complexity of the transceiver architecture. CapEx reduction is addressed resorting to photonic integrated devices (e.g. Silicon photonics ODC) that guarantee high performance at a reasonable cost. As for Energy consumption, compliance with the QSFP form factor is targeted as a reasonable reference value.

5.2.3 Elastic transponders with low-resolution DAC and ADCs for metro networks

Metro networks are often heterogeneous, i.e. they consist of legacy 10 Gb/s channels with dispersion managed optical links, mixed with higher capacity coherent channels (e.g. 100 Gb/s). They are also more cost-sensitive than long-haul networks and at the same time less constrained by reach and hence propagation impairments, thus promoting innovations in DSP [29]. Coherent transponders are flexible and can operate at various symbol rates, modulation formats (e.g. QPSK, 16QAM, 64-QAM) and employ Nyquist pulse-shaping to be highly spectrally efficient. For such functionalities, DACs are mandatory and represent the major part (40 %) of the overall DSP power consumption [30]. Customarily, coherent transponders employ 6- or 8-bit DACs that were originally developed for long-haul applications. These high-resolution DACs are mainly limited by their electronic bandwidth, which can be mitigated using pre-emphasis algorithms [31] whose implementation increases the overall DSP power consumption. A solution to reduce the DSP power consumption is to lower the DAC resolution down to 4 bits and below [30], [32] but with the disadvantage of increasing quantization noise. Recent efforts focus on assessing the quantization noise penalty due to a limited ADC resolution [33].

We propose a model to predict the system performance (i.e. signal to noise ratio, SNR) when using low *physical* resolution DACs/ADCs without restricting to specific signal categories and with going further than the traditional ENoB indicator (further details could be found in). For this, we use the theory developed in [34], [35] to model the performance fluctuations induced *specifically* by quantization and clipping, treated separately because of their different origins and properties. We present a two-step model. First, we compute the mean square error (MSE) due to quantization and to clipping. Second, we translate the MSE into SNR, carefully accounting for the operating parameters (sampling frequency, symbol rate). We then confront our model with simulations and experiments in an optical set-up using a low-resolution DAC/ADC and show that SNR predictions can be done with less than 0.5dB of error. We use this model to establish resolution requirements for next generation optical systems.

We experimentally evaluated our model on a back-to-back optical set-up. At transmitter (Tx), we use an 8-bit DAC at 92 GS/s. An optical attenuator before an amplifier ensures a constant optical power into the coherent mixer, and we vary the optical signal to noise ratio (OSNR) by ASE loading. We express the SNR as in [36] but isolate the low-resolution DAC/ADC contributions:

$$\frac{\mathbf{1}}{\boldsymbol{SNR}} = \frac{\mathbf{1}}{\boldsymbol{\xi OSNR}} + \frac{\mathbf{1}}{\boldsymbol{SNR_{TRx}}} + \frac{\mathbf{1}}{\boldsymbol{SNR_{DAC}}} + \frac{\mathbf{1}}{\boldsymbol{SNR_{ADC}}}$$

We calibrate the system with 8-bit DAC/ADC such that $1/SNR_{DAC}$ and $1/SNR_{ADC}$ are negligible. At Tx, employing a 4-bit DAC versus 8-bit gives -2.1dB of performance loss at the C^2 = -6.46dB, which is consistent with prediction (solid line), and for small C^2 the measured SNR is around 0.4dB below the prediction and we attribute this difference to filtering effects that may affect the noise before Rx. As in simulations, when clipping noise dominates, the model and the measurements disagree.

With a reduced ADC resolution, we also observe performance loss, partially compensated by the relatively high oversampling factor (200/46 ≈ 4.35). If the ADC sampling frequency is divided by 2, the SNR additively loses 1dB at the optimal C^2 = -7.95dB at the ADC, as in Figure 23(c). Finally, in all presented results, and at the highest measured SNR, the measurements and the model differ by less than 0.5dB.

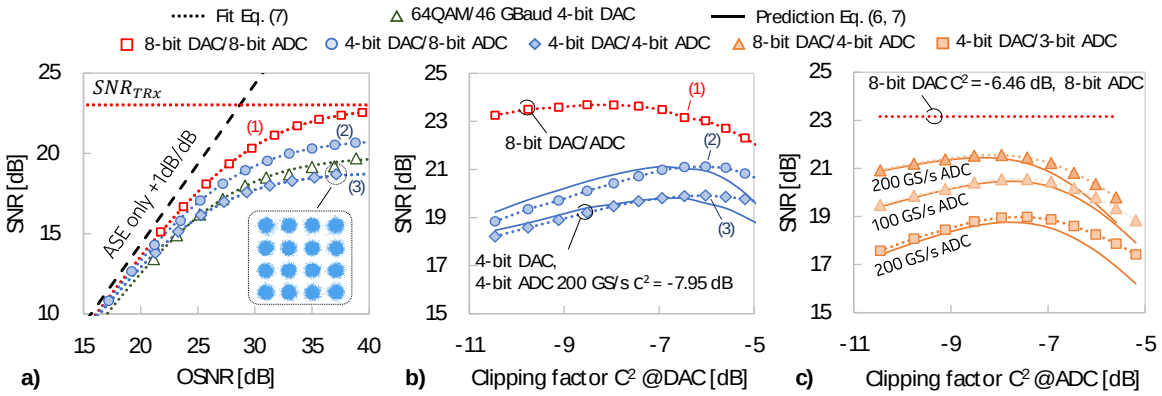

Figure 23: Experiments. (a) SNR versus OSNR for various DAC/ADC configurations. (b-c) SNR floor at best OSNR versus clipping factor at DAC or ADC. Curves (1), (2) and (3) in (a) correspond to the highlighted points in (b)

For performance prediction with quantization and clipping, the useful parameters are the quantizer resolution N and the number of SPS. Thus, we report in

Figure 24 the maximum modulation forma, which can be theoretically carried by a low-resolution DAC or ADC assuming a Gaussian distributed input, for generality. For 640 Gb/s, a 4-bit DAC enables 32QAM 64 GBaud. We also observe that, at the optimum SNR, even if the quantization noise is uniformly distributed, the receiver match-filtering makes it Gaussian distributed (see example in the inset of Figure 23(a)), as per the central limit theorem, such that BER relations in AWGN channel apply.

We assess physical resolution requirements for 600 Gb/s and beyond transceivers and show that a 4-bit resolution is enough for 32QAM 64 GBaud (640 Gb/s gross). We experimentally show that our

SPS (Symb. Rate)	3 bits	4 bits	5 bits
2.85 (32 GBaud)	32-QAM (320 Gb/s)	64-QAM (380 Gb/s)	256-QAM (510 Gb/s)
2 (46 GBaud)	16-QAM (360 Gb/s)	64-QAM (550 Gb/s)	128-QAM (640 Gb/s)
1.44 (64 GBaud)	8-QAM (380 Gb/s)	32-QAM (640 Gb/s)	128-QAM (900 Gb/s)
1 (92 GBaud)	8-QAM (550 Gb/s)	32-QAM (920 Gb/s)	128-QAM (1.3 Tb/s)

Figure 24: Maximum achievable modulation formats (targeting an SNR for 10-3 bit error ratio) for a DAC or an ADC

model is accurate as we found less than 0.5dB signal to noise ratio error prediction for all investigated configurations in the regime of interest.

On parallel of our performance model, we also investigate a dynamic performance optimization to reduce the complexity of the overall DSP and to decrease the power consumption. Indeed, to keep maximum Quality of Transmission (QoT) performance, *soft-decision* FEC techniques, such as iterative Low-Density Parity Check (LDPC) decoding [37] can be used, where several iterations are performed. Notwithstanding the number of iterations can be adjusted as a function of the pre-FEC BER, a fixed number of iterations is usually performed for simplicity, targeting at reaching the desired post-FEC

BER under a wide number of scenarios and connection lengths. In fact, according to [37], up to 82% power savings could be potentially achieved by adjusting the number of LDPC iterations according to connection's length; note that the longer the connection, the higher the number of iterations. Specifically, connections shorter than 1,200 km need no additional LDPC iterations, which opens the possibility to reach maximum power savings in metro networks where connections' length are shorter.

However, low-resolution ADC-based transmission systems are more sensitive to physical fluctuations, such as the state of polarization (SOP) rotation [38]; SOP fluctuations can be caused by external events like hitting, bending or shacking. In fact, fluctuations causing a fast variation on the polarization state can drastically affect system margins planned by the operator [39]. In low-margin networks, the impact of soft-failures (i.e., fiber bending) that could lead to hard failures (fiber cut) increases with margin reduction [40]. Note that pre-FEC might be noticeably impacted by SOP fluctuations [41], and therefore, the number of LDPC iterations needs to be configured to a high conservative value to ensure robust transmission at the expense of higher power consumption.

The solution, given the infrequent nature of such events, is to work toward intelligent approaches able to adapt the FEC decoder configuration to the actual needs, targeting at reducing power consumption without compromising QoT. To that end, Machine Learning (ML) techniques based on monitoring data [42], can be applied to build autonomic transmission systems able to self-adapt their configuration in response to changing conditions. ML-based algorithms need to focus on the anticipated detection of events (e.g., SOP fluctuations) that can potentially produce a burst of errors to enable decision making, resulting in the reconfiguration of the receiver or the transmitter.

Table 11: Power consumption versus #LDPC iterations

	Static config	**ATA**		
		normal	*warning*	*critical*
# LDPC iters	10	2	2.18	10
Pow consum (W)	25	3.5	6.92	25

While, for concision, we will not develop the whole architecture here, an Autonomic Transmission Agent was developed to follow the exposed idea.

Table 11 summarizes the average number of iterations and power consumption of the LDPC module for the three ATA states defined for decision making detailed in [43] and observed in the experimental data. We can see that only under the *critical* state (i.e., close to the pre-FEC BER threshold), ATA power consumption is that of the static configuration. For any other scenario, even in the *warning* state (i.e., fluctuations causing number LDPC iterations to increase), power consumption is noticeably reduced due to the small average number of LDPC iterations actually required. Figure 25 shows total power consumption as a function of the probability (p) of fiber stressing events requiring LDPC iterations to increase. In particular, three cases are compared: *i*) the static configuration where the conservative maximum number of iterations is setup; *ii*) the average operation of ATA under those events observed in the *warning* state; and *iii*) a worst case where all events lead to the *critical* state. Note that the latter meets the static one in the (unlikely) case of p=1. Putting the spotlight on a remarkably large probability, i.e. p=0.01, ATA allows achieving power

consumption savings around 80% compared to the static operation. Since ATA also guarantees zero post-FEC errors, we can finally validate our proposed ATA as a smart solution.

To conclude, these two studies can be included in the pluggable modules with no modification, which reducess the consumption of the module. Pluggable modules such as CFP2-DCO target a 12W power consumption.

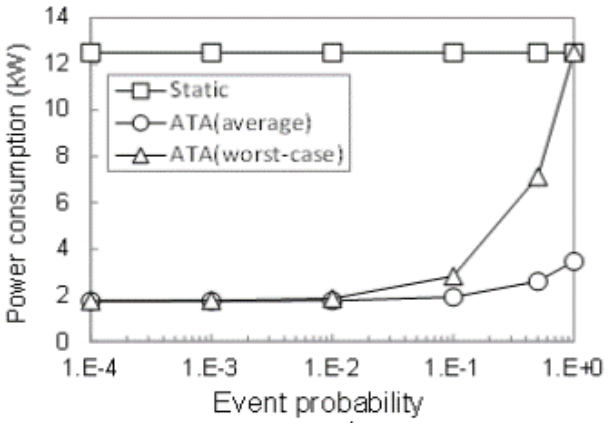

Figure 25: Power consumption saving

5.2.4 A digital sliceable bandwidth variable transponder for filterless networks

While the component D7 implements a programmable sliceable transceiver based on multicarrier modulation and IM/DD, the component D11 implements a similar concept based on full vectorial field modulation and coherent detection.

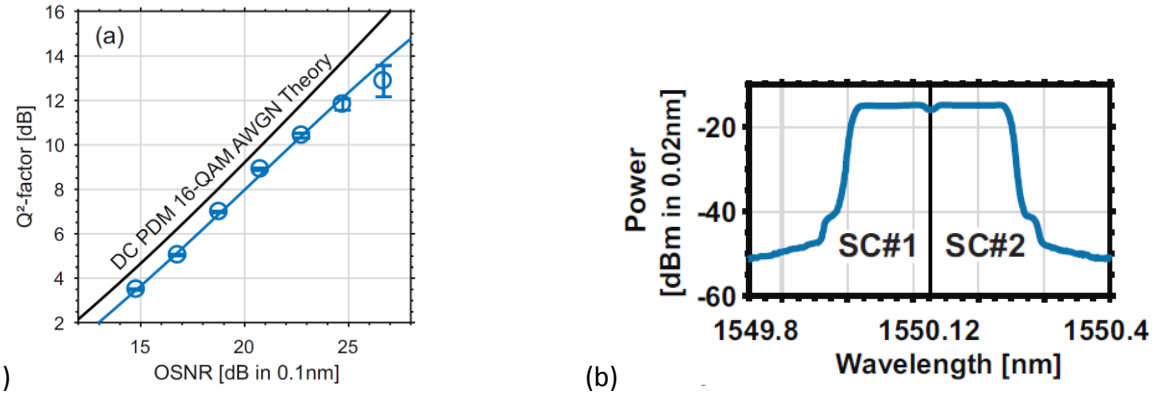

Figure 26: (a) B2B performance of 2×16-GBd digital dual-carrier (DC) PDM 16-QAM and (b)corresponding measured an optical spectrum

The digital sliceable bandwidth-variable transponder (DS-BVT) is proposed in METRO-HAUL as an efficient and flexible transponder architecture for filterless optical networks. A DS-BVT digitally modulates a certain spectral range (e.g. several ITU-T flexgrid slices). The spectral range is limited by the analogue bandwidth of its components such as the DAC, ADC, optical modulator, driver amplifiers and TIAs.

A block diagram of the DS-BVT was shown in deliverable 3.1. The DSP part at the transmitter consists of an FEC encoder, subcarrier modulation and pulse shaping, as well as a nonlinear pre-distortion stage to compensate for transmitter component impairments. At the receiver DSP, the received subcarriers are demultiplexed after the optical frontend has been compensated. The target subcarriers are further processed by standard single-carrier DSP before FEC decoding. The prototype currently supports a DAC sample rate of up to 92 GS/s. Flexible subcarrier generation is supported on the ITU-T 6.25-GHz center frequency grid with subcarrier spacings of 6.25 GHz, 12.5 GHz and 25 GHz. Mixed spacings are possible. Single-carrier operation is also supported. Each subcarrier is modulated with M-QAM and flexible FEC code rate. This allows achieving a fine granularity in net data rate per subcarrier.

Table 12: DS-BVT specifications

Transponder Feature	Specification
Tunability range	191.5 - 196.25 THz in C-band, 186.35 - 191.1 THz in L-band
WDM Flexgrid	6.25 GHz centre frequency and 12.5 GHz spectral slice width granularity
Line Rate	12-768 Gb/s per subcarrier depending on symbol rate and modulation
Net Line Rate	10-600 Gb/s per subcarrier depending on symbol rate and modulation
Line Coding/FEC	M-QAM with rate-adaptive TPC/LDPC
Baud rate	6-64 Gbaud per subcarrier
Output power	C-band: -2.4 dBm, L-band: -3.4 dBm typical output power
Output OSNR	>31 dB in 0.1 nm at the output of the transmitter
Reconfigurable Parameters	Laser frequency, operational mode (modulation format, FEC code, symbol rate, no. of sub-carriers)
Monitoring Parameters	Pre-FEC BER, chromatic Dispersion, ESNR, Q-value

Table 12 reports DS-BVT features and their specifications. The multi-carrier capability is achieved by adding functionality in the transmitter and receiver DSP. By using low-complexity approaches for demultiplexing filterbanks, the increase in DSP complexity compared to a single-carrier DSP is negligible. Therefore, the DS-BVT is expected to scale according to standard coherent transponders in power consumption and module form factor (cf. e.g. [44]). For example, 400G class DCO (digital coherent optics) could fit into OSFP or QSFP-DD form factors as discussed by OIF 400ZR.

exemplarily shows the measured back-to-back (B2B) performance of the DS-BVT prototype in a 2×16-GBd dual-carrier polarization-division multiplexed (PDM) 16-QAM configuration and the corresponding optical spectrum. The DS-BVT prototype also features an advanced nonlinear compensator, which operates on a per-symbol basis after the carrier phase recovery block in the receiver DSP [45]. The nonlinear compensator has been extensively tested for different system configurations relevant in the metro segment. Figure 27 shows an evaluation of the performance for the symbol rates 16 GBd, 32 GBd and 64 GBd over a distance of 120 km standard single-mode fiber (SSMF). The modulation format is dual-polarization (DP) 64-QAM. As a reference, the figure also reports corresponding pre-FEC BER at 10^{-2}, 10^{-3} and 10^{-4}.

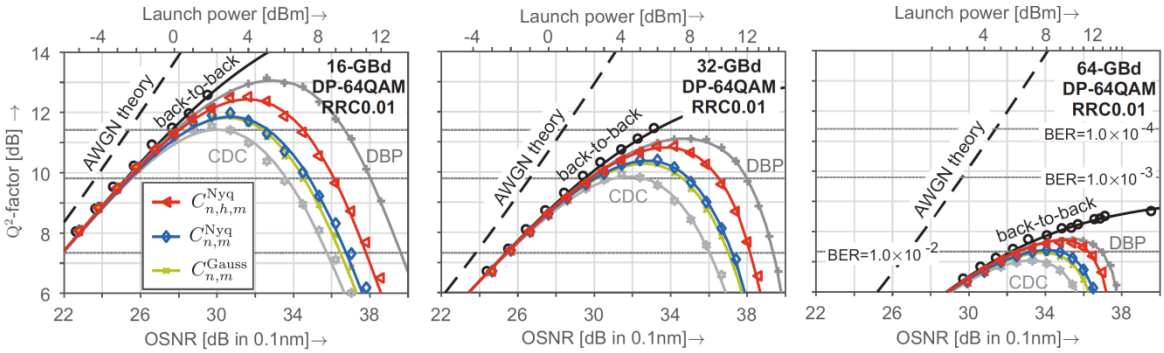

Figure 27: Experimental performance validation of the DS-BVT for variable symbol rate and DP-64QAM modulation over a 120 km SSMF link using the novel nonlinear compensator $C^{Nyq}_{n,h,m}$ as compared to just standard linear chromatic dispersion compensation (CDC), alternative nonlinear compensators from literature ($C^{Nyq}_{n,m}$ and $C^{Gauss}_{n,m}$) and ideal nonlinearity compensation by digital back-propagation (DBP).(From [45])

The functionality of this prototype was extended within METRO-HAUL by a NETCONF agent, which allows for NETCONF-based OpenConfig-compliant configurability. As such, the DS-BVT is fully programmable and configurable through the NETCONF agent based on the OpenConfig model, which was developed within METRO-HAUL. For example, the transponder can be configured concerning symbol rate, modulation format, FEC code rate, number of sub-carriers, and others. Since the transponder prototype is based on offline processing, a python script/add on to the driver, that is a bridge between the driver and the hardware and software parts of the DS-BVT was implemented. This script can receive and send data to MATLAB through a socket, making the process fast and effortless. At this moment the parameters: “PRE-FEC-BER”, “ESNR”, “Q-VALUE”, “FREQUENCY” and “CHROMATIC-DISPERSION” are implemented as part of the scripts. After the communication has been opened, the NETCONF agent communicates all of the configuration data, through a socket, to the driver. The driver then saves the configuration in a Config.txt file or potentially transmits it for further communication to external devices. The driver also has the possibility to return data to the agent in order to monitor the parameters.

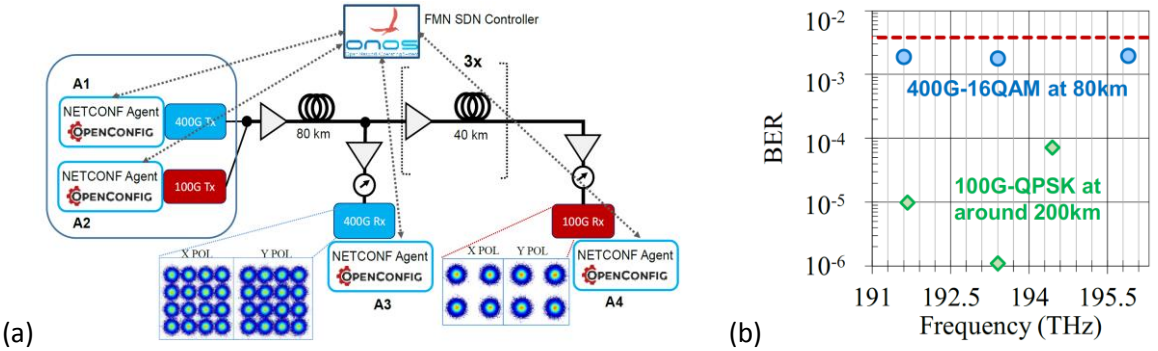

Figure 28: (a) Experimental control plane setup; Inset: received constellations at 193.4 THz. (b) BER results on data plane setup. (From [46])

An experimental data and control plane validation have recently been published at OFC in a joint work of CNIT and HHI targeting a filterless metro network scenario with variable modulation format and FEC codes. [46]. Figure 28 reports the corresponding experimental control plane setup and the results obtained in the data plane setup at 100G and 400G.

Future works in METRO-HAUL target an extension of the parameters, which are controllable by the agent as well as an extension of monitoring parameters, which can be made available by the DS-BVT prototype.

5.2.5 Discussion of peculiarities and diversities for the four transmission solutions.

Within METRO-HAUL project, different candidate, metro transport network architectures, addressing various network scenarios have been defined and detailed description is provided in deliverable D2.3 [5]. To satisfy different possible requirements, a diversified "portfolio" of transmission solutions is proposed and investigated, offering a range of technological solutions enabling the implementation of metro transport networks technologically capable of supporting 5G service. As detailed in sections 5.2.1 to 0, each solution offers innovative features and peculiar functionalities concerning the state-of-the-art. Nevertheless, all proposed solutions share a common paradigm of increasing network performance while maintaining cost and complexity reasonably low and affordable for the metro scenario. Table 13 briefly summarizes the four main different transceiver solutions proposed within METRO-HAUL. While solutions D7 and D8 rely on direct detection aiming at significantly pushing performances beyond state of the art, D10 and D11 exploit the huge and well-known potential of coherent detection targeting cost and complexity reduction to make these solutions favourable for implementation also in the metro segment. All solutions support NETCONF/YANG and are equipped with OpenConfig agents for interface with control plane for dynamic (re)configuration.

Table 13. Summary of METRO-HAUL transmission solutions

Component	Description
D7	**Programmable S-BVT based on multicarrier modulation** A programmable sliceable transceiver based on multicarrier modulation adopting direct detection. The scheme exploits DSP generation and reception of the DMT/OFDM signals with modular architecture providing sliceability, flexibility and adaptability with very fine granularity, trading DSP complexity against advanced functionalities/performance.
D8	**Transceiver solutions for dispersion-tolerant direct detection** High bit rate and enhanced tolerance to chromatic dispersion are provided while maintaining cost and complexity comparable with conventional NRZ. Photonic-integrated optical dispersion compensating modules are embedded in the transceiver and operate together with alternative dispersion-tolerant modulation formats.
D10	**Elastic transponders with low-resolution DAC and ADCs for metro networks** Coherent solutions for Metro transport networks, relying on low-resolution DAC and ADC to reduce DSP power consumption enabling up to 600Gbps/channel.
D11	**Digital sliceable bandwidth variable transponder for filterless networks** A digital sliceable bandwidth-variable transponders (DS-BVT) for application, e.g. in filterless D&W architectures. Several subcarriers are digitally generated and received in the frequency domain, potentially serving different destinations.

D7 transceiver (developed by CTTC) is based on multicarrier modulation and adopts direct detection: this solution represents a medium/long term solution suitable for metro aggregation networks. The scheme exploits DSP (performed offline) for the generation and reception of the DMT/OFDM signals. Thanks to the implementation of MCM and the adoption of a modular architecture, unique flexibility and adaptability are achieved with very fine granularity, trading DSP complexity against advanced functionalities/performance. The proposed S-BVT is composed of two BVTs that can handle two different slices at different data rates. The S-BVT modular design facilitates the scalability and a suitable sizing of the solution according to the network segment or specific node requirements, promoting a grow/pay-as-you-need approach.

Additionally, a high degree of (re)configurability is provided, enabling spectral manipulation with sub-/super-wavelength granularity. Bit rate/bandwidth variability enables adaptive transmission over different metro network paths, without adding any dispersion compensator for the target capacity/reach. **D8** transceiver (developed by TEI/CNIT) offers enhanced tolerance to chromatic dispersion for high bit rate while maintaining very low requirements in terms of cost and complexity (only marginally higher than conventional NRZ). While the receiver consists of a conventional direct detection NRZ receiver without additional DSP other than standard HD-FEC, the transmitter is embedded with programmable photonic integrated optical dispersion compensating modules and adopts amplitude and phase modulation with increased tolerance to chromatic dispersion that turns to NRZ after direct intensity detection. Additional flexibility as a BVT can be provided as option exploiting a low-resolution DAC. METRO-HAUL has also been investing significant efforts on the realization of cost-effective coherent reception transceivers to make this solution affordable also in the metro transport networks. Indeed, while the performance offered by coherent transponders can fully satisfy metro transport requirements in terms of capacity, reach and flexibility, their cost (both CapEx and OpEx) has been so far unsustainable for this segment. One of the most critical aspects for coherent is the DSP power consumption. METRO-HAUL coherent transceiver **D10** (developed by NOKIA) operates with reduced DSP power consumption by lowering the DAC/ADC resolution down to 4 bits and below offering performance as high as 600 Gb/s and beyond based on 32QAM at 64GBaud. METRO-HAUL coherent transceiver **D11** (developed by HHI) is a digital sliceable bandwidth-variable transponders (DS-BVT) and is particularly as an efficient and flexible transponder for application in filterless D&W architectures. By digitally generating and receiving several subcarriers in the frequency domain, a DS-BVT can set up several optical flows to different destinations, e.g. serving several AMENs. Flexible subcarrier generation is supported on the 6.25-GHz center frequency grid with subcarrier spacings of 6.25 GHz, 12.5 GHz and 25 GHz. Mixed spacings are possible. Table 14 summarizes the main technical features for the four transmission solutions developed within METRO-HAUL, offering an overview of the different technological options available.

Table 14. METRO-HAUL transmission solutions: technical features

	Modulation format	Tx DSP	Tx Front-end	Rx Front-end	Rx DSP	Bitrate per channel	Dispersion Compensation	Optical Reach
D7	DMT/OFDM (Adaptive BPSK/M-QAM per subcarrier)	yes	DAC + MZM	DD	Yes	Up to 50G	DSP and SSB	50G: 40/50km 40G: 100km 30G: 200km
D8	CAPS or IQDuobinary	Optional	IQ-MZM	DD	No	Up to 50G	Si-integrated ODC or legacy DCF (Not required up to 15km at 50Gbps)	50G: 50km 25G: 100km 12.5G: >250km
D10	M-QAM	yes	Low-res DAC + IQ-MZM	CO	yes	Up to 600G	DSP	Depending on configuration
D11	M-QAM	yes	DAC + IQ-MZM	CO	yes	Up to 360G	DSP	Depending on configuration

5.3 PON termination to metro nodes and abstraction

In the most general case, the AMEN comprised connectivity, computing and storage resources. A generic AMEN layout is given in Figure 29 where the connectivity infrastructure may include PON (or Ethernet P2P) interfaces towards Access while it includes optical elements like ROADMs, couplers (in case of filterless systems), blockers (in case of semi-filterless systems) etc. and transceivers towards the Metro network. Key AMEN element is an L2 switch that is tasked to forward traffic from Access PON terminals either towards a local Datacentre (computing and storage resources, including a disaggregated L3 switch) or towards Metro and vice versa.

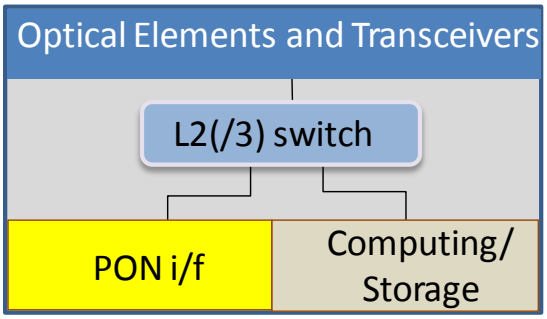

Figure 29: A generic AMEN layout

The generic solution of Figure 29 is limited to the switching capacity of the L2 switch and in particular to the available number of ports commercially available products may support. In turn, this limits the number of end-users that are served by an AMEN.

To overcome this limitation, the adopted two-fold strategy is the following: a) PON systems are extensively used instead of Ethernet systems to provide connectivity either to Access end-users or between the servers within the local Datacentre as in [47]; b) the adoption of a modular AMEN architecture to ensure a scalable solution.

To implement the above, we are considering a "cloud-box", that becomes the main building block of an AMEN, that incorporates an L2 switch, PON interfaces (connectivity resources) and server blades (with computing and storage resources). Therefore, an AMEN is constructed by a cascade of lower capacity/switch ports cloud boxes. The cloud boxes are interfaced to an optical bus topology bi-directional link using a passive coupler, appropriate band filters (BF) and a band (de)multiplexer as shown in Figure 30.

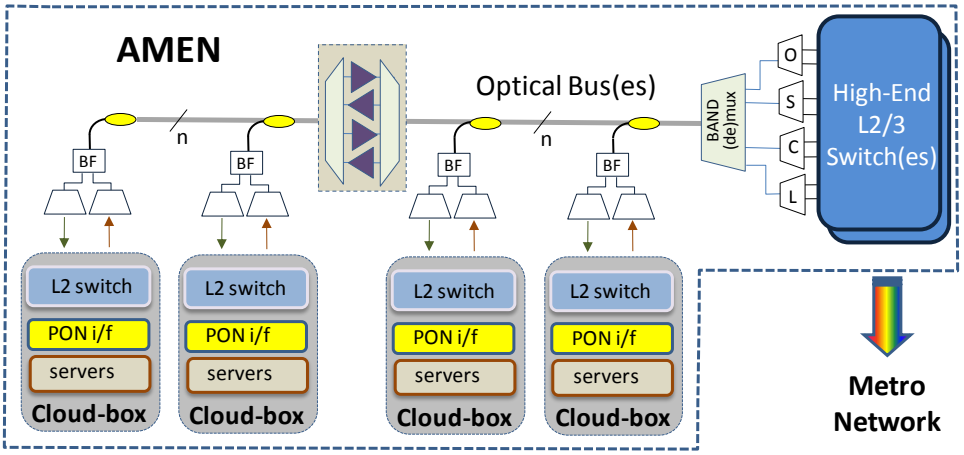

Figure 30: Schematic layout of a cloud-integrated AMEN architected as a DataCentre

Under this connectivity scheme, traffic from a cloud-box towards either the Metro network or another cloud-box is transported to the High-End L2/3 Switch using several WDM channels. The

WDM channels from all cloud boxes form the WDM upstream (US) comb employing optical multi-band transmission in, e.g. the O or S bands. The WDM channels are either dedicated to the particular cloud-box (P2P), or they are TDM(A)-shared between two or more cloud-boxes (P2MP). To ensure scalability of this passive connectivity architecture 90:10 couplers are preferred, for low losses on the bus. If 3-dB couplers are used, an optical amplification stage may be needed consisting of two band mux/demux in tandem where band-optimised optical amplifiers are connected in parallel.

The US channels are terminated into the High-End (HE) L2/3 switches, where the traffic flows are aggregated and are either forwarded towards the Metro or towards cloud-boxes forming the downstream (DS) traffic. The latter is transported using WDM channels in optical bands different to the US, e.g. in the C and L bands. In this way, the US and DS traffic are completely decoupled. It is pointed out that there is no direct connectivity between two different cloud-boxes as this is solely performed by an HE L2/3 switch. Also, it is pointed out that the total physical length of this LAN is of the order of 100-200 meters. The proposed architecture is modular as cloud-boxes are added per optical bus while several optical buses may operate in parallel.

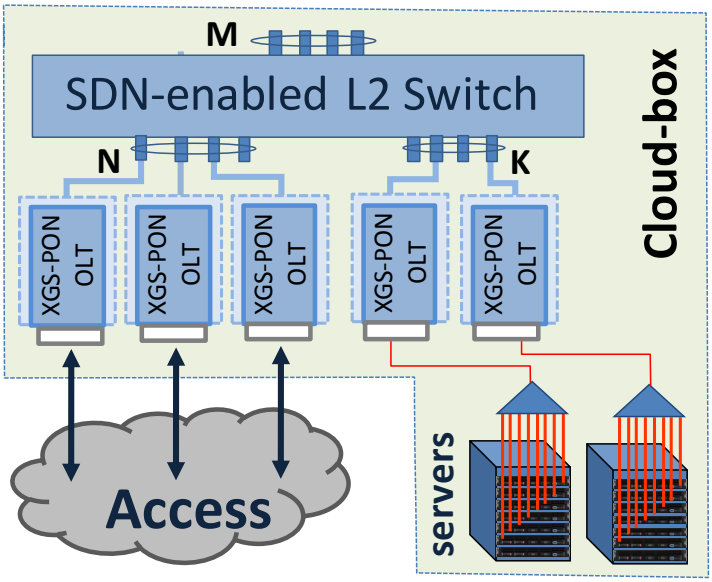

Figure 31: Detailed view of a Cloud-box

Figure 31 shows in more detail a cloud-box: the L2 switch has several physical south/northbound ports. N of the southbound ports is interfaced to 10G OLTs that terminate traffic flows from Access. At the same time, there are K ports that terminate local PON-systems which are connected to server blades (Tier-1; Figure 1 and 2 of [47]). Therefore, the L2 switch of a cloud-box may interconnect traffic flows between Access and the local server blades while forwarding traffic towards the HE L2/3 switch and other cloud-boxes. For the latter function, the M physical northbound ports of the L2 switch are used.

In any case, PON becomes the preferred technology to intra and inter-AMEN connectivity, and we proceed to present the architecture for PON abstraction and virtualisation. This is important in the quest for SDN-enabled control-plane that integrates the heterogeneous systems of an AMEN while it allows the dynamic handling of the corresponding resources

5.3.1 PON abstraction methodology

The SDN architecture for a PON exploits the abstraction scheme described in D3.1 where the active elements in the US/DS paths, i.e. the OLTs and ONUs, are represented as legacy OpenFlow/NETCONF L2 switches as depicted in Figure 32. Under this abstraction, the north/southbound physical ports of

a PON that are used for its interconnect to a network infrastructure, i.e. the upstream port of OLT the (p1) and the downstream ports of the ONUs (p2-p5), are portrayed as the logical ports of a switch.

The proposed abstraction scheme is offering two advantages: a) it is hiding the PON specific details related to forwarding and control/management operations; b) vendor-specific configuration commands are automatically translated and executed by the PON components. Therefore, the forwarding command messages are exchanged using the standard OpenFlow protocol, while (re)configuration is realized using the NETCONF protocol. In detail, the Metro abstraction was realised using the legacy-switch YANG model to which the BroadBand Forum's GPON QoS queue models [48] were incorporated. This allows us to capitalize on the extensively developed SDN-framework while offering two advantages: a) standard OpenFlow/NETCONF protocols are used without extensions; b) the vendor-specific configuration details are automatically translated and executed based on the OpenFlow forwarding flows and NETCONF model.

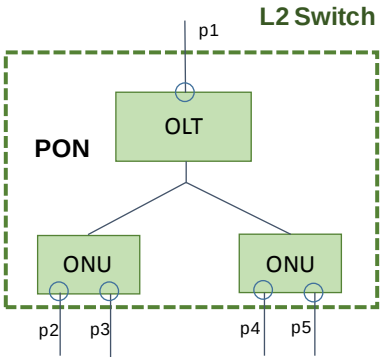

Figure 32: Schematic representation of PON abstraction;

The building blocks of the SDN control-plane are depicted in Figure 33, and they consist of: the ConfD [49] configuration management system, the PON Configuration Agent (PCA), the PON Network Flow Agent (PNFA), the L2 Switch Agent (SA) and the Docker Management Agent (DMA).

ConfD is responsible for retaining the configuration status of the Metro network. The ConfD framework is a model-driven framework. Therefore, it automatically renders all the management interfaces from a data-model (the abstracted PON YANG model in our case). When the configuration/status parameters of this model are changing, the changes are automatically updated to the corresponding management interfaces. As ConfD also supports transactions, it provides transaction-safe configuration changes on the NETCONF interface towards the network controller (NetConf client in our case).

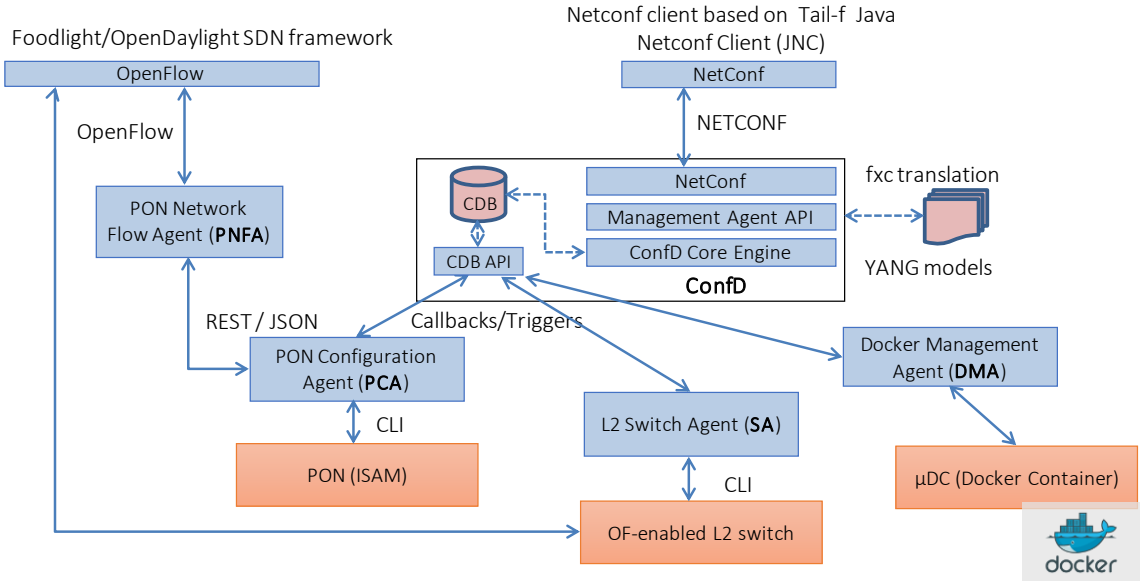

Figure 33: A schematic representation of the SDN architecture

This means that the configuration state of the PON rolls back to the previous stable state in case of unsuccessful configuration attempts due to connection failures or unexpected problems. These operations offer operational simplifications to an operator since they ensure a fully consistent configuration state for the PON.

The entire configuration status is stored at the Core engine DataBase (CDB) of ConfD. When configuration requests arrive from the application layer via the North Bound Interface (NBI), the ConfD Core Engine Agent retrieves the data stored in CDB and updates the configuration. Moreover, through the Application Programming Interface (API) of the CDB, it informs the other entities, in real time, for the changes made in the configuration status.

Further, the PCA, that communicates with the ConfD via the API of the CDB, it is responsible for realizing the requested configuration changes in the US/DS elements using the Command Line Interface (CLI): when the configuration is modified, the CDB engine informs the PCA for the changes and the PCA generates the appropriate CLI commands and executes them directly to the corresponding PON.

For the PCA, we have implemented a set of configuration capabilities that enable the dynamic operation of the PON (see Table 15). These functionalities are exposed to ConfD and towards the network controller (NetConf client) through the appropriate YANG representation while their realisation is implemented via a set of callback modules that trigger specific actions at the CLI. Moreover, the PCA exposes the port configuration details to the PNFA which is responsible for the representation on the OpenFlow Controller at the abstracted view of the network (as L2 switch) together with the translated OpenFlow flows through the available REST interface.

Table 15. PCA Configuration Capabilities

Category		Configuration capabilities
PON element configuration:	VLANs	Management of VLANs
	VPLS	Management of Virtual Private LAN Services (VPLSs)
	ports	Management of ports • Bridging/ unbridging of ports
	bandwidth profiles	Management of bandwidth profiles • QoS parameters: committed-info-rate (CIR), assured-info-rate (AIR), excessive-info-rate (EIR), delay-tolerance
	queue	Management of queues • Generation of priority bit to queue mapping • Assignment of bandwidth profiles to upstream queues • Management of ingress QoS queue profiles and assignment to VLANs
PON status monitoring		Retrieve the status of OLT, ONU, VPLS, VLAN, port, queue, bandwidth profile

Similarly, the PNFA implements the flow management of the infrastructure. The PNFA uses the OpenFlow protocol to receive OpenFlow requests from the OpenFlow controller and forwards them to the PCA. The PCA is responsible for translating these requests to the appropriate element mapping (e.g. VLAN to queue) and execute the appropriate commands. When a new PON is activated, the PNFA is also responsible for informing the OpenFlow controller the activation of a new abstraction switch, and to setup the initial configuration OpenFlow flows.

The servers of the AMEN are deployed as a VM, in which a set of containers (Docker containers) are hosted and managed. The VM is also responsible for forwarding traffic to the appropriate container (using e.g. port forwarding). For experimentation purposes, Ubuntu Docker images in which the following tools are deployed: a) iputils-ping: for enabling pin commands; b) net-tools: for enabling networking information (e.g. ipconfig etc.); c) iperf3: for generating and receiving traffic from/to container. The Docker Management Agent (DMA) is responsible for instantiating and executing Docker images in the VM in an ad-hoc manner. The DMA module is triggered by the ConfD through the CDB API.

Finally, the L2 Switch agent (SA) creates the appropriate VLANs on the switch for the forwarding of traffic either to the local DC facilities or to the remote DC (cloud), and OpenFlow is used for the creation of the appropriate forwarding rules based on VLAN tagging

The events and interactions between the different components above are illustrated in the sequence diagram of Figure 34.

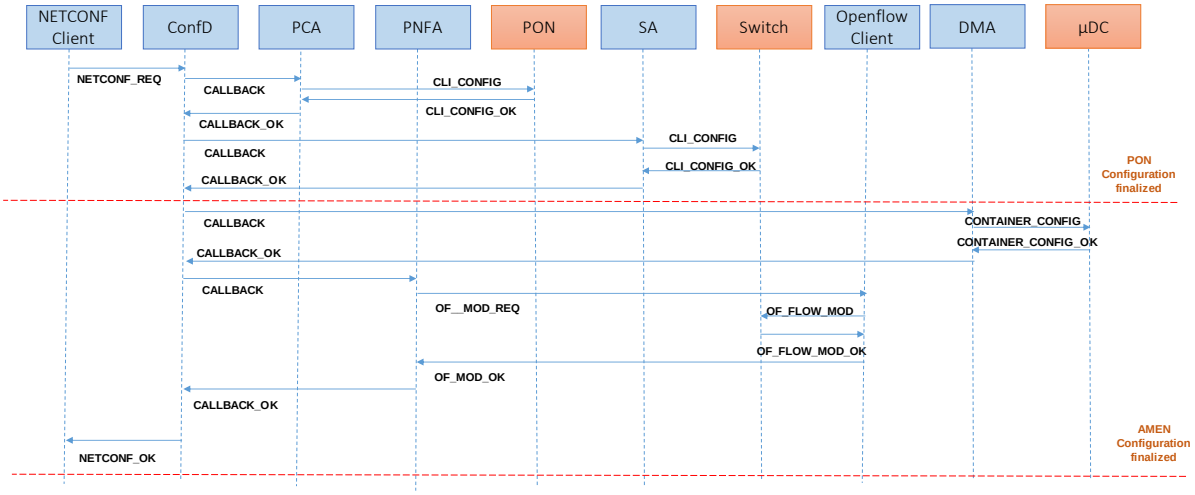

Figure 34: Sequence diagram of the interactions between the components

According to the sequence diagram, initially, NETCONF Client sends a NETCONF request message (NETCONF_REQ) to the ConfD using the NETCONF API of ConfD. The message contains the new PON configuration which follows the abstracted YANG model described above. The ConfD, based on the new configuration and current configuration decides on the configuration actions to be executed. Based on this decision, ConfD triggers the PCA through its CDB API. The PCA module is responsible for realising the new configuration on the actual PON hardware by executing a set of CLI commands (CLI_CONFIG) through its CLI interface. When all the commands are finalised, the PCA module informs the ConfD that the actual configuration is finalised (CALLBAK_OK). Also, in cases that the L2 switch needed to be configured (e.g. CLAN configuration) ConfD triggers the SA module, which is responsible for applying the new switch configuration to the actual switch using CLI commands (CLI_CONFIG). When the configuration is finalised, the ConfD is informed (CALLBAK_OK). As a next step, the µDC configuration follows. In order, the containers of µDC το de deployed/configure, ConfD communicates with the DMA. The DMA deploys, configures or executes selected containers in the VMs of µDC using standard Docker commands. Finally, ConfD triggers the PNFA module, which is responsible for executing the appropriate OpenFlow flow modification commands on the OpenFlow Controller. These commands are realized in the actual L2 switch through the OpenFlow Controller. When all the set of triggers are executed successfully (all CALLBAK_OK messages received), ConfD replies to the NETCONF Client with the NETCONF_OK message.

5.3.2 PON abstraction Validation

For the validation of the PON SDN architecture, we implemented the PCA and PNFA components, and we integrated all the already available components (like ConfD). Regarding the PON equipment, a GPON system (ISAM 7330) provided from NOKIA was utilised.

The test scenarios employed were designed to alter the characteristics of a network slice (which translates to modification of the actual parameters of upstream queues in the GPON network):

- Shaping the bandwidth profile of a queue
- Activation/deactivation of queue profiles
- Assigning bandwidth to queues

Several different traffic loads were generated using the Iperf software for (TCP and UDP flows) and the VLC Server/Client (for VBR video flows) The results were evaluated in terms of

- Control plane latency for applying the new configuration
- Data plane interruption time

Table 16: PON queue configuration

The upstream queue configuration profile	TCONT type	Fixed BW	Assured BW	Maximum BW
Initial queue profile	TCONT-1	5	5	5
Queue profile after time t1	TCONT-5	5	7	7
Queue profile after time t2	TCONT-5	5	10	20

The different queue configurations through time are depicted in Table 16. According to the scenario, initially, the queue is of TCONT-1 with a bandwidth of 5 Mbit/s. At time t1 the queue configuration is modified to TCONT-5 with a bandwidth of 7 Mbit/s, while at time t2 the queue configuration is modified to TCONT-5 with a maximum bandwidth of 20Mbit/s. During the experiment, both data and control plane statistics were collected.

Table 17: Control Plane latency

KPI	Average	Min	Max
Latency in PCA for PON reconfiguration (ms)	960	666	1373
Latency in PCA for PON reconfiguration causing DATA interruption (ms)	798	512	1221
Total latency in PCA	1300	975	1756
Total NETCONF configuration cycle (request-update-response) (ms)	1855	1503	2288

The results of control plane latency are depicted in Table 17, measured over 30 iterations of the experiment.

Figure 35: Data interruption time for VBR video traffic

Figure 35 illustrates the performance results on an already established VBR video streaming flow (average bitrate=7Mbit/s) generated using the VLC server/client.

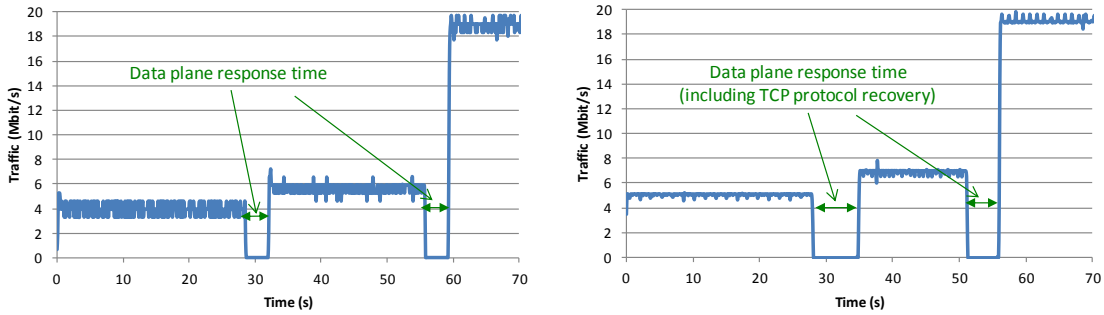

Figure 36: Data interruption time for (a) UDP traffic, and (b) TCP traffic

Figure 36 (a) and (b) present the same results in the case of UDP and TCP flows respectively generated using the iperf traffic generator.

To summarize, we measured a control plane latency in PCA of around 1s and a total control plane latency for the whole reconfiguration cycle of about 2s. This cycle includes all the steps between the NETCONF client and the PON equipment, described in the sequence diagram of Figure 34 (steps from the start of the sequence until the dotted line of PON configuration finalization). The data interruption time depended on flow and protocol characteristic and was found to span between 3 - 3.5s (UDP) and 5 - 7s (TCP, including TCP protocol recovery).

5.4 Programmable packet switching solution for interconnection

The University of Bristol proposes a disaggregated edge node that can be programmed on demand to support multiple front-haul/back-haul protocols such as CPRI/eCPRI and Ethernet. This node provides aggregation/disaggregation of any optical access traffic with stringent synchronization requirements and different bandwidth granularities, optical transport based on time slot switching in a programmable way. Furthermore, the same node can offer access to highly programmable coherent variable bandwidth transponders suitable for spectrally elastic long-haul transmission.

5.4.1 Edge Node Architecture

The proposed edge node architecture is based on the integration of three major components: a Voyager switch, one or more aggregation Field Programmable Gate Array (FPGA), and two Wavelength Selective Switch (WSS). A more detailed description of the equipment is presented in Section 5.4.2.

In addition to the above-mentioned equipment, both the FPGAs and WSSs have dedicated agents to configure them. Also, these agents provide RESTful API communication with the corresponding driver implemented in the southbound OpenConfig Agent. Since the Voyager has a REST server implementation on it, a dedicated agent is not required.

Next, an extra agent provides compatibility and compliance with OpenConfig YANG models. The OpenConfig Agent has specific drivers to communicate with the three components of the node using RESTful API. The design of a single agent was chosen due to restrictions on the ONOS controller drivers, since a Transponder Device which interfaces the packet network with the optical network and vice versa, is represented as a single terminal device in ONOS. Currently, the terminal device drivers in ONOS are based on OpenConfig and are part of the official ONOS source code as contributed under the ODTN and METRO-HAUL project, hence the choice of OpenConfig agent in southbound is justified. In future, if the ONOS implementation allows, this single agent could be replaced by individual agents for each of the components in the node.

Finally, the communication between the ONOS controller and the OpenConfig Agent is performed using the NETCONF protocol. The agents used are based on the CNIT agents described in Section 6.2. The described node architecture is presented in Figure 37:

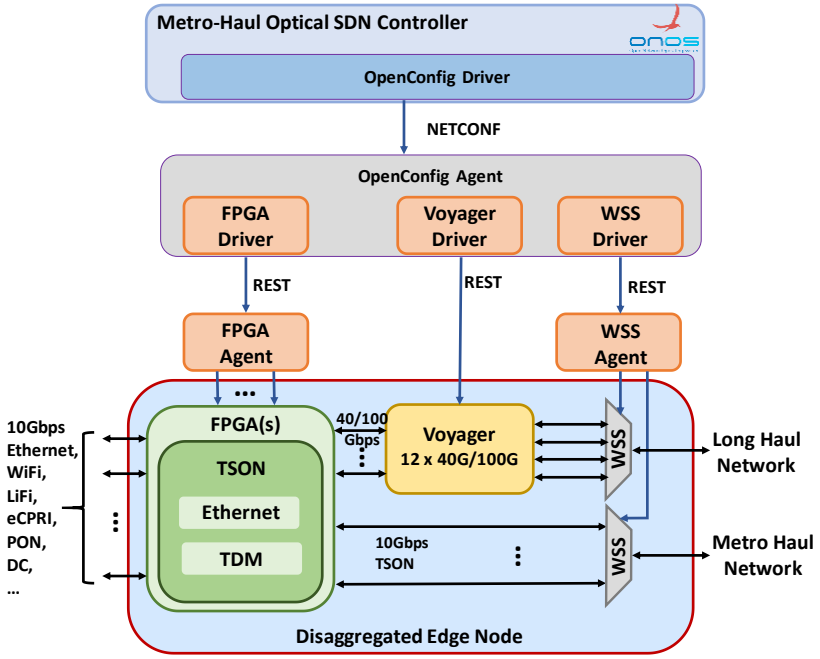

Figure 37: Disaggregated Edge Node Architecture

5.4.2 Data Plane Equipment

5.4.2.1 FPGA

FPGA platform is used to implement aggregation/disaggregation function. This component of the edge node is fully programmable by using an SDN controller. It also supports two transport mode, which are TSON and Ethernet. Both functions, TSON and Ethernet, can operate together depending on the demand sent by an SDN controller. Indeed, the aggregation and the disaggregation using a specific transport function and selecting specific input and output ports can be programmed.

TSON technology is an active Wavelength Division Multiplexing (WDM) solution which can be used in the dynamic optical transport network. It is the first multi-protocol programmable interface that meets 5G KPIs. It provides variable subwavelength switching granularities and the ability to dynamically allocate optical bandwidth elastically with a unique time-sharing mechanism. Hence, diversified Quality of Services (QoS) can be satisfied through the dynamic connectivity with the different granularities of bandwidths with a time-sharing mechanism.

This edge node contains two types of FPGA implementation (Figure 38):

- The ingress node: responsible for the parsing, aggregation and mapping any input traffic combination with different bandwidths (less than 10Gbps) into either 10Gbps TSON outputs or the converged 40Gbps Ethernet output.
- The egress node: disaggregates traffic from transport network to different output traffic with different granularities.

Since the OpenConfig agent from CNIT is used currently, the control plane design will be more focused on the ethernet mode as required by the METRO-HAUL project.

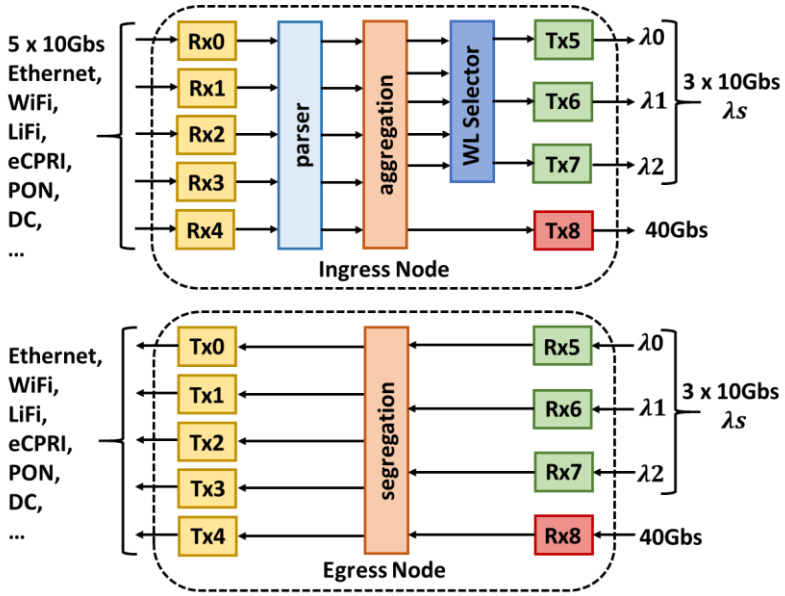

Figure 38: Architecture for Disaggregated Edge Node

5.4.2.2 Voyager and WSS

The Voyager and WSS are also part of our edge node. Under the SDN control, any access traffic combination from the FPGA can be aggregated/disaggregated to/from a transport network based on the operator or service provider requirements.

We use the Voyager, a Broadcom Tomahawk-based switch, as the optical transponder in the proposed edge node. It supports Dense Wavelength Division Multiplexing (DWDM) and hosts multiple Bandwidth Variable Transponders (BVTs) that can allocate variable spectral width and reach dynamically by modifying corresponding device parameters. The Voyager agent is responsible for changing such parameters, such as physical interfaces, modulation formats, the link speed, the power and the Forward Error Correction (FEC). Three types of modulation formats, namely PM-QPSK, 8-QAM, and 16-QAM, can be chosen for different line rates up to 200Gbps. Additionally, it can switch traffic on a configurable wavelength on its transponders and thus, act as a gateway between the packet and optical domains for the network. Voyager has 12 QSFP/QSFP28 Ethernet ports and four DWDM ports that can be configured from the control plane. The Ethernet ports are internally connected to the Broadcom Tomahawk ASIC (BCM56960 SERIES), and they receive the aggregated traffic from the FPGA which is encapsulated to OTN signals at the transponder ports.

The WSS, filtering and switching of the optical signal, is used as a programmable 4x16 optical switch that multiplexes and demultiplexes the optical signals to specific ports. There are two WSSs in the edge node architecture (shown in Figure 37:), one is connected to the voyager, and another is to the FPGA short range optical ports. The WSS multiplex and demultiplex four wavelengths with different bandwidth from the voyager and FPGA ports.

5.4.3 Control Plane

The control plane consists of an ONOS SDN controller, and device agents are implemented on the top of the disaggregated edge node to bring flexibility and scalability to this architecture. It allows the programming and dynamic configuration of different components of the disaggregated edge node. The SDN controller consists of the OpenConfig driver which programmes the disaggregated edge node.

Currently, in ONOS, the configuration of the terminal device is one client port (e.g. Ethernet) to one line port (OCh) mapping. This will be extended so that multiple ports on the client side will be mapped to a line port; where the SDN controller will receive a REST request containing the description of the network services to be deployed. This request will specify the FPGA ingress and Voyager egress ports, and optionally VLAN tags, modulation format, FEC, power and central frequency of the voyager BVT. Based on this request, the driver in the SDN controller sends corresponding parameters to the device agent. Several agents can be connected to the same driver.

The OpenConfig agent receives port information, including ingress/egress ports. Then, it translates the information to program the FPGA configuration registers via its Peripheral Component Interconnect Express (PCIe). The voyager receives the configuration parameters consisting of VLAN tags, ports, modulation format, FEC and power. The WSS agent receives the optical parameters including central frequencies, associated bandwidths, and port interconnection, thus creating a configuration file and sending it to the WSS, effectively configuring it.

5.4.4 OpenConfig Representation

The described OpenConfig Agent is based on the agent developed by CNIT and further described in Section 6.2. Hence, this section focuses on the specifics for the equipment, as mentioned in Section 5.4.2.

The agent is based on abstractions of the aggregation FPGA, Voyager, and WSS devices. Each device is represented by multiple OpenConfig YANG models, mainly the Terminal Device (openconfig-terminal-device.yang) and the Platform (openconfig-platform.yang) models.

The OpenConfig Platform model represents a system component inventory, which can include hardware or software (e.g., ports, transceivers, and fibers). Such components may or may not have their own model, e.g., port and transceiver and their specific models: openconfig-platform-port.yang and openconfig-platform-transceiver.yang, respectively. Furthermore, the OpenConfig Terminal Device model represents a terminal optics device of a WDM transport network. One of the most important elements of the model is the logical channel, used to represent a flow of information between components and other channels.

Figure 39 shows the relationship between the OpenConfig Agent, the equipment abstraction, and the drivers. The components of the FPGA are: n Ports, n Transceivers, and one Optical Channel. Each Port is associated with one Transceiver, and each Transceiver is connected to one Logical Channel (LC1, ..., LCn). These Logical Channels represent the traffic flow related to the client-side of the FPGA. Next, these client-side Logical Channels can be connected to another Logical Channel (LC n+1), that is connected to the Optical Channel. This latter line-side Logical Channel (LC n+1) represents the connection of the FPGA with the fiber.

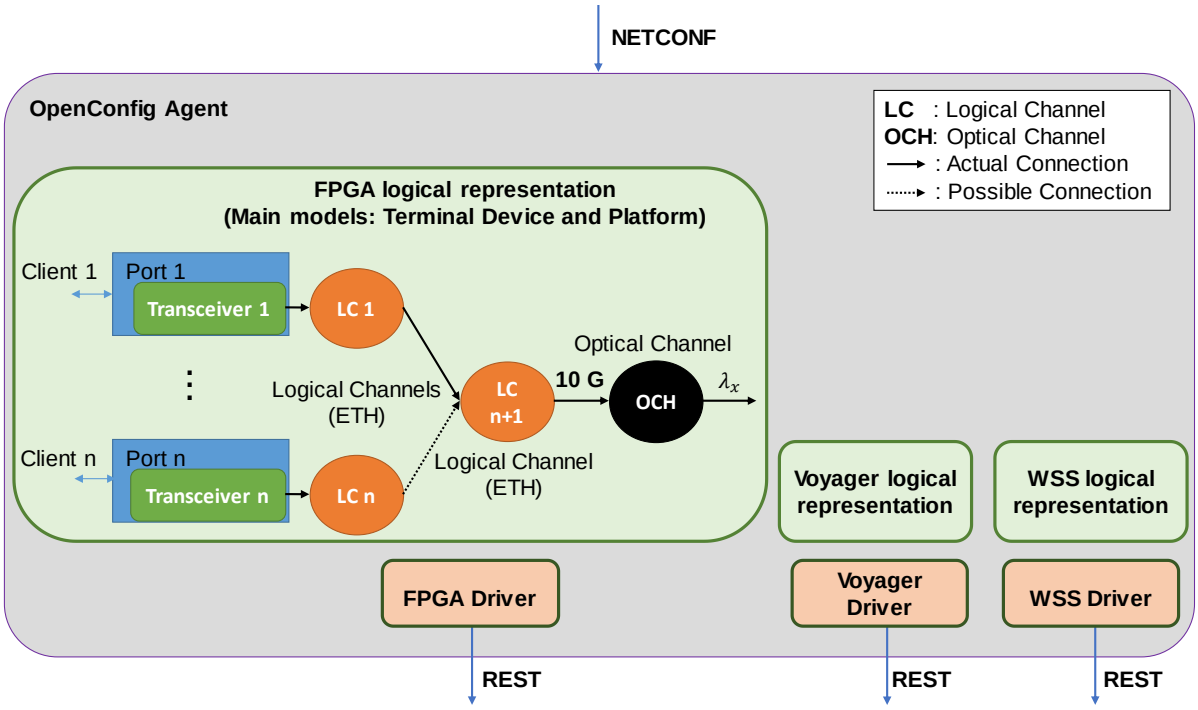

Figure 39: Example of the schema for FPGA modelling based on OpenConfig YANG models

Both the Voyager and the WSS modelling are still in progress, following the same logic.

5.4.5 Edge Node Data Plane Validation

We have adopted a Xilinx FPGA vcu108 evaluation board for the implementation. Each edge node contains two FPGAs. Figure 40 shows the testbed setup architecture with two disaggregated edge nodes. Edge nodes are connected from one side to 10 x 10 Gbps Ethernet traffic analysers and from the other side to the Bristol City Metro Network and 100 km/200 km optical fibre link. The 10Gbps traffic can be aggregated to 40Gbps traffic that is sent to either long-distance network through Voyager and WSS or transmitted to the metro network according to different control policies.

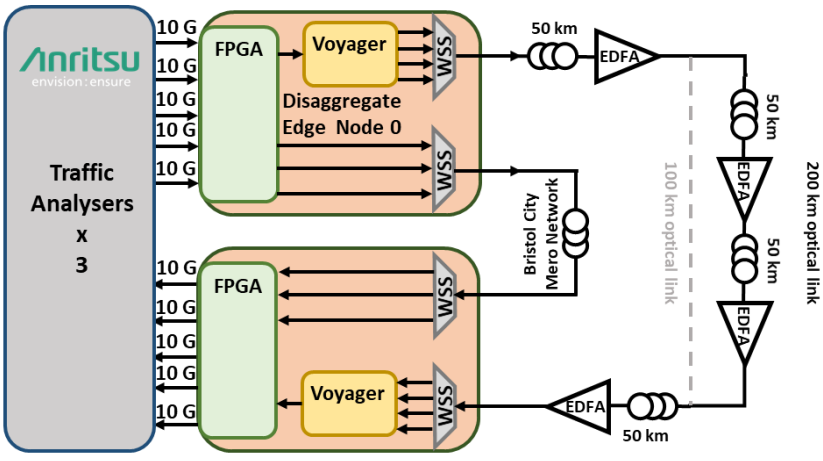

Figure 40: Disaggregated Edge Nodes Testbed Setup Architecture

Three different network scenarios are considered for the experimental evaluation of the metro and long-haul networks. The first scenario involves using the Bristol City metro network connecting two disaggregated edge nodes for both networks. The second scenario is for over 100km/200km of optical fibre. We have used a fixed frame of 1500B length to evaluate the proposed scenarios. Fine

and coarse bandwidth granularities have been considered to evaluate the 100km/200km case. In the fine granularity case, the packet size is the same as the Ethernet frame, i.e. 1500B with 10Gbps bandwidth. In the coarse granularity case, the packet size is 15000B with 50% utilisation, which means that two 5Gbps Ethernet clients are mapped to one wavelength to use the full line rate capacity of 10Gbps. The Ethernet performance parameters under consideration include Bit Error Rate (BER) and latency, which refers to the time difference between the arrival of a frame at the analyser and its departure from the analyser.

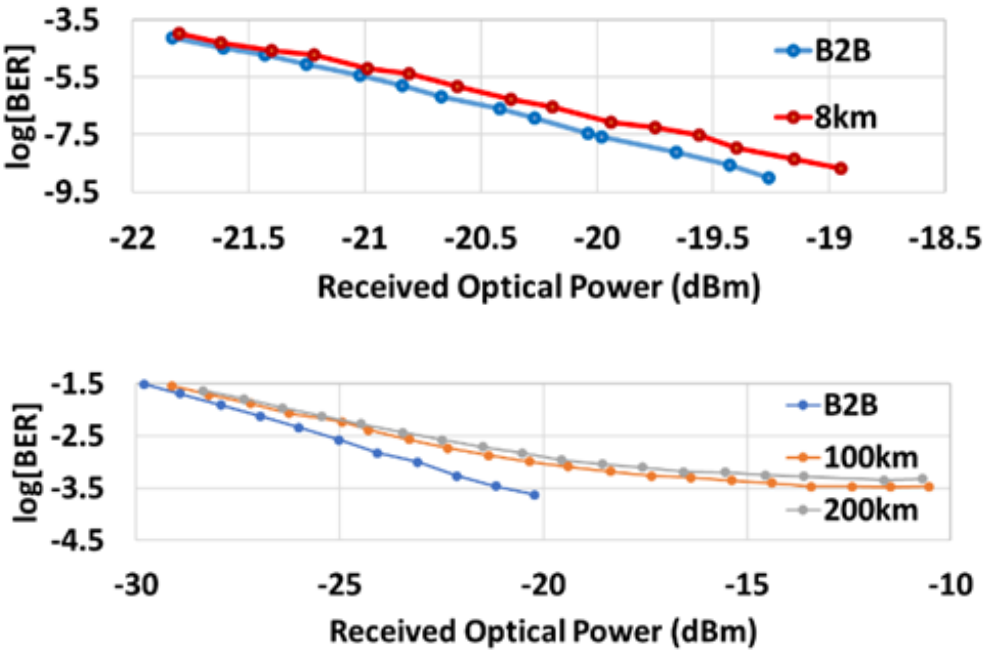

Figure 41: (a) Metro Network BER, (b) Long-Haul Network (100km/200km) BER

Figure 41 (a) displays the BER for the metro network. Comparing to the B2B scenario, the penalty for 8km transmission is lower than 1dB and can be neglected. Figure 41 (b) shows the BER for the long-haul network, where the worst-case scenario corresponds to the voyager modulation of 16QAM. Due to the dispersion on the optical fibre transmission and the noise of amplifier, the BER for 100km and 200km transmission are increased.

5.5 Monitoring probes

Within the project, several monitoring systems have been developed, ranging from the optical layer to the data-link layer. This section is devoted to the data-link layer.

To monitor the network at the data-link layer, two different types of probes have been developed: active and passive network probes. Passive network probes are covered in this work package, whereas active network probes are covered in WP4.

5.5.1 Description

This element is in charge of monitoring the system at the packet layer, composed of a set of network traffic probes watching which service is being provided by the underlying layers. The obtained measurements are made available to the monitoring and data analytics system. These elements are needed to design a monitoring system with big-data analytics framework supporting cognition.

Passive probes capture and measure existing network traffic at the packet level. In Metro Haul project, these measurements have been developed for 100 Gbps Ethernet links.

5.5.2 Sub-components

- D14 - Passive Traffic Probe at 100 Gbps, developed in this work package, and described in this deliverable.
- D15 - Active Network Probe at 100 Gbps, developed in WP4 (for more information, please refer to deliverable D4.2).

5.5.3 Status

Current development is now able to provide time series (1s resolution) of bytes, packets and flows.

Measurements from the network (flows, bytes and packets per second) are stored on the probe for later use/analysis.

There have not been any deviations w.r.t D3.1

A first version is to be released at the end of 1H2019.

5.5.4 Related testbed and platform

The probe is being validated in the Naudit 100G local testbed in Madrid, and will be further validated in the Berlin Demo testbed, measuring the delays in the network. The integration with Berlin demo is expected for M30.

5.5.5 Functional Tests

To test the passive probe, a traffic generator is used, based on existing network traces. However, these traces have been obtained at 10Gbps, so we have to mix them to have something similar to a 100Gbps trace. Based on the received traffic, the probe collects the data and generates the time series.

The passive probe has to be integrated with two other components:

- Network switches: network traffic is captured from these elements. For this, there are two possibilities:
    - Mirror port in the switch.

- Network taps in the link from the switch to the transponder.

Currently, the network probe has been tested with the mirror port option.

- Network Monitoring and Analysis System: network measurements are sent to this element. The integration was tested and already presented at OFC'18.

5.5.6 KPIs

KPI Description	Bytes time series
Context	It provides information on the volume of the network traffic that is transmitted in a link. They are useful to let a network manager know the occupancy of a link and if it is necessary to establish a new link.
Target	Time series values are provided every second.
Assessment	The probe passively counts the bytes of the captured packets.
Relationship to project KPIs	This KPI can help to measure the MH6 (Capacity of METRO-HAUL infrastructure) KPI, and reduce the MH5 (Fault/degradation detection time).

KPI Description	Packets time series
Context	It provides information on the packets that are switched in a link. They are useful to let a network manager know the load of the switching elements in the network.
Target	Time series values are provided every second.
Assessment	The probe passively counts the captured packets.
Relationship to project KPIs	This KPI can help to measure the MH6 (Capacity of METRO-HAUL infrastructure) KPI, and reduce the MH5 (Fault/degradation detection time).

KPI Description	Flows time series
Context	It provides information on the flows that are traversing a link. They are useful to let a network manager decide how to work with the traffic in a multilayer scenario.
Target	Time series values of active flows are provided every second.
Assessment	The probe passively counts the flows from the captured packets.
Relationship to project KPIs	This KPI can help to measure the MH6 (Capacity of METRO-HAUL infrastructure) KPI, and reduce the MH5 (Fault/degradation detection time).

5.5.7 Availability

The hardware development is not publicly available at this moment, but an FPGA bitstream can be made available to other partners on request to be used for other project tasks.

The software development associated with the hardware can be released at the project Gitlab if necessary.

5.5.8 Interfaces

To export these measurements to a collector, IPFIX records are exported from the passive network probe and sent to the MDA system.

6 Agents

The METRO-HAUL consortium, as reported in D3.1, has adopted the OpenROADM model for the optical network equipment (O-NE) performing optical switching (e.g., WSS-based ROADM, photonic integrated switching matrices) and the OpenConfig YANG model for O-NE of type transponder. In this deliverable, the implementation of the software agents for either type of O-NE is reported.

Each agent software architecture has been designed to account for the support of different specific O-NE hardware implementations. For example, the OpenConfig agent implementation is composed of two main sets of software components. The first set is common for any type of transponder implementation and includes the NETCONF-based OpenConfig YANG model and the telemetry service. The second set of software components, python-based, is specifically designed to interface the first common components with the underlying vendor/system-specific hardware. Thanks to this approach, only the latter software component has to be adapted to provide OpenConfig support to any transponder implementation, significantly limiting integration effort. A similar approach has been adopted for the design and implementation of the OpenROADM agent.

Specific YANG model extensions have also been designed and implemented, enhancing the standard models to support the innovative transmission and switching solutions designed within the METRO-HAUL project and detailed in the previous chapters (e.g.,[50]).

In the next sub-sections, the two METRO-HAUL OpenConfig and OpenROADM Agent software implementations are summarized. Both implementations, in line with Milestone 3.5, include all expected functionalities and have been successfully tested in preliminary validations of disaggregated scenarios. WP5 will adopt them for integrated METRO-HAUL demonstrations.

6.1 OpenROADM Agent

OpenROADM is a Multi-Source Agreement, led by AT&T and composed of more than 20 among vendors and network operators, aiming at defining interoperability specifications for ROADMs, transponders and pluggable optics. Specifications consist of both interoperability at the optical level as well as YANG data models for the control and management of the optical infrastructure.

The MSA specifies YANG models at device, network and service level. At the optical network equipment (O-NE) level, only the first specification applies.

The OpenROADM device YANG data model defines the following objects to abstract the implementation of a ROADM device:

- **Info**: provides general node information, including node name, IP address, etc.
- **Shelves:** provides shelf information. A node can consist of one or more shelves.
- **Circuit Packs:** represents a physical piece of equipment which contains a group of hardware functional blocks such as common equipment, cards, plug-in-units and pluggable optics.
    - The **Ports** container defines the ports associated with a circuit pack or pluggable optics and the associated port attributes
- **Internal Links:** reflects the connectivity within each circuit pack. These objects are read-only and report attributes of the circuit pack themselves.
- **Physical Links:** reflects the connectivity between ports across different circuit packs. The controller pushes this data to the device and reflects the actual inter-card fibering/cabling.
- **External Links:** these objects are placeholders for data about the far end device. Data for these objects are pushed from the controller.

- **Degrees:** defines the grouping of circuit packs that form a line degree.
- **Shared Risk Groups:** defines the grouping of circuit packs that form a colorless/directionless add/drop bank.
- **Connection Map:** is wavelength agnostic and reflects any connectivity restrictions / blocking in the device (not wavelength contention).
- **Interfaces:** defines supported interface types and the association with Port objects.
- **Roadm-connections**: lists the cross-connections between couples of interfaces (two line interfaces or one line interface and one add-drop interface)

The NETCONF agent has been implemented using Netopeer [51] and the transAPI tool [52], both based on libnetconf, through which it is possible to create a Netconf server focusing the development solely on the management of the device. Using the transAPI, it is possible to invoke a specific call-back function whenever an *edit-config rpc* operation performs changes on a branch of the configuration. The agent has, therefore, call-back functions that manage the controller requests for the creation of the interfaces that, according to the OpenROADM device model, are required for connection setup and, in turn, the request for the connection itself.

To decouple the OpenROADM model processing from the action required by the underlying hardware, the agent can load specific drivers at runtime. Drivers are coded as Linux dynamic libraries associated with a *circuit-pack* having a specific *circuit-pack-type* and loaded by the main module when an *edit-config rpc* creates a new *circuit-pack*. Figure 42 shows the agent architecture.

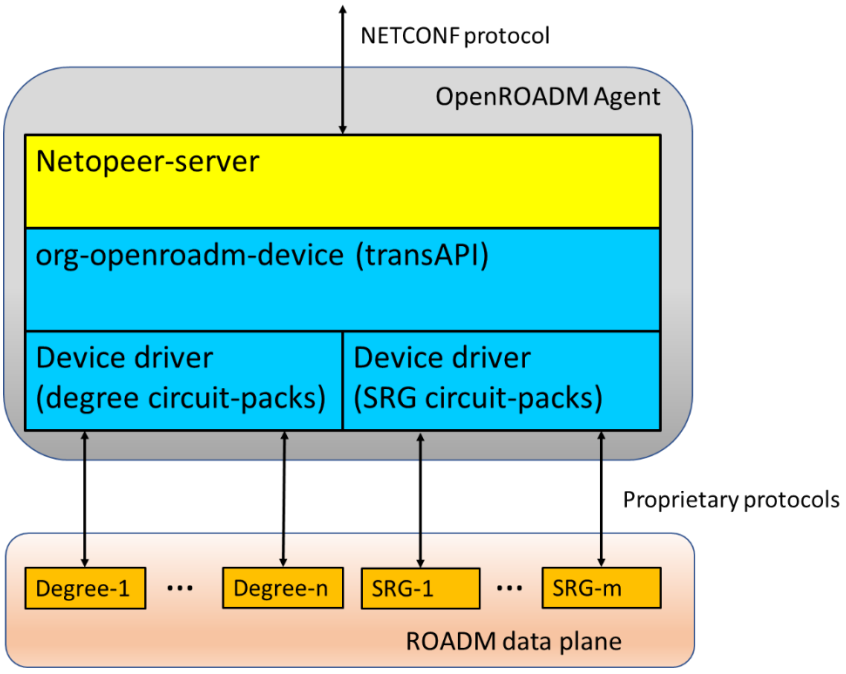

Figure 42: NETCONF OpenROADM agent architecture

The driver module should implement a few functions to perform actions on the corresponding circuit-packs. For the time being, a module can implement the following actions:

- **init**: called during agent startup, it is in charge of setting up the communication session and of the initial device setup.
- **close**: called at agent closing to free all the allocated resources.
- **get_inventory**: called when the agent needs circuit pack inventory info.
- **get_port_operational_state**: called to get the operational state of a circuit pack port.

- **make_connection**: cross-connection (spectral window) creation between circuit-pack ports.
- **delete_connection**: cross-connection removal.

All functions are optional (to cope with circuit packs that have no programmability, such as mux-demux) but the followings constraints apply:

- If *init* function is defined, the *close* function must be present.
- If *make_connection* function is defined the *init* function must be present.
- If *make_connection* function is defined the *delete_connection* function must be present.

Other functions could be added in future releases of the agent, for example to manage power settings.

The current software architecture is flexible enough to manage ROADMs composed of circuit-packs from different vendors and allows easy implementations of emulators, since it is possible to create "dummy" drivers that perform no actions.

The OpenROADM Agent has been designed and implemented by TIM. An emulator of a colorless/directionless 3 degrees and 1 add/drop port ROADM has been released as a docker container available in the project GitLab [53].

The previous release of the agent, implementing the same core functions but devoted to the TIM-ROADM, has been successfully tested and demonstrated at the ECOC 2018 demo session in a configuration where an ONOS instance controlled a disaggregated optical network composed of Coriant transponders and TIM ROADMs. The current version will be used during the control plane demo at EuCNC 2019.

Within the Project, the agent is expected to be used in WP5 to control the ROADM under development at TU/e.

6.2 OpenConfig Agent

OpenConfig is a working group of network operators, led by Google, devoted to the definition of vendor-neutral data models to be adopted to simplify and standardize the control and management of the optical infrastructure by mean of SDN scheme. Concerning optical transponders, a set of YANG models have been introduced to provide a common way to configure, through NETCONF, the main transponder parameters. More specifically, the root of the tree (*<terminal-device>*) represents an *xPonders* node in a modular structure composed by logical channels associated with physical ports. By exploiting the exposed *<config>* parameters (i.e., target-output-power, central-frequency and operational-mode), the SDN Controller is able to enforce in a standard way a specific configuration to the underlying network devices. Moreover, *<state>* fields are adopted in the data-model in order to store both the key OTN parameters (to be monitored in order to check the status of an active connection, such as pre-FEC-BER, post-FEC-BER, Q factor, ESNR) and the physical parameters at hardware level (i.e., output-power, input-power, chromatic dispersion).

In METRO-HAUL, we provide an open-source implementation of an SDN agent that includes the OpenConfig NETCONF agent enhanced with a gRPC-based telemetry service.

Figure 43 shows the considered optical node architecture. In the bottom part of the figure, the data plane optical node is represented, where xPonders (i.e., several transponders and/or muxponders) are installed. On the top of the figure the control plane software architecture of the SDN agent is shown. Its main functional blocks are:

- the NETCONF agent,
- the device driver (HW-specific).
- the telemetry server.

The NETCONF agent has been implemented using ConfD software [49], adopting the OpenConfig YANG modules. It exposes a North Bound Interface (NBI) to the SDN controller based on NETCONF protocol, allowing the configuration and the monitoring of the main key transmission parameters of the underlying transponders, exploiting the *edit-config rpc* and the *get-config rpc*. Those parameters are maintained in a database (DB) organized according to the OpenConfig YANG modules. The NETCONF agent has been equipped with two ad-hoc defined sockets (i.e., config socket and monitoring socket) to enable the communication with the device driver module. The syntax adopted over the sockets is custom and text-based.

The device driver, developed in python, has two main functions: enforce the configuration received on the config socket to the physical transponder(s) and periodically collect the required key parameters from the physical device and pushing them to the NETCONF agent through the monitoring socket. The communication with the physical device is performed adopting proprietary APIs provided for the control of the devices (i.e., HW-specific).

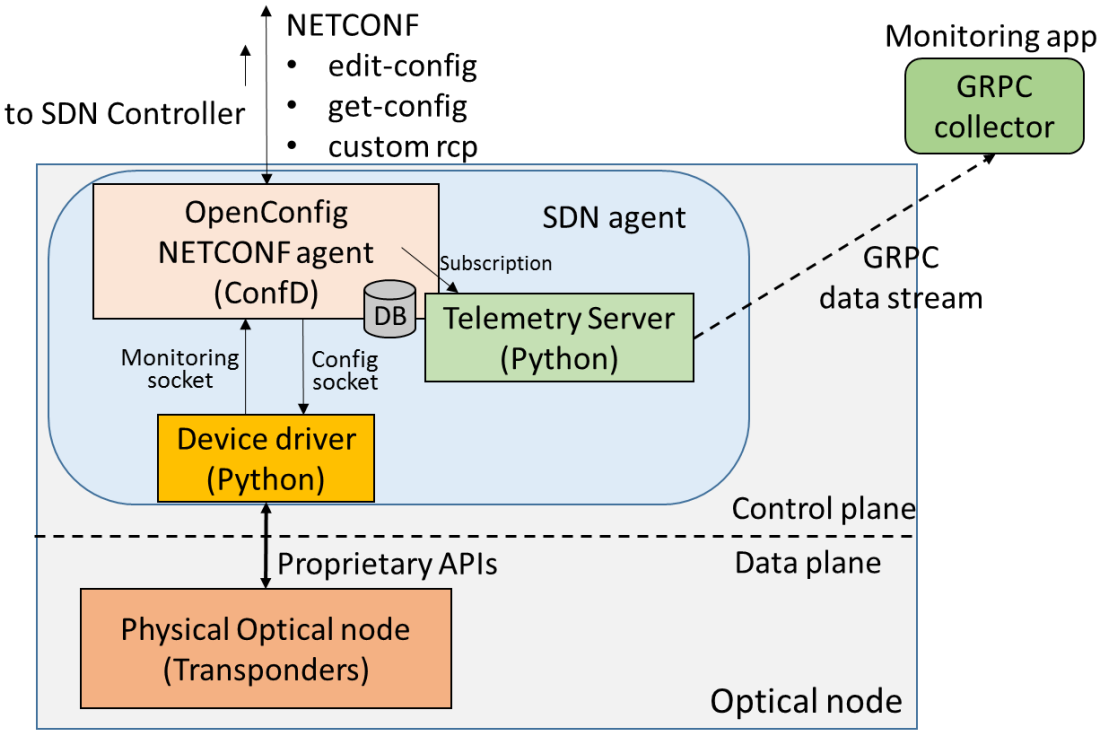

Figure 43: NETCONF OpenConfig agent architecture

The telemetry server is a module devoted to handle the telemetry requests and enable the stream of telemetry information. The telemetry has been implemented using the open-source Python implementation of the gRPC with protobuf protocol. According to the OpenConfig model, the telemetry subscriptions are received via NBI by the NETCONF agent. The NETCONF agent submits the proper gRPC subscription to the Telemetry server, including in the request the remote gRPC collector (i.e., IP address and port), the list of parameters to be monitored (more parameters can be included in the same data stream), the period and the duration of the stream. Then, the telemetry server enables the telemetry stream to the collector, retrieving the data directly from the NETCONF database.

A first experimental validation of the proposed OpenConfig Agent has been performed on the network testbed shown in Figure 44 where two xPonders nodes are equipped with the SDN agent described in the previous section. Each node presents three muxponders: one commercial 100Gb/s with coherent reception, two commercial 10Gbps with direct detection reception. On the link between the 2 ROADMs, we connected a Variable Optical Attenuator (VOA), to induce possible performance degradations on the considered connections. We focused our validation on the xPonders nodes, managed through OpenConfig NETCONF agents, while the ROADMs devices were managed using different (OpenROADM) NETCONF agents.

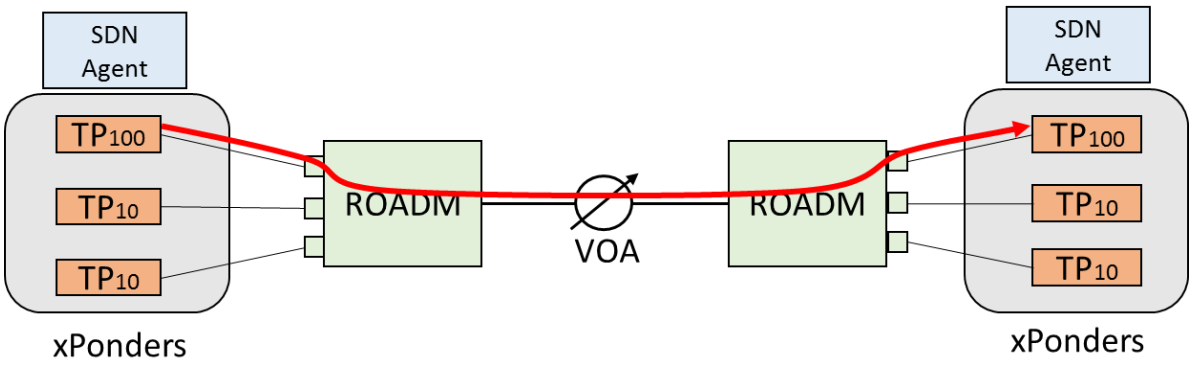

Figure 44: SDN Controller messages and results

Initially, we configured a connection between the pair of 100Gbps transponders. Figure 45 shows the message sent by the SDN controller to configure the two transponders. More specifically, the transponder with index 10102 (i.e., the TP_{100}) was configured with central frequency 192.5 THz (expressed in MHz), output power 0 dBm and the related optical-channel enabled.

After the setup of the connection, the SDN Controller performed the telemetry subscription at the receiver transponder by sending the XML message shown in Figure 45(b). The subscription request includes: IP address and port of the remote collector that will receive the data stream (i.e., 10.30.2.24 and 50083, respectively), the duration (i.e., sample-interval) and the period of the samples (i.e., heartbeat-interval) expressed in milliseconds (60 and 3 seconds, respectively), the option to suppress samples equal to the previous one (disabled), protocol and encoding type (gRPC and PROTO3, respectively) and the list of the required parameters (in the example instantaneous ESNR and instantaneous pre-FEC BER of transponder 10102, expressed according to the OpenConfig hierarchy).

During the experiment, we induced the degradation of the link between the two ROADMs by increasing the attenuation at the VOA. This operation resulted in a soft failure of the connection. The telemetry stream, that included the instantaneous values of ESNR and pre-FEC BER, reported updated data to the remote collector. In Figure 45(c) and d the trends of both pre-FEC-BER, in logarithmic scale, and the ESNR of the connection are reported, respectively. In normal condition (i.e., without the VOA attenuation) the connection presented a pre-FEC BER around $3.7E^{-7}$ and an ESNR of 25.3dB. Once the soft failure occurred, the performance of the connection degraded, resulting in a pre-FEC BER around $4.3E^{-4}$ and an ESNR of 13.5dB. The telemetry functionality allowed the monitoring system to detect the degradation of the performance of the connection (i.e., soft failure) and perform the required operations to recover from the failure or eventually reroute the connection before the connection is a break.

Additional experimental validations have been performed in the context of filterless C+L networks, as reported in [50].

b)

```
<telemetry-system xmlns="http://openconfig.net/yang/telemetry">
  <subscriptions>
    <dynamic-subscriptions>
     <dynamic-subscription>
       <id>1</id>
       <state>
          <id>1</id>
          <destination-address>10.30.2.24</destination-address>
          <destination-port>50083</destination-port>
          <sample-interval>60000</sample-interval>
          <heartbeat-interval>3000</heartbeat-interval>
          <suppress-redundant>false</suppress-redundant>
          <protocol xmlns:t="http://openconfig.net/yang/
                    telemetry-types">t:STREAM_GRPC</protocol>
          <encoding xmlns:t="http://openconfig.net/yang/
                    telemetry-types">t:ENC_PROTO3</encoding>
       </state>
       <sensor-paths>
         <sensor-path>
           <path>/terminal-device/logical-channels/channel
                [10102]/otn/state/pre-fec-ber/instant</path>
           <state>
            <path>/terminal-device/logical-channels/channel
                 [10102]/otn/state/pre-fec-ber/instant</path>
           </state>
         </sensor-path>
         <sensor-path>
           <path>/terminal-device/logical-channels/channel
                    [10102]/otn/state/esnr/instant</path>
           <state>
             <path>/terminal-device/logical-channels/channel
                      [10102]/otn/state/esnr/instant</path>
           </state>
         </sensor-path>
       </sensor-paths>
     </dynamic-subscription>
    </dynamic-subscriptions>
  </subscriptions>
</telemetry-system>
```

a)

```
<components xmlns="http://openconfig.net/yang/
   platform">
  <component>
    <name>channel-10102</name>
    <optical-channel xmlns="http://openconfig.net/yang/
        terminal-device">
      <config>
        <frequency>192500000</frequency>
        <target-output-power>0</target-output-power>
      </config>
    </optical-channel>
  </component>
</components>
<terminal-device xmlns="http://openconfig.net/yang/terminal-
   device">
  <logical-channels>
    <channel>
      <index>10102</index>
      <config>
        <admin-state>ENABLED</admin-state>
      </config>
    </channel>
  </logical-channels>
</terminal-device>
```

c)

d)

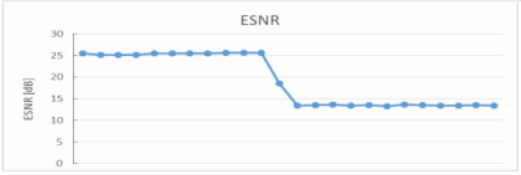

Figure 45: SDN Controller messages and results.

The OpenConfig Agent has been designed and implemented by CNIT. It will be released as open source by the end of the METRO-HAUL project. This will further stimulate the adoption of the OpenConfig standard within the Telecommunication Community.

Within the Project, the Agent is expected to be used in WP5 to control the following O-NEs of type transponders (See D5.2).

METRO-HAUL prototypes:

- OpenConfig Agent for the programmable sliceable transceiver based on multicarrier modulation (MCM) by CTTC (D7)
- OpenConfig Agent for the transceiver solutions for dispersion-tolerant direct detection by CNIT/Ericsson (D8)
- OpenConfig Agent for the elastic transponders with low-resolution DAC and ADCs for metro networks by Nokia (D10)
- OpenConfig Agent for the digital sliceable bandwidth variable transponder for filterless networks by HHI (D11)

Commercial transponders:

- OpenConfig Agent for Muxponder 100G Ericsson SPO (D16)
- OpenConfig Agent for Coriant Groove (D17)
- OpenConfig Agent for ADVA Muxponder (D18)
- OpenConfig Agent for Voyager Muxponder (D19)

7 METRO-HAUL node control and Management environment

7.1 Monitoring and Data Analytics (MDA) and node integration

In this section, we present our architecture to support active and passive monitoring, telemetry, and data analytics.

The proposed monitoring and data analytics architecture shown in Figure 46 consists of a multi-node agent, referred to as MDA agent, managed by the centralized MDA system in the control and management (COM) plane. The number of MDA agents may vary depending on the size of the network, geographical extension, and any other criteria.

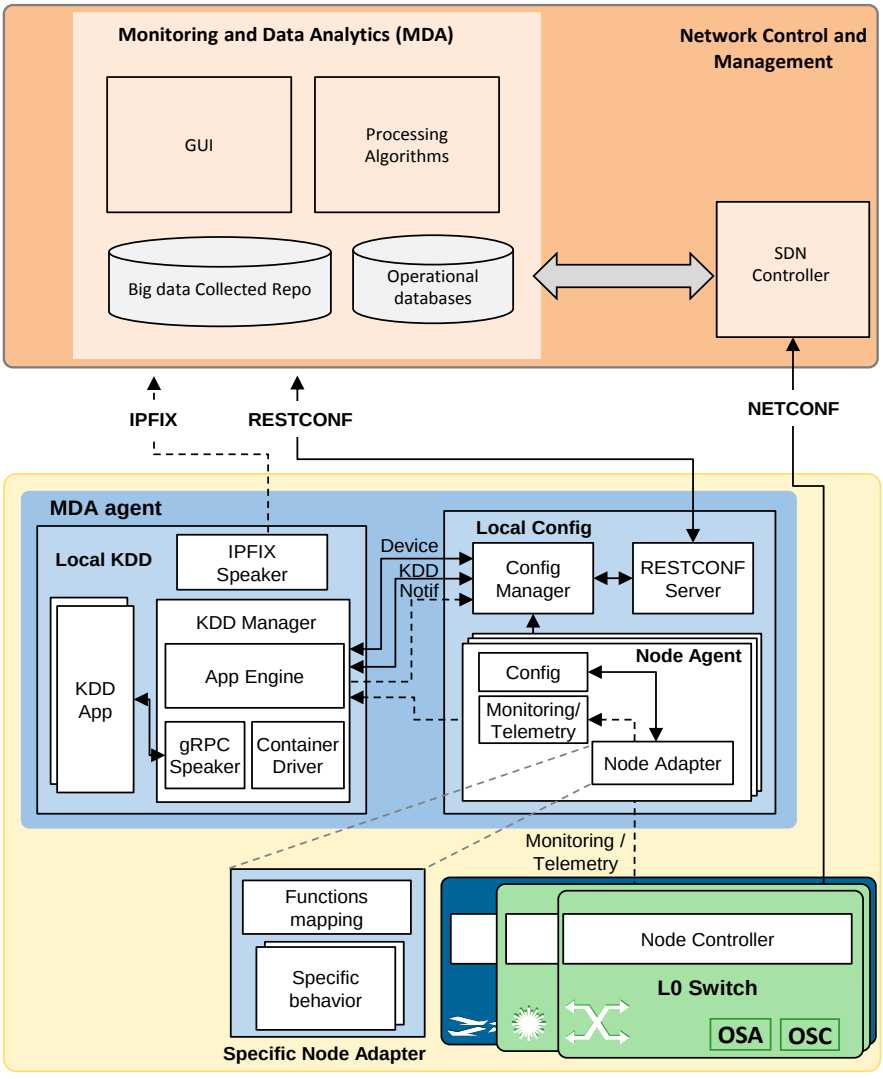

Figure 46 MDA architecture and interfaces

MDA agents are designed to configure monitoring and telemetry, as well as to collect measurements from one or more nodes in the disaggregated data plane. While each node controller usually controls one single node and exposes one single interface toward the SDN controller, MDA agents are designed to be in charge of monitoring and telemetry of a set of nodes. MDA agents consist of two building blocks, the *local configuration* module and the *local KDD* module. The local configuration module is in charge of receiving configuration and exposes a RESTCONF-based North-Bound Interface (NBI) to the MDA system. Finally, several node adapters (one per node) are used to implement the

specific protocols exposed by every node controller for node configuration and for monitoring data collection.

A specific node adapter is being currently defined and developed to be able to collect telemetry from the gRPC-based telemetry service in the NETCONF agent defined in the previous section. The telemetry is based on the open source Python implementation of the gRPC with protobuf protocol.

The MDA controller is in charge of collecting monitoring data from the underlying infrastructure; It includes operational databases (e.g., topology and LSP databases) synchronized from the SDN controller. With operational databases synchronized, the MDA system is able not only to collate measurements from the nodes, but also to correlate them with the route of an LSP for failure localization purposes and applying data analytics techniques on these data, while generating useful notifications of detected events and issuing recommendations to the SDN controller for network automation. Therefore, sophisticated procedures can be developed correlating measurements with topology and LSP data.

7.2 Active Measurements

The metro network has to provide Key Performance Indicators (KPI) such as capacity, delay or packet loss, with very stringent requirements. To check that the deployed optical paths meet these requirements, it is necessary to test them before they are put in operation. This section shows how active measurements at 100 Gbit/s are performed to check that the requested KPIs are met before the optical path is put in operation. Given the foreseen heterogeneity in the optical network, with different equipment providers, these preliminary measurements are essential for the network operator to assure the Quality of Service (QoS) provided to the users, and complement passive measurements performed during the optical path lifetime. Integration of the MDA controller and active monitoring devices allows adding active measurements to the MDA capabilities. This combination can help network providers to operate 5G optical networks.

Let us assume an infrastructure where a multi-layer network interconnects Central Offices (CO). The multi-layer interconnection network is controlled by a hierarchical SDN architecture COM. A parent SDN controller is on top of per-layer SDN controllers, one for the packet layer and another one for the optical layer (see Figure 47).

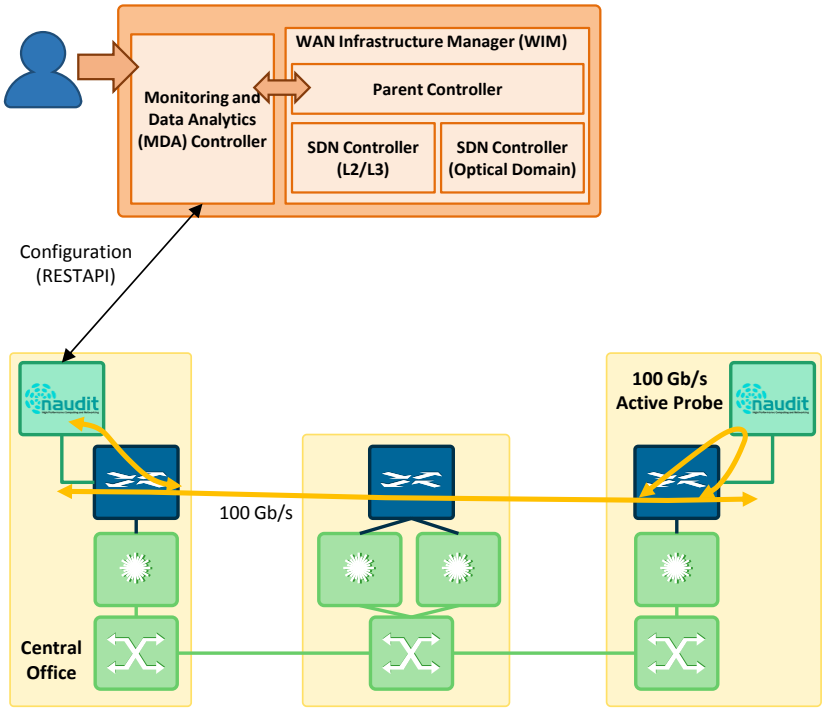

Figure 47 Example of active probes and MDA controller integration

In particular, one of the main aspects of network automation is to guarantee that provisioned connections meet the requested performance, e.g., in terms of end-to-end latency and throughput in the case of the packet layer. In that regard, this section shows the use of active probes at the packet layer to measure the performance of packet layer connections. The active probes are installed in every CO and connected through a 100GE interface of a layer 2 (L2) switch in the internal CO network.

Given that the active probes are connected to interfaces configured in trunk mode, the probes can tag the generated Ethernet frames with the desired VLAN ID, selecting the VLAN to be measured. The process of measuring a packet connection consists in injecting a train of numbered and timestamped Ethernet frames, which arrive the other end of the connection, where the remote active probe loops back them. Following this procedure, packet circuit performance, i.e., round-trip packet delay, jitter, packet loss and throughput, can be measured.

The active probes have been developed to be integrated into the above-described COM system. To that end, they expose a REST-API-based northbound interface (NBI) through which the MDA controller can initiate a measurement session on a specific packet circuit.

To achieve precise measurements at 100 Gbit/s, we have implemented the active probe in hardware, using a Field Programmable Gate Array (FPGA). To do so, a Virtex Ultrascale+ FPGA device is being used. In particular, the ADM-PCIE-9V3 High-Performance Network Accelerator card, which includes two 100GE interfaces, 8 GB of DDR4 memory and a XCVU3P-2-FFVC1517 FPGA. The QSFP28 physical cages are mapped directly to the FPGA. An integrated 100G Ethernet interface is in charge of communicating the FPGA side with the physical network. The FPGA internally works with a bus of 512-bit width of data and is clocked at 322 MHz (3.1 ns) to reach the needed throughput, even with smallest frames.

The packet train technique has been implemented in the FPGA at 100 Gbit/s. Packets are timestamped at the transmitter and at the receiver. Receiver timestamps are useful to calculate the

achieved throughput, whereas transmitter timestamps allow a precise calculation of round-trip delay with the clock implemented in the FPGA, without needing to synchronise the transmitter and receiver clocks.

The development is split into two independent designs, which reside in the same FPGA. In one hand, the transmitting side, a synthetic packet generator has been developed. On the other hand, the receiving side is in charge of filtering the packets, analysing them and generating a summary. In what follows, both elements are detailed.

7.2.1 Synthetic Packet Generator

This piece of hardware is written in Verilog and implemented as a Finite State Machine (FSM). In this way, the behavior is completely deterministic, and it provides the most accurate measurements. This module is in charge of generating UDP packets that will carry useful information for the measurement. The packets can be generated at the maximum throughput, which is extremely close to the theoretical value in 100G Ethernet links.

When a measurement is requested, some of the fields in the packets can be set, such as VLAN, source and destination IP addresses, source and destination ports, packet size, and Bit Error Rate Test (BERT) type used for the payload. Moreover, each UDP packet carries a payload with the following fields:

- Local timestamp (8 bytes).
- Extended identifier (4 bytes).
- Total amount of packets configured by the user (4 bytes).
- Burst identifier (2 bytes).
- 4 free bytes, reserved for future use.
- BERT payload, filling the rest of the packet size

Additionally, other configurable parameters are the number of packets in the burst and the inter-packet gap. All those configurations are done through an interface from a program running in the computer hosting the FPGA card.

The following BERT types have been implemented in the payload of the packets, so the active measurements can also be used to check if the optical modulation and the Forward Error Correction (FEC) implemented in the optical path are working properly:

- PRBS (Pseudo Random Binary Sequence): binary sequence that is difficult to predict and exhibits statistical behavior similar to a truly random sequence.
- All zeros: A sequence of all zeros.
- All ones: A sequence of all ones.
- 1:1: A sequence composed of alternating ones and zeroes.
- 1:7: Also referred to as “1 in 8”. It has only a single one in an eight-bit repeating sequence.
- 2:8: A pattern that contains a maximum of four consecutive zeros and only two ones.
- 3:24: A pattern that contains the longest string of 15 consecutive zeros with only three ones

7.2.2 Packet Filtering

In the receiver side, packets are timestamped at the moment they reach the FPGA side. The packet handler module is in charge of filtering packets by type. For instance, ARP and UDP packets are taken into account in this implementation. After that, UDP packets are parsed, and those fields that are configurable are verified to check if the packets match with the required configuration. If so, the useful information is extracted to compute the packet train parameters. This information is fed to

the statistics generator, which collects it. The results of the burst are then returned to the MDA once the burst has been completely received or after a timeout.

7.2.3 Demonstrative workflow

The workflow of the demonstration is as follows (see Figure 48-left):

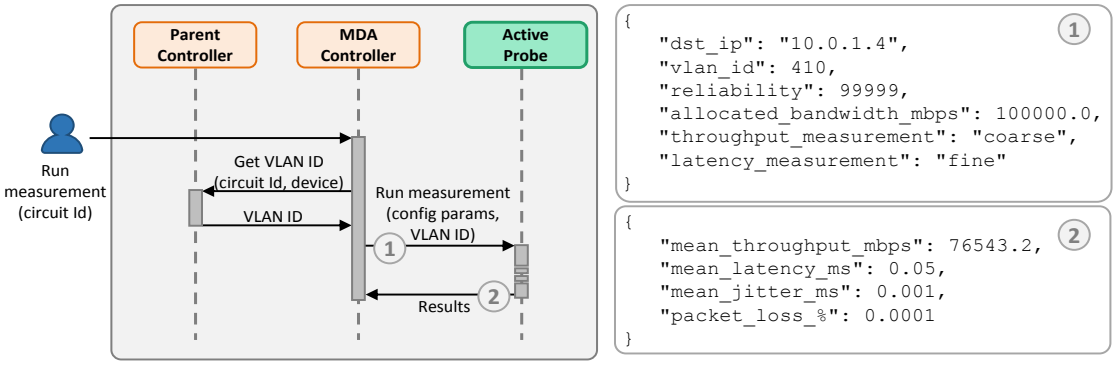

Figure 48 Workflow and messages details

- The operator requests to measure the performance of a packet circuit through the MDA controller's GUI; to this end, the circuit is selected by its circuit Id.
- The MDA controller uses the circuit Id to ask the parent controller about the VLAN IDs that have been used for the circuits, which are next sent to the active probe to be used for tagging the generated Ethernet frames.
- To measure the performance of a circuit, the active probe in a CO injects trains of Ethernet frames that are received by the active probe in the remote CO, which loops back them to the sender.
- Once the performance of a circuit is measured, the obtained values are replied. Such values are shown in the MDA controller' GUI to the operator that can in such way verify the performance of the set-up circuits.

Figure 48-right shows examples of the JSON messages exchanged between the MDA controller and the parent SDN controller, as well as the MDA controller and the active probe. As shown, for the latter case, the MDA controller requests a measurement with some parameters, such as the reliability -five '9' will generate measurements with one million packets-, allocated bandwidth -measurement can be adjusted to values below 100 Gbit/s if necessary-, and if the measurement is throughput or latency oriented -maximum transmission unit (MTU) packets will be used for fine throughput measurements, whereas minimum size packets will be used for fine latency measurements. By default, if not indicated, the used BERT type is PRBS. As a result, the probe provides the following values: achieved throughput in Mbit/s, latency and jitter in ms, and observed packet loss percentage.

8 Conclusions

In this D3.2 document, we have summarized the result of the second year of activities in WP3 of the METRO-HAUL project.

During the first year of the project, we provided the reference framework together with a selection and preliminary implementation of candidate metro node architectures and optical technology options for future metro networks, aiming at supporting 5G and the new heterogeneous services including the emerging “vertical actors”.

In this deliverable D3.2 we focus on three selected classes of metro optical WDM transport systems that have been identified within the METRO-HAUL project as the most suitable solutions for the evolution of metro networks. The three classes differ in terms of switching and transmission technologies, overall guaranteeing cost-effectiveness and high-performance despite of the specific metro application scenario which could vary quite significantly according to the considered optical reach (from few tens of km up to 150-200km), fiber availability and topology (ring, mesh, horseshoe), geographic/demographic conditions (e.g., rural to densely populated areas), etc.

The three identified classes of systems are:

- WDM-Sys1: Flexible, high capacity WDM transport System based on MD-ROADMs;
- WDM-Sys2: Low cost, simple topology WDM transport System based on degree-2 ROADMs;
- WDM-Sys3: Low cost, simple topology WDM transport System based on Filterless OADMs.

These classes rely on innovative devices and subsystems designed and validated within METRO-HAUL. In terms of optical switching technologies, the Project has designed and preliminarily validated low-cost MD-ROADM, semi-filterless and filterless solutions, and innovative filtered photonic integrated solution. In terms of transceivers, we reported on four different solutions: (i) a programmable sliceable transceiver based on multicarrier modulation (MCM); (ii) a transceiver solution for dispersion-tolerant direct detection; (iii) an elastic transponder with low resolution DAC and ADCs for metro networks; and (iv) a digital sliceable bandwidth variable transponder for filterless networks. Such solutions have been discussed and compared in terms of their capacity, complexity, and suitability for the above classes of systems.

To provide a comprehensive solution, also Passive Optical Network (PON) termination to metro nodes, programmable packet switching solution for interconnection at the edge, and monitoring probe-based solutions at the data-link layer have been discussed and preliminarily validated.

All the aforementioned node and transceiver solutions have been designed to operate under common open API. In this deliverable, we reported on the design, implementation and preliminary validation of the software components serving as subsystem agents. More specifically, an OpenROADM compliant software agent has been implemented for the optical network equipment performing optical switching and the OpenConfig compliant model for transponders.

Finally, the implementation of the monitoring and data analytics (MDA) system, introduced in D3.1, has been reported and preliminary validates.

This D3.2 document feeds WP2 for the design of next-generation cost-effective metro architectures, WP4 for the implementation of the overall control framework and WP5 for the experimental demonstrations including verticals.

List of acronyms

Acronym	Description
ABNO	Application Based Network Operations
ACO	Analog Coherent Optical module
ACTN	Abstraction and Control of Traffic-Engineered Networks
ADC	Analog to Digital Converter
AMEN	Access-Metro Edge Node
API	Application Programming Interface
ASE	Amplified Spontaneous Emission
ATA	Autonomic Transmission Agent
A-WDM	Analog-WDM
AWGN	Additive White Gaussian Noise
BER	Bit Error Rate
BL/PL	Bit/Power Loading
BSS	Business Support System
B2B	Back to Back
BVT	Bandwidth Variable Transponder
CapEx	Capital Expenditure
CAPS	Combined Amplitude and Phase Shift
CDB	Core Engine Database
CFP	C Form-factor Pluggable
CLI	Command Line Interface
CNC	Customer Network Controller
CO	Central Office
COM	Control, Orchestration and Management
CORD	Central Office Re-architected as a Data-center
CP	Control Plane
CPE	Customer Premises Equipment
CPRI	Common Public Radio Interface
CW	Continuous Wavelength
DAC	Digital to Analog Converter
DC	Data Center
DCO	Digital Coherent Optical module
DD	Direct Detection
DMA	Docker Management Agent
DP	Data Plane
DP-*n*QAM	Dual Polarization QAM of order *n*
DS-BVT	Digital S-BVT
DSP	Digital Signal Processing
DS	DownStream
DWDM	Dense WDM

EDFA	Erbium Doped Fiber Amplifier
ETSI	European Telecommunications Standards Institute
FBG	Fiber Brag GrATING
FEC	Forward Error Indicator
FMN	Filterless Metro optical Networks
FODAM	Fixed OADM
FPGA	Field Programmable Gate Array
GMPLS	Generalized Multi-Protocol Label Switching
gNMI	gRPC Network Management Interface
gRPC	Google's Remote Procedure Call
HD-FEC	Hard Decision FEC
HE	High End
(I)FFT	Inverse Fast Fourier Transform
IHSDN	Interface between the parent controller (Orchestrator) and the packet / optical controllers
IM/DD	Intensity Modulation with DD
IO2	Operator – VIM for Authentication (Keystone), Instantiation of VMs (Nova), Basic Intra-node connectivity (Neutron)
IO3	Operator – NFVO (OSM). Based on OSM interfaces and APIs.
IO4	Operator – Monitoring
IOS	Interface between Orchestrator – WIM [NFVO-TSDN, follow OSM]
IP	Internet Protocol
IPFIX	IP Flow Information Export
IPNFVO	NFVO – Planning Tool – Interface for planning and placement
IPON	Interface to the SDN PON controller – Controller Specific
IPSDN	SDN – Planning Tool – Interface for planning (SDN) [Complements IPNFVO]
IPVIM	VIM – Planning Tool – Interface for planning and placement (VIM) [Complements IPNFVO]
JSON	JavaScript Object Notation
KDD	Knowledge Discovery from Data
KPI	Key Performance Indicator
LAN	Local Area Network
LDPC	Low Density Parity Check
LE	Label Extractor
LP	Label Processor
MAN	Metro Area Network
MANO	Management and Orchestration
MCEN	Metro-Core Edge Node
MCM	MultiCarrier Modulation

MCOM	Interface between the monitoring system and the SDN controller (parent) or the NFVO
MDA	Monitoring and Data Analytics
MDSC	Multi-Domain Service Coordinator
MD-ROADM	Multi Degree-ROADM
MH	METRO-HAUL
ML	Machine Learning
MPLS	Multi Protocol Label Switching
MSA	Multi Source Agreement
MSE	Mean Square Error
MWI	Multi Wavelength Interface
MZM	Max-Zehnder Modulator
NBI	North Bound Interface
NE	Network Element
NETCONF	NETwork CONFiguration protocol
NFV	Network Function Virtualization
NFVI	NFV Infrastructure
NFVO	NFV Orchestration
NIC	Network Interface Card
NOS	Network Operating System
OA	Optical Amplifier
OADM	Optical Add Drop Multiplexer
OAM	Operation Administration and Maintenance
OCh	Optical Channel
OCP	Optical Dispersion Compensator
ODC	Open Line System
OLS	Open Line System
OLT	Optical Line Terminator
O-NE	Optical-Network Element
ONOS	Open Network Operating System
ONSR	Optical SNR
ONU	Optical Network Unit
OOK	On/Off Keying
OpEx	Operational Expenditure
OSS	Operations Support System
OST	Optical Sub-System

OT	Open Terminal
P2MP	Point to Multi-Point
P2P	Point to Point
PAM	Pulse Amplitude Modulation
PCA	PON Configuration Agent
PDM	Polarization Division Multiplexed
PNC	Provisioning Network Controller
PNFA	PON Network Flow Agent
PoP	Point of Presence
PON	Passive Optical Network
QAM	Quadrature Amplitude Modulation
QoT	Quality of Transmission
QPSK	Quadrature Phase Shift Keying
QSFP	Quad Small Form-factor Pluggable
ROADM	Reconfigurable OADM
RPC	Remote Procedure Call
SA	Switch Agent
SBI	South Bound Interface
S-BVT	Sliceable-BVT
SD-FEC	Software Decision FEC
SDN	Software Defined Network
SNR	Signal to Noise Ratio
SOA	Semiconductor Optical Amplifier
SOP	State Of Polarization
SSB	Single Side Band
SMF	Single Mode Fiber
SSMF	Standard SMF
SWI	Single Wavelength Interface
TCP	Transport Control Protocol
TDM	Time Division Multiplexing
TIA	Trans-Impedance Amplifiers
TLS	Tunable Laser Source
UDP	User Datagram Protocol
US	UpStream
VIM	Virtual Infrastructure Manager

VLAN	Virtual LAN
VM	Virtual Machine
VNF	Virtual Network Function
VOA	Variable Optical Attenuator
VPN	Virtual Private Network
VTEP	Virtual Tunnel End Point
VXLAN	Virtual Extensible LAN
WDM	Wavelength Division Multiplexing
WIM	WAN Infrastructure Manager
WB	Wavelength Blocker
WSS	Wavelength Selective Switching
YANG	Yet Another Next Generation

References

[1] Victor Lopez, Oscar Gonzalez de Dios, Juan Pedro Fernandez-Palacios, “Whitebox Flavors in Carrier Networks”, Optical Fiber Communications Conference and Exhibition (OFC), 2019

[2] E. Riccardi, P. Gunning, O. Gonzalalez de Dios, M. Quagliotti, Victor Lopez, and A. Lord, “An Operator view on the Introduction of White Boxes into Optical Networks”, JOURNAL OF LIGHTWAVE TECHNOLOGY, VOL. 36, NO. 15, AUGUST 1, 2018

[3] D3.1: METRO-HAUL Selection of metro node architectures and optical technology options

[4] A. Sgambelluri et al., “Fully disaggregated ROADM white box with NETCONF/YANG control, telemetry, and machine learning-based monitoring”, OFC Demo 2018

[5] D2.3: Network Architecture Definition, Design Methods and Performance Evaluation

[6] H. Miyata et al., "Fully dynamic and reconfigurable optical add/drop multiplexer on 0.8 nm channel spacing using AOTF and 32-wave tunable LD module," Optical Fiber Communication Conference. Technical Digest Postconference Edition. Trends in Optics and Photonics Vol.37 (IEEE Cat. No. 00CH37079), Baltimore, MD, USA, 2000, pp. 287-289 vol.4. doi: 10.1109/OFC.2000.869486

[7] G. Serafino et al., "Semi Filter-Less Drop & Waste Network Demonstration with Integrated SOI Optical Filter," 2017 European Conference on Optical Communication (ECOC), Gothenburg, 2017, pp. 1-3. doi: 10.1109/ECOC.2017.8346157

[8] Annika Dochhan, Robert Emmerich, Pablo Wilke Berenguer, Colja Schubert, Johannes K. Fischer, Michael H. Eiselt, Jörg-Peter Elbers, “Flexible metro network architecture based on wavelength blockers and coherent transmission” ECOC2019, Dublin (submitted)

[9] M. Eiselt, K. Grobe, “Wavelength Division Multiplexing: A Practical Engineering Guide”, Wiley, 1st Edition, 2013

[10] R. Emmerich, R. Elschner, C. Schmidt-Langhorst, et al., "Colorless C-band WDM system enabled by coherent reception of 56-GBd PDM-16QAM using an high-bandwidth ICR with TIAs," 2017 Optical Fiber Communications Conference and Exhibition (OFC), Los Angeles, CA, 2017, paper M2C.3, pp. 1-3, doi: https://doi.org/10.1364/OFC.2017.M2C.3

[11] R. Jensen, A. Lord, and N. Parsons, “Colourless, Directionless, Contentionless ROADM Architecture Using Low-Loss Optical Matrix Switches”, ECOC 2010 Proceeding, paper Mo.2.D.2, 2010.

[12] Toshio Watanabe, Kenya Suzuki, Takashi Goh, Kuninori Hattori, Atsushi Mori, Tetsuo Takahashi, Tadashi Sakamoto, Keiichi Morita, Shunichi Sohma, and Shin Kamei: “Compact PLC-based Transponder Aggregator for Colorless and Directionless ROADM” Proc OFC 2011, paper OTuD3.

[13] S. Gringeri, B. Basch, V. Shukla, R. Egorov, and T. J. Xia, “Flexible Architectures for Optical Transport Nodes and Networks,” IEEE Commun. Mag. 48, 40-50, 2010

[14] Dan M. Marom, et al., "Survey of Photonic Switching Architectures and Technologies in Support of Spatially and Spectrally Flexible Optical Networking [Invited]," J. Opt. Commun. Netw. 9, 1-26, 2017

[15] P. Colbourne and B. Collings, “ROADM Switching Technologies,” OFC 2011 Proceeding, paper OTuD1, 2011

[16] F. Paolucci, R. Emmerich, F. Fresi, I. Sackey, L. Potì, C. Schubert, J.K. Fischer, F. Cugini , “Filterless Optical WDM Metro Networks exploiting C+L Band”, in Proc. ECOC 2018, Rome, paper Tu.1.D, 2018

[17] Robert Emmerich, António Eira, Nelson Costa, Pablo Wilke Berenguer, Colja Schubert, Johannes Karl Fischer, João Pedro, “Low-cost Dual Node Architecture for C+L-band Transmission in Metro Transport Networks” ECOC 2019, Dublin (submitted)

[18] OpenConfig web site, Mar. 2018. [Online]. Available: http://www.openconfig.net/

[19] Hideki Isono, “Recent standardization activities for client and networking optical transceivers and its future directions ”, vol. 10131, SPIE OPTO, San Francisco, 2017

[20] Hideki Isono, “Latest standardization status and its future directions for high speed optical transceivers”, Photonics West, vol. 10946, February, 2019

[21] Muñoz, R., Nadal, L., Casellas, R., et al., “The ADRENALINE Testbed: An SDN/NFV Packet/Optical Transport Network and Edge/Core Cloud Platform for End-to-End 5G and IoT Services”, Proc. of European Conf. on Netw. and Comm. (EUCNC), Oulu, Finand, June 2017

[22] Fàbrega, J.M., Svaluto Moreolo, M., Martín, L., et al., "On the filter narrowing issues in elastic optical networks," *J. of Optical Communications and Networking*, Vol. 8, No. 7, pp. A23-A33, July 2016

[23] E. Forestieri and G. Prati, “Novel optical line codes tolerant to fiber chromatic dispersion,” J. Lightwave Technol. **19**(11), 1675–1684, 2001

[24] E. Forestieri, M. Secondini, F. Fresi, G. Meloni, L. Potì, and F. Cavaliere, “Extending the reach of short-reach optical interconnects with DSP-Free direct-detection,” J. Lightw. Technol. 35(15), 3174-3181, 2017

[25] F. Fresi , M. Morsy-Osman, E. Forestieri, M. Secondini, F. Cavaliere, D. V. Plant, S. Lessard, L. Potì, “50 Gb/s Transmission over Uncompensated Link up to 20 km Exploiting DSP-Free Direct-Detection”, in Proc. CLEO 2018, San Jose, CA, USA, paper STu3C.1, 2018

[26] F. Fresi, G. Meloni, M. Secondini, F. Cavaliere, L. Potì, and E. Forestieri, “Short-reach distance extension through CAPS coding and DSP-free direct detection receiver,” in *Proc. Europ. Conf. Optical Commun. (ECOC)*, Düsseldorf, Germany, paper Th.2.P.2, 2016

[27] C. K. Madsen et al., "Integrated all-pass filters for tunable dispersion and dispersion slope compensation," IEEE Photonics Technology Letters, vol. 11, no. 12, pp. 1623-1625, 1999

[28] V. Sorianello, G. De Angelis, F. Fresi, F. Cavaliere, L. Potì, M. Midrio, M. Romagnoli, “100Gb/s PolMux-NRZ Transmission at 1550nm over 30km Single Mode Fiber Enabled by a Silicon Photonics Optical Dispersion Compensator”, in Proc. Optical Fiber Communication Conference 2018, San Diego, CA, USA, W2A. 31, 2018

[29] P. Layec, A. Dupas, D. Verchère, K. Sparks, and S. Bigo, “Will Metro Networks Be the Playground for (True) Elastic Optical Networks?” J. of. Lightw. Technol, vol. 35, no. 6, pp. 1260-1266, 2017

[30] T. Kupfer, A. Bisplinghof, T. Duthel, C. Fludger, and S. Langenbach, “Optimizing Power Comsumption of a Coherent DSP for Metro and Data Center Interconnects,” in Proc. OFC’17

[31] A. Napoli, M.M. Mezghanni, T. Rahman, D. Rafique, R. Palmer, B. Spinnler, S. Calabrò, C. Castro, M. Kuschnerov, and M. Bohn, “Digital Compensation of Bandwidth Limitations for High-Speed DACs and ADCs,” J. of. Lightw. Technol., vol. 34, no. 13, pp. 3053–3064, Jul. 2016

[32] G. Böcherer, F. Steiner, and P. Schulte, “Bandwidth Efficient and Rate Matched Low-Density Parity-Check Coded Modulation,” IEEE Trans. Commun., vol. 63, no. 12, pp. 4651–4665, Dec. 2015

[33] X. Chen, S. Chandrasekhar, S. Randel, W. Gu, and P. Winzer, “Experimental Quantification of Implementation Penalties from Limited ADC Resolution for Nyquist Shaped Higher-Order QAM,” presented at the Optical Fiber Communication Conf. Exhibition, Paper W4A.3, 2016

[34] Sripad A., Snyder D., 'A Necessary and Sufficient Condition for Quantization Errors to be Uniform and White', IEEE Trans. Acoust. Speech, Signal Process., 1977, 25, 5, pp. 442-448, DOI:10.1109/TASSP.1977.1162977

[35] Widrow B., Kollar I., Liu M.-C., 'Statistical Theory of Quantization', IEEE trans. Instrum. Meas., 1996, 45, 2, pp. 353-361, DOI:10.1109/19.492748
[36] Jennevé P., Ramantanis P., Dubreuil N. et al., 'Measurement of Optical Nonlinear Distortions and Their uncertainties in Coherent Systems', Journal of Lightwave Technology, 2017, 35, 24, pp. 5432-5439, DOI: 10.1109/JLT.2017.2773204
[37] C. Dorize, O. Rival, and C. Costantini, "Power scaling of LDPC decoder stage in long haul networks," in Proc. PS, 2012
[38] X. Chen *et al.*, "Experimental Quantification of Implementation Penalties from Limited ADC Resolution for Nyquist Shaped Higher-Order QAM," in Proc. ECOC, 2016
[39] J. Auge, "Can we use Flexible Transponders to Reduce Margins?," in Proc. OFC 2013
[40] I. Sartzetakis, K. Christodoulopoulos, and E. Varvarigos, "QoT Aware Adaptive Elastic Optical Networks," in Proc. OFC, 2017
[41] F. Boitier et al., "Proactive fiber damage detection in real-time coherent receiver," in Proc. ECOC, 2017
[42] D. Rafique and L. Velasco, "Machine Learning for Optical Network Automation: Overview, Architecture and Applications," IEEE/OSA Journal of Optical Communications and Networking, vol. 10, pp. D126-D143, 2018
[43] Marc Ruiz, Fabien Boitier, Behnam Shariati, Patricia Layec, and Luis Velasco, "Predictive Autonomic Transmission for Low-Cost Low-Margin Metro Optical Networks", JOCN, (accepted, to be published)
[44] F. Frey et al., "Estimation of Trends for Coherent DSP ASIC Power Dissipation for different bitrates and transmission reaches," ITG-Fachbericht 272: Photonische Netze, Leipzig, Germany, pp. 137-144, May 2017
[45] F. Frey et al., "Improved Perturbation-based Fiber Nonlinearity Compensation," ECOC 2018, Rome, Italy, Sep. 2018
[46] P. Paolucci et al., "OpenConfig Control of 100G/400G Filterless Metro Networks with configurable Modulation Format and FEC," OFC 2019, San Diego, USA, paper Tu3H.4, Mar. 2019
[47] C. Matrakidis, T. Orphanoudakis, A. Stavdas, et al, "Low-Power/Cost Intra-Datacentre Architecture Exploiting Transmission and Multiplexing in the Interconnection Fabric", proceeding of ECOC, Valencia Spain, September 2015
[48] "ITU-T PON YANG Modules", BroadBand Forum, WT-385, May 2017
[49] ConfD, https://www.tail-f.com/confd-basic/
[50] F. Paolucci, A. Sgambelluri, R. Emmerich, A. Giorgetti, P. Castoldi, C. Schubert, J. K. Fischer, and F. Cugini, "OpenConfig Control of 100G/400G Filterless Metro Networks with configurable Modulation Format and FEC," in Optical Fiber Communication Conference (OFC) 2019, OSA Technical Digest (Optical Society of America, 2019), paper Tu3H.4.
[51] https://github.com/CESNET/netopeer
[52] https://rawgit.com/CESNET/libnetconf/master/doc/doxygen/html/d9/d25/transapi.html
[53] https://gitlab.com/METRO-HAUL/openroadm-agent/tim-agent